Voltage-Gated Sodium Channel β1 Subunit Processing by BACE1 and γ-secretase: Regulatory
Mechanisms and Downstream Signaling

by

Alexandra A. Bouza

A dissertation submitted in partial fulfillment
of the requirements for the degree of
Doctor of Philosophy
(Pharmacology)
in the University of Michigan
2020

Doctoral Committee:

    Professor Lori L. Isom, Chair
    Professor Pierre Coulombe
    Research Assistant Professor James Offord
    Professor Yoichi Osawa
    Professor Manoj Puthenveedu

Alexandra A. Bouza

bouzaa@umich.edu

ORCID iD: 0000-0002-7610-5517

Acknowledgements

First, I would like to thank my mentor, Dr. Lori Isom, for her incredible support and guidance throughout the duration of my graduate studies. I feel very fortunate to have been trained in the Isom lab with a mentor who is so passionate about not only research, but graduate education. I would also like to thank the additional members of my thesis committee: Drs. Pierre Coulombe, Jim Offord, Yoichi Osawa, and Manoj Puthenveedu. The insight and advice during both committee and individual meetings greatly helped advance my thesis project and my own progression as a scientist. In particular, I would like to thank Dr. Jim Offord for sharing his over 30 years of experience with me each day in the lab to help turn a chemist into a molecular biologist/pharmacologist. Next, I would like to thank all current and previous members of the Isom lab. Thank you for providing the most kind and supportive environment to learn and thank you all for your great passion for food and a good happy hour.

I would also like to thank the many collaborators for their contributions to this thesis as well as those who included me in their own work. To Julie Philippe, thank you for loving β1 palmitoylation as much as I do. Without you, the β1 palmitoylation project truly would not have been possible. Nnamdi Edokobi and Dr. Luis Lopez-Santiago, thank you for completing the many of the electrophysiological experiments presented in this thesis. I so appreciate the large amount of time you committed to moving my project forward. Dr. Gemma Carvill, thank you for your advice and analysis on the β1 proteomic study presented. Thank you to the incredible University

Table of Contents

List of Tables

List of Figures

Abstract

Voltage-gated sodium channels (VGSCs) are heterotrimeric proteins comprised of one pore-forming, α subunit and two non-pore forming, β subunits. Variants in *SCN1B,* the gene which encodes VGSC β1 subunits, are linked to human diseases with high incidence of sudden death including Early Infantile-Developmental and Epileptic Encephalopathy (EI-DEE) and cardiac arrhythmia. *Scn1b*-null mice are a model of EI-DEE, including a cardiac phenotype, and 100% of mice die by approximately postnatal day 21. β1 subunits are classically known for their role in modulating the gating, kinetics, and localization of the ion channel pore. In addition, β1 is a member of the immunoglobulin super family of cell adhesion molecules (CAMs). β1 functions in both homophilic and heterophilic cell adhesion with downstream roles in neurite outgrowth and neuronal pathfinding and fasciculation. Although these functions explain a portion of *SCN1B*-linked disease, the underlying mechanisms for differential gene expression observed in the *Scn1b*-null model of EI-DEE remained poorly understood.

Studies presented in this thesis sought to understand the contribution of β1 to transcriptional changes in *Scn1b*-null animals. We and others have shown, in addition to the aforementioned functions of β1, β1 is a substrate for sequential cleavage by β-site APP cleaving enzyme 1 (BACE1) and γ-secretase. We created a cell culture based assay to study the molecular mechanisms that regulate cleavage and its subsequent downstream signaling. Using biochemical approaches,

we demonstrated β1 is post-translationally palmitoylated, the addition of a 16-carbon fatty acid chain to a cysteine residue by a thioester bond, at p.C162. β1 palmitoylation promotes β1 localization to the plasma membrane and consequently promotes β1 processing by BACE1 at the plasma membrane. Sequential cleavage generates a small, soluble peptide, the β1-intracellular domain (β1-ICD). β1-ICD is translocated to the nucleus where it modulates transcription. Expression of the β1-ICD generally downregulates gene expression of genes implicated in proliferation, the immune response, calcium ion binding, and voltage-gated potassium channels. Interestingly, these same Gene Ontology (GO) groups are upregulated in cardiac ventricle isolated from *Scn1b*-null mice, where this pathway is deleted, compared to wild-type. Subsequent increases in potassium current are observed in acutely isolated ventricular myocytes from *Scn1b*-null mice. In heterologous cells, expression of the β1-ICD increases *Scn4a* and *Scn5a* transcripts and decreases *Scn3a* transcripts. Expression of the β1-ICD does not lead to increases in sodium current density, nor does it act directly on the Na$_v$1.5 α subunit when the peptide is profused during patch clamp. This work identified a novel function of a species of the β1 subunit, β1-ICD, as both a transcriptional modulator. Identification of this pathway provides a direct mechanism by which loss of β1 in the *Scn1b*-null model of EI-DEE, and potentially in patients with loss-of-function *SCN1B* variants, results in changes in gene expression and altered excitability.

Chapter 1 Introduction

Alexandra A. Bouza and Lori L. Isom, PhD

Summary

Voltage-gated sodium channels are protein complexes comprised of one pore forming α subunit and two, non-pore forming, β subunits. The voltage-gated sodium channel β subunits were originally identified to function as auxiliary subunits, which modulate the gating, kinetics, and localization of the ion channel pore. Since that time, the five β subunits have been shown to play crucial roles as multifunctional signaling molecules involved in cell adhesion, cell migration, neuronal pathfinding, fasciculation, and neurite outgrowth. Here, we provide an overview of the evidence implicating the β subunits in their conducting and non-conducting roles. Mutations in the β subunit genes (*SCN1B-SCN4B*) have been linked to a variety of diseases. These include cancer, epilepsy, cardiac arrhythmias, sudden infant death syndrome/sudden unexpected death in epilepsy, neuropathic pain, and multiple neurodegenerative disorders. β subunits thus provide novel therapeutic targets for future drug discovery.

The basics of the voltage-gated sodium channel β subunits

There are five voltage-gated sodium channel (VGSC) β subunits, which are encoded by four genes, *SCN1B-SCN4B (O'Malley and Isom 2015)*. *SCN1B* encodes the β1 subunit and the developmentally regulated splice variant, β1B, while the β2, β3, and β4 subunits are encoded by *SCN2B-SCN4B*, respectively (Table 1.1**)** (Isom, De Jongh et al. 1992); (Isom, Ragsdale et al. 1995); (Kazen-Gillespie, Ragsdale et al. 2000);(Morgan, Stevens et al. 2000); (Patino, Brackenbury et al. 2011); (Qin, D'Andrea et al. 2003); (Yu, Westenbroek et al. 2003). β subunits each contain a large, extracellular V-set immunoglobulin (Ig) domain, making them part of the Ig superfamily of cell adhesion molecules (CAMs) (Brackenbury and Isom 2011);(O'Malley and Isom 2015). β1B differs from the other subunits in that it is the only one that is not a type I transmembrane protein, but rather, a soluble, secreted CAM expressed during embryonic development in brain and throughout development, into adulthood, in heart. The C-terminal domain of β1B is encoded by a retained intron, resulting in a unique polypeptide sequence that does not contain a transmembrane segment (Patino, Brackenbury et al. 2011). β subunit Ig domains are stabilized by two completely conserved cysteine residues in the extracellular portion, maintaining the β-sheet structure, as established by the X-ray crystal structures of β3 and β4 (Gilchrist, Das et al. 2013); (Namadurai, Balasuriya et al. 2014).

VGSC α subunits		VGSC β subunits	
Gene	Protein	Gene	Protein
SCN1A	Nav1.1	*SCN1B*	β1
SCN2A	Nav1.2	*SCN1B*	β1B
SCN3A	Nav1.3	*SCN2B*	β2
SCN4A	Nav1.4	*SCN3B*	β3
SCN5A	Nav1.5	*SCN4B*	β4
SCN8A	Nav1.6		
SCN9A	Nav1.7		
SCN10A	Nav1.8		
SCN11A	Nav1.9		

Table 1.1: VGSC genes and their encoded proteins.

VGSCs are comprised of one pore-forming α subunit and two different β subunits, either a β1 or β3 and a β2 or β4 (Fig. 1.1) (O'Malley and Isom 2015). β1 and β3 non-covalently associate with α, while β2 and β4 associate with α by cysteine disulfide bonds, Cys-26 and Cys-58, respectively, both of which are located in the extracellular Ig domain (Chen, Calhoun et al. 2012); (Gilchrist, Das et al. 2013); (McCormick, Isom et al. 1998); (Meadows, Malhotra et al. 2001); (Spampanato, Kearney et al. 2004). While there is no biochemical evidence to show that β1B associates with α subunits by co-immunoprecipitation, co-expression of β1B and Nav1.5 in heterologous systems results in plasma membrane retention of β1B and increased sodium current density, implicating association with α (Patino, Brackenbury et al. 2011); (Watanabe, Koopmann et al. 2008). Heterologous co-expression of β1B with Nav1.2 results in changes in current activation and inactivation, while co-expression with Nav1.3 results in subtle alternation of current properties, again suggesting a functional association (Kazen-Gillespie, Ragsdale et al. 2000); (Patino, Brackenbury et al. 2011).

VGSC β subunits are expressed in many tissues and cell types, not all of which are excitable (Brackenbury and Isom 2011). The expression of each specific β subunit is also developmentally regulated. In rodent brain, β1B and β3 are most highly expressed during embryonic development and early life. This differs from heart, in which β1B and β3 expression continues into adult life (Kazen-Gillespie, Ragsdale et al. 2000); (Patino, Brackenbury et al. 2011); (Shah, Stevens et al. 2001). β1 and β2 display peak expression in brain during adulthood (Isom, De Jongh et al. 1992); (Isom, Ragsdale et al. 1995). The developmental regulation of β4 subunit expression is yet

to be determined. β subunits are localized to a variety of specific sub-cellular compartments. In the brain and peripheral nervous system, β subunits are highly enriched the axon initial segment and nodes of Ranvier (Buffington and Rasband 2013);(Chen, Bharucha et al. 2002); (Chen, Westenbroek et al. 2004); (Dhar Malhotra, Chen et al. 2001); (O'Malley, Shreiner et al. 2009). These sites are important in the initiation and propagation of action potentials in neurons and have a high density of VGSC α subunit expression (Brackenbury, Calhoun et al. 2010). In heterologous cells, the β1 C-terminal domain interacts with the scaffolding protein, ankyrin-G, in a tyrosine phosphorylation-dependent manner and a similar mechanism is proposed at the axon initial segment and nodes of Ranvier (Malhotra, Kazen-Gillespie et al. 2000). In cardiomyocytes, the phosphorylation of β1 may regulate its sub-cellular localization. Tyrosine phosphorylated β1 subunits are localized to the intercalated disks, while non-phosphorylated β1 subunits are localized to t-tubules (Malhotra, Thyagarajan et al. 2004).
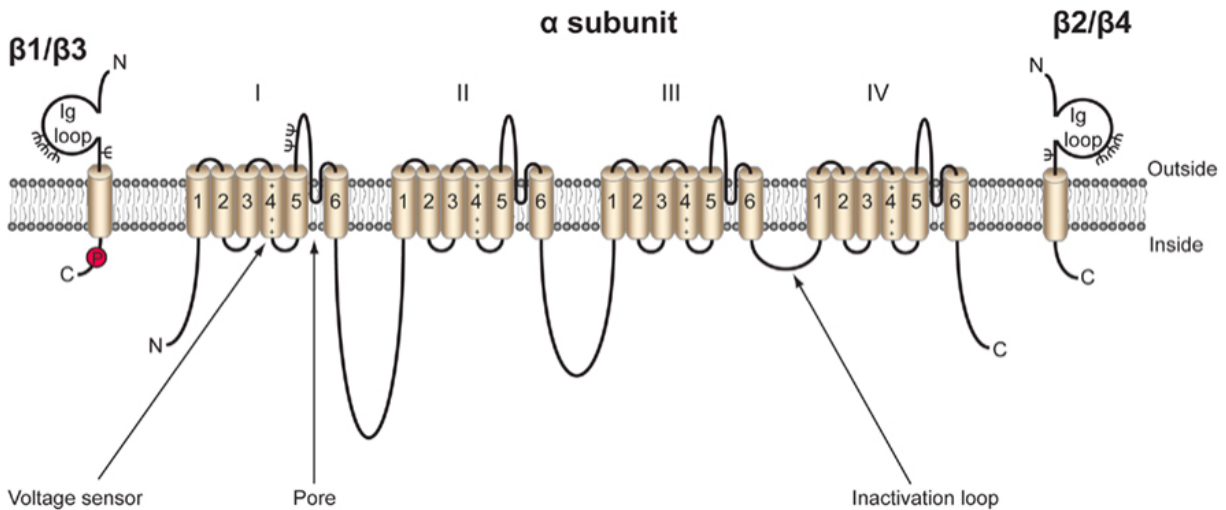
Figure 1.1: Cartoon diagram of the voltage-gated sodium channel (VGSC). VGSCs are comprised of one pore-forming, or α subunit, and one or two non-pore forming β subunits. The α subunit is made up four domains each of which contain six transmembrane segments. The voltage sensor is located in transmembrane segment four of each domain (Catterall). There are five β subunits, β1-β4, and the developmentally regulated β1B. β1-β4 all contain an intracellular C-terminal domain, a single transmembrane domain, and a large extracellular immunoglobulin (Ig) domain (Isom, De Jongh et al. 1994). β1B also possesses an Ig domain, but does not contain an intracellular or transmembrane domain, resulting in a soluble, secreted protein (Patino, Brackenbury et al. 2011). β1 and β3 are non-covalently linked to the α subunit, while β2 and β4 are linked by disulfide bonds. Each β subunit is heavily glycosylated, denoted by Ψ, and β1 also contains an intracellular phosphorylation site at tyrosine 181 (Malhotra, Thyagarajan et al. 2004). Figure reproduced from (Brackenbury and Isom 2011).

In addition to phosphorylation, the β subunits are post-translationally modified by glycosylation and proteolytic cleavage. All 5 β subunits are highly N-linked glycosylated (Isom, De Jongh et al. 1992). This heavy glycosylation of mature β subunits accounts for about 12 kilodaltons (kDa) of the ~36 kDa total molecular weight. β subunit glycosylation impacts their surface expression and channel modulatory properties (Johnson, Montpetit et al. 2004). Lastly, the transmembrane β subunits are also substrates for sequential cleavage, or regulated intramembrane proteolysis (RIP), by the β-site amyloid precursor protein cleaving enzyme-1 (BACE1) and γ-secretase (Wong, Sakurai et al. 2005). Initially, BACE1 cleaves β subunits on the extracellular side of the membrane, shedding the Ig domain, which may function as a soluble CAM, similar to β1B. Subsequently, γ-secretase cleaves the β subunits in the lumen of the membrane, generating an intracellular domain (ICD) (Fig. 1.2) (Haapasalo and Kovacs 2011); (Wong, Sakurai et al. 2005). Evidence shows that the β2 subunit ICD translocates to the nucleus where it increases expression of the Nav1.1 α subunit (Kim, Carey et al. 2007). A similar mechanism has been proposed, but not shown, for the other β subunits. Sequential cleavage of β subunits may play important roles in mediating neurite outgrowth, migration, and cell adhesion (Brackenbury and Isom 2011); (Kim, Ingano et al. 2005).
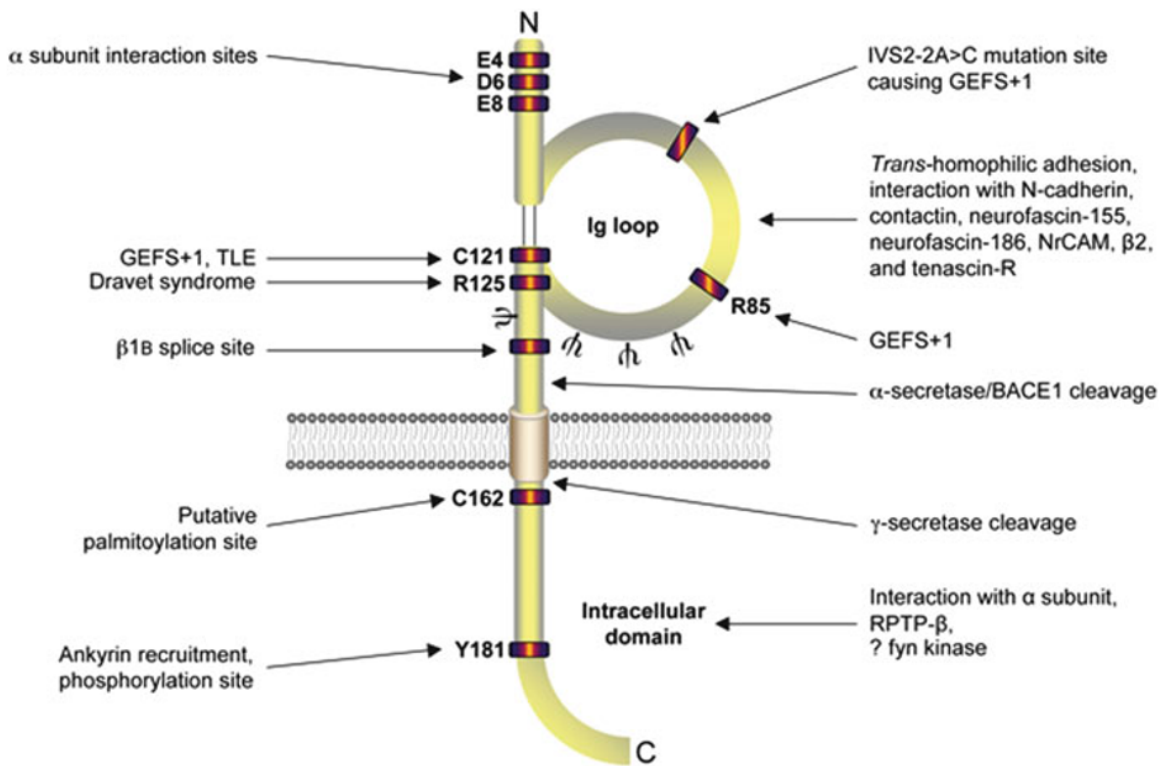
Figure 1.2: Cartoon diagram of β1/β1B topology. Both intracellular and extracellular residues on β1 are important for interacting with the α subunit (McCormick, Isom et al. 1998, Spampanato, Kearney et al. 2004). Epilepsy-linked mutation sites are clustered in the Ig domain (Wallace, Wang et al. 1998, Meadows, Malhotra et al. 2002, Wallace, Scheffer et al. 2002, Audenaert, Claes et al. 2003, Scheffer, Harkin et al. 2007, Patino, Claes et al. 2009). The alternative splice site for β1B, ankyrin interaction site (Kazen-Gillespie, Ragsdale et al. 2000, Qin, D'Andrea et al. 2003, Patino, Brackenbury et al. 2011), α-secretase/BACE1/γ-secretase cleavage sites (Wong, Sakurai et al. 2005), N-glycosylation sites (Ψ) (McCormick, Isom et al. 1998), tyrosine phosphorylation site (Malhotra, Thyagarajan et al. 2004), and the putative palmitoylation and fyn kinase interaction site are designated (McEwen and Isom 2004, Brackenbury, Davis et al. 2008). Figure reproduced from (Brackenbury and Isom 2011).

Modulation of the ion channel pore by β subunits

VGSC β subunits are traditionally known for their functions in modulating the gating and kinetics of the VGSC pore (Calhoun and Isom 2014). In Xenopus oocytes, expression of Nav1.2 mRNA alone results in sodium currents that are activated and inactivated much slower than those recorded in neurons. Co-injection of β1 or β2 mRNA altered the sodium current parameters (Isom, De Jongh et al. 1992). Co-expression β1 with Nav1.2 increased peak sodium current density, shifted the voltage-dependence of inactivation negatively, and accelerated activation and inactivation in comparison to Nav1.2 alone (Isom, De Jongh et al. 1992). Co-expression of β2 with Nav1.2 also resulted in increased peak sodium current density and accelerated current inactivation. Expression of the three subunits together, β1, β2, and Nav1.2, yielded the largest peak sodium currents and the most rapidly inactivating channels, most closely mimicking that observed in neurons (Isom, Ragsdale et al. 1995).

In addition to modulating VGSC activity, β1 can also act on Kv1.1, Kv1.2, Kv1.3, Kv1.6, Kv4.2, Kv4.3, and Kv7.2 in Xenopus oocytes or heterologous cells (Deschenes and Tomaselli 2002); (Nguyen, Miyazaki et al. 2012). Interestingly, β1 and Kv4.2 co-immunoprecipitate from mouse brain. Kv4.2 is a major contributor to A-type potassium current. Knockdown of β1 decreases A-type potassium current and prolongs action potential waveforms in cultured cortical neurons. β1 expression also increases the stability of Kv4.2 in HEK293 cells, leading to increased total and cell surface expression of Kv4.2 (Marionneau, Carrasquillo et al. 2012).

In addition to oocytes, heterologous mammalian cell lines have been utilized to study VGSC modulation by the β subunits. Although these models are more physiologically relevant, they cannot fully replicate VGSC activity in native excitable cells, such as neurons and cardiomyocytes. In Chinese Hamster Lung (CHL) cells, co-expression of Nav1.2 with β1 increases peak current density and causes a negative shift in the voltage-dependence of activation and inactivation, although to a lesser extent than observed in Xenopus oocytes (Isom, De Jongh et al. 1992, Isom, Ragsdale et al. 1995, Patino, Claes et al. 2009). Co-expression of Nav1.2 and β2 in CHL cells does not recapitulate the results observed in Xenopus oocytes, instead resulting in sodium currents that are unchanged or reduced in comparison to the expression of Nav1.2 alone (Kazarinova-Noyes, Malhotra et al. 2001); (McEwen, Meadows et al. 2004). In addition to altering kinetics of the ion channel pore, co-expression of β1 and/or β2 with Nav1.2 affects α subunit surface expression. Co-expression of β1 with Nav1.2 increases α subunit cell surface expression (Isom, Ragsdale et al. 1995). When β2 is added to the experiment, the cell surface expression of α subunits is even further increased, even though β2 cannot generate this effect in the absence of β1 (Kazarinova-Noyes, Malhotra et al. 2001). The modulatory and localization effects of β subunits on α subunits are impacted by the presence of other Ig-superfamily CAMs. In the case of the CAM, contactin, co-expression with Nav1.2 and β1 increases α subunit cell surface expression and sodium current density approximately four-fold over that observed with Nav1.2 plus β1. This is also displayed with NF186, although to a lesser extent than the effects observed with contactin. β1B co-expression with Nav1.2 in CHL cells also increases α subunit surface expression and peak sodium

current density, although, this combination only has a modest effect on channel activation and inactivation (Kazen-Gillespie, Ragsdale et al. 2000); (Patino, Brackenbury et al. 2011).

The effects of the β subunits on a variety of α subunits have also been studied in Chinese Hamster Ovary (CHO) cells and Human Embryonic Kidney (HEK) cells. β1 or β3 co-expression with Nav1.3 in CHO cells results in a negative shift in the voltage dependence of inactivation, but does not influence the rate of inactivation. In this same system, co-expression of β2 with Nav1.3 had no effect on the gating or kinetics of the ion channel pore (Meadows, Malhotra et al. 2002). Co-expression of β3 with Nav1.5 in CHO cells results in a negative shift in the voltage dependence of inactivation, but decreases the rate of inactivation (Ko, Lenkowski et al. 2005). Co-expression of β1B with Nav1.3 in CHO cells has no effect on Nav1.3 cell surface expression or sodium current density, different from the large effect of β1B observed in CHL cells (Kazen-Gillespie, Ragsdale et al. 2000); (Patino, Brackenbury et al. 2011). In HEK cells, co-expression of Nav1.5 and β4 results in a negative shift in the voltage dependence of inactivation in comparison to expression of Nav1.5 alone (Medeiros-Domingo, Kaku et al. 2007). The β4 subunit, when expressed with Nav1.2 or Nav1.4, induces a negative shift in the voltage dependence of activation (Yu, Westenbroek et al. 2003). This is also the case for co-expression of β4 with Nav1.1, although this results in increased levels of non-inactivating current (Aman, Grieco-Calub et al. 2009). Also in HEK cells, β1 and β3 subunits each modulate activity, cell surface expression, and glycosylation state of Nav1.7. β1 or β3 co-expression with Nav1.7 resulted in shifted activation and inactivation and increased sodium current density. Co-expression of β1 also resulted in alternative glycosylation of Nav1.7, while co-expression with β3 led to increased expression of fully-glycosylated Nav1.7

(Laedermann Cé, Syam et al. 2013). Overall, studies on β subunit modulation of VGSCs in heterologous systems have revealed cell type, β subunit, and α subunit specific effects.

The most physiologically relevant method to study VGSC modulation by the β subunits is to utilize primary cells, e.g. neurons or cardiomyocytes. In these native cells, β subunit effects are, in general, more modest than observed in heterologous over-expression systems. *Scn1b*-null mice, lacking both β1 and β1B, model the epileptic encephalopathy Dravet syndrome, and exhibit spontaneous seizures, ataxia, and premature death around post-natal day (P) 19 (Chen, Westenbroek et al. 2004). Acutely isolated P10-P18 *Scn1b*-null pyramidal and bipolar hippocampal neurons show no differences in VGSC activity compared to age-matched wild-type animals (Chen, Westenbroek et al. 2004); (Patino, Claes et al. 2009). However, slice recordings from this age range revealed hyperexcitability in the *Scn1b*-null CA3 hippocampal region as well as epileptiform activity in the hippocampus and cortex, suggesting altered VGSC activity in axons or dendrites (Patino, Claes et al. 2009). There are altered sodium currents and decreased excitability in cultured *Scn1b*-null cerebellar granule neurons (CGNs) (Brackenbury, Calhoun et al. 2010). In contrast, acutely isolated *Scn1b*-null dorsal root ganglion (DRG) neurons are hyperexcitable (Brackenbury, Calhoun et al. 2010); (Lopez-Santiago, Brackenbury et al. 2011). These results suggest that the effects of β1 and β1B in brain are neuronal cell-type specific, consistent with that observed in heterologous cells. Similar to that observed in heterologous systems, β1/ β1B expression in vivo affects the expression of α subunits, especially Nav1.1 and Nav1.3. In the *Scn1b*-null hippocampal CA3 region, Nav1.1 expression is decreased, while Nav1.3 expression is increased (Chen, Westenbroek et al. 2004). β2 also modulates VGSC gating and

kinetics in vivo. Acutely isolated *Scn2b*-null hippocampal neurons display a negative shift in the voltage dependence of inactivation in comparison to neurons from age-matched, wild-type mice (Chen, Bharucha et al. 2002). Acutely isolated *Scn2b*-null small-fast DRG neurons have decreased sodium current density and decreased rates of TTX-sensitive sodium current activation and inactivation (Lopez-Santiago, Pertin et al. 2006). Importantly, the β4 intracellular domain is postulated to play a role in resurgent sodium current, or the influx of sodium ions through the ion channel pore during repolarization. β4 knockdown in mouse CGNs showed reduced resurgent sodium current and repetitive firing (Bant and Raman 2010). Furthermore, expression of a β4 intracellular domain peptide in CA3 neurons, which do not endogenously express β4 subunits, generates resurgent sodium current (Grieco, Malhotra et al. 2005). This activity is particularly important in high-frequency firing neurons. *Scn4b*-null mice have defects in sodium current modulation. *Scn4b*-null mice have reduced resurgent sodium current and repetitive firing in medium spiny neurons of the striatum, as well as increased failure rates of inhibitory postsynaptic currents with repetitive stimulation (Miyazaki, Oyama et al. 2014). β1 and β1B are also implicated in regulating resurgent sodium current in the cerebellum, as *Scn1b*-null CGNs have normal transient sodium current, but decreased resurgent sodium current, even though the overall protein expression of β4 is unchanged (Brackenbury, Calhoun et al. 2010). Together, these data indicate that modulation of sodium current by the β subunits in vivo is cell-type-, subcellular domain-, β subunit-, and α subunit-specific.

VGSC β subunits are also important regulators of excitability in the heart. In ventricular cardiomyocytes isolated from *Scn1b*-null mice, transient and persistent sodium currents are

increased due to increased *Scn5a* and Nav1.5 expression, resulting in prolongation of action potential repolarization and the QT interval (Lin, O'Malley et al. 2014); (Lopez-Santiago, Meadows et al. 2007). Furthermore, *Scn1b*-null mice display increased susceptibility to polymorphic ventricular arrhythmias. *Scn1b*-null ventricular cardiomyocytes also have increased tetrodotoxin (TTX)-sensitive sodium current, increased Nav1.3 mRNA levels, increased incidence of delayed after-depolarizations, delayed Ca^{2+} transients, and frequent spontaneous Ca^{2+} release. Addition of TTX prevented the majority of changes in Ca^{2+} handling, indicating mutations in *Scn1b* may result in disrupted intracellular Ca^{2+} homeostasis in ventricular myocytes (Lin, O'Malley et al. 2014). *Scn2b* deletion in mice leads to atrial and ventricular arrhythmias and increased levels of atrial fibrosis. These animals exhibit region-specific effects in heart. *Scn2b*-null ventricular myocytes show reduced sodium and potassium currents, with conduction slowing in the right ventricle compared to wild-type. *Scn2b*-null atria had normal levels of sodium current compared to wild-type (Bao, Willis et al. 2016). *Scn3b*-null mice also show abnormal cardiac excitability, with ventricular tachycardia from electrical stimulation that is not observed in wild-type mice. *Scn3b*-null hearts also demonstrate atrial tachycardia during atrial burst pacing (Hakim, Gurung et al. 2008).

The β subunits as cell adhesion molecules

All five β subunits have an extracellular Ig domain and belong to the Ig superfamily of CAMs (Isom and Catterall 1996). Importantly, β subunits have also been shown experimentally to function as CAMs (Isom 2002). An especially large body of work in this area has been completed

on the β1 subunit. In Drosophila S2 cells expressing either β1 or β2, large aggregates form, suggesting these molecules can participate in trans homophilic cell adhesion in vitro (Malhotra, Kazen-Gillespie et al. 2000). Upon β1-β1 trans homophilic cell adhesion in Drosophila S2 cells, ankyrin is recruited to the point of cell-cell contact (Meadows, Malhotra et al. 2001). Ankyrin binds to the β1 subunit via the intracellular C-terminal domain in a tyrosine phosphorylation-dependent manner. When residue Y181 of β1 is phosphorylated, ankyrin is unbound, while when Y181 is not phosphorylated, ankyrin binds to β1, indicating that downstream signaling events occur in response to cell-cell adhesion (Malhotra, Koopmann et al. 2002). In addition, β1 subunits can form heterophilic interactions with other CAMs, including contactin, N-cadherin, NrCAM, neurofascin-155, neurofascin-186, and the VGSC β2 subunit as well as the extracellular matrix protein, tenascin-R (Fig. 1.3) (Xiao, Ragsdale et al. 1999, McEwen and Isom 2004). β2 subunits can also participate in heterophilic adhesion in vitro with both tenascin-R and tenascin-C (Srinivasan, Schachner et al. 1998, Xiao, Ragsdale et al. 1999). Drosophila S2 cells expressing β3 subunits do not aggregate, suggesting that β3 does not participate in trans homophilic adhesion (McEwen, Chen et al. 2009). In contrast, β3 subunits expressed in HEK cells participate in trans heterophilic adhesion with other CAMs, although this does not result in β3-ankyrin binding (Ratcliffe, Westenbroek et al. 2001, McEwen and Isom 2004, McEwen, Chen et al. 2009). The function of β4 in cell adhesion remains more poorly understood (Brackenbury and Isom 2011). Insights from crystallographic, mutagenic, and photo-crosslinking studies have revealed the structural importance of an antiparallel interface between β4 subunits in trans homophilic adhesion (Shimizu, Miyazaki et al. 2016). Recent evidence shows that β4 Ig domains interact in a parallel

manner involving a disulfide bond between cysteine 58 and hydrophobic and hydrogen bonding interactions between residues 30 through 35. Deletion of the β4 N-terminal domain led to decreased cell adhesion and increased association with the α subunit, revealing the importance of β4 cis dimerization (Shimizu, Tosaki et al. 2017).
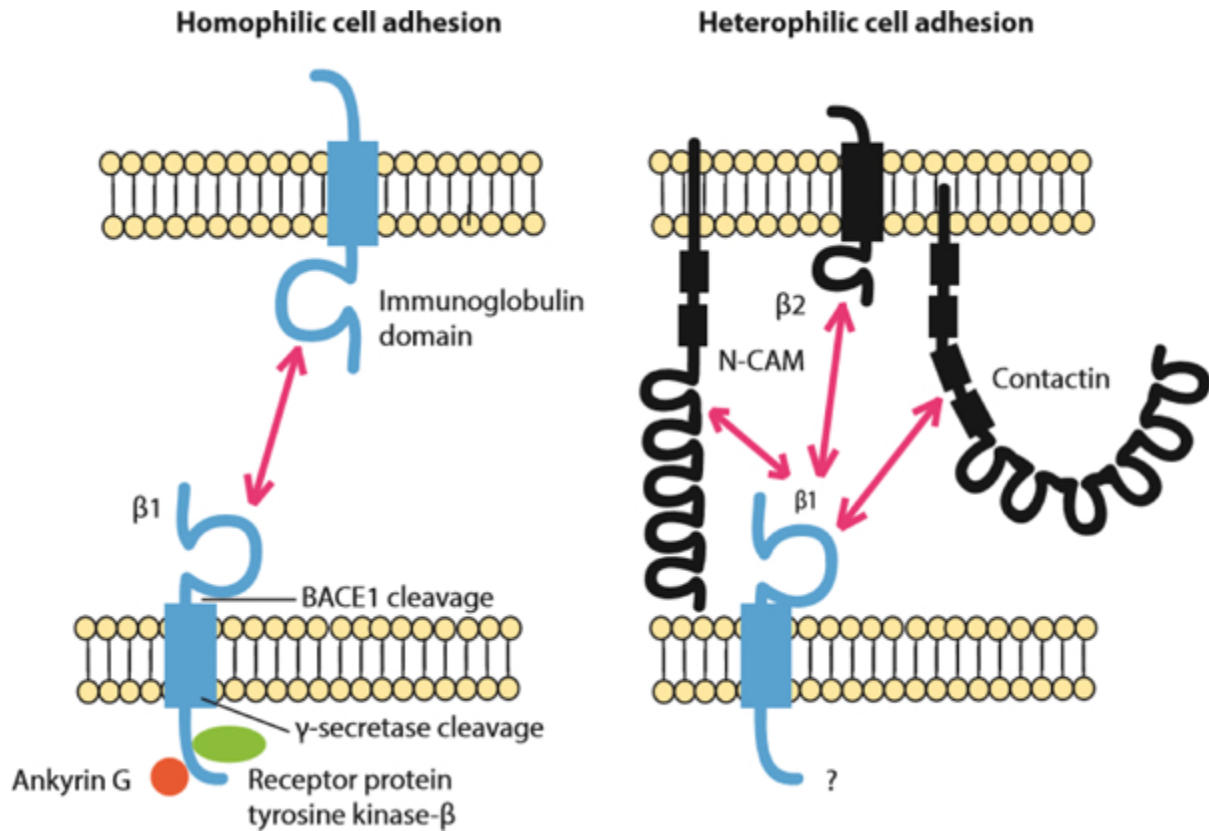
*Figure 1.3: β1 participates in homophilic and heterophilic cell adhesion(Malhotra, Kazen-Gillespie et al. 2000). **Left:** Schematic of β1-β1 homophilic cell adhesion and its downstream signaling. At points of cell-cell contact β1 binds to ankyrin in a phosphorylation-dependent manner. When β1 is not phosphorylated it is bound to ankyrin, while when tyrosine 181 is phosphorylated it is not bound to ankyrin (Malhotra, Kazen-Gillespie et al. 2000, Malhotra, Koopmann et al. 2002). In rat brain β1 interacts with receptor protein tyrosine kinase-β which may contribute to regulating the β1 phosphorylation state (Ratcliffe, Qu et al. 2000). **Right:** β1 participates in heterophilic cell adhesion with N-CAM, VGSC β2 subunits, and contactin.*

Consistent with the role of β1 and β2 in cell adhesion, these molecules have been identified to mediate neurite outgrowth in CGNs (Davis, Chen et al. 2004). In this series of experiments, CGNs were grown on a monolayer of CHL cells that either did, or did not, express β subunit proteins. When β1-β1 trans homophilic cell adhesion occurred between the CGN and the monolayer expressing β1, neurite length was longer than when it did not. In contrast, β2-mediated homophilic adhesion resulted in decreased neurite length while β4 had no effect on this biological output. These data suggest that β1-β1 trans homophilic cell adhesion initiates a signal transduction cascade to drive neurite outgrowth in vitro while β2-mediated signaling may be inhibitory. Cell adhesion-mediated neurite outgrowth has been shown to occur through two downstream pathways: either via an epidermal growth factor receptor (EGFR) or fibroblast growth factor receptor (FGFR) mediated signal transduction cascade, or through the fyn kinase pathway (Brackenbury, Davis et al. 2008). Inhibitors of FGFR and EGFR had no effect on β1-mediated neurite outgrowth in CGNs. In contrast, CGNs isolated from fyn-null mice grown on a CHL monolayer expressing β1 did not show extended neurite length, suggesting that β1-mediated neurite outgrowth signals through a pathway that involves fyn kinase. This hypothesis is further supported by results showing that β1 subunit peptides associate with fyn in detergent-resistant membrane fractions solubilized from mouse brain (Brackenbury, Davis et al. 2008). The proteolytic processing of β1 by BACE1 and γ-secretase is also important for β1-mediated neurite outgrowth, as inhibitors of γ-secretase block β1-mediated neurite outgrowth (Fig. 1.4) (Brackenbury and Isom 2011). The secreted *Scn1b* splice variant, β1B, increases neurite outgrowth to a similar extent as full-length β1 (Patino, Brackenbury et al. 2011)Outside of the central nervous system, the β1 subunit can induce the growth of neurite-

like features from cultured breast cancer cells, suggesting a possible developmental role for β1 in other cell-types (Nelson, Millican-Slater et al. 2014).
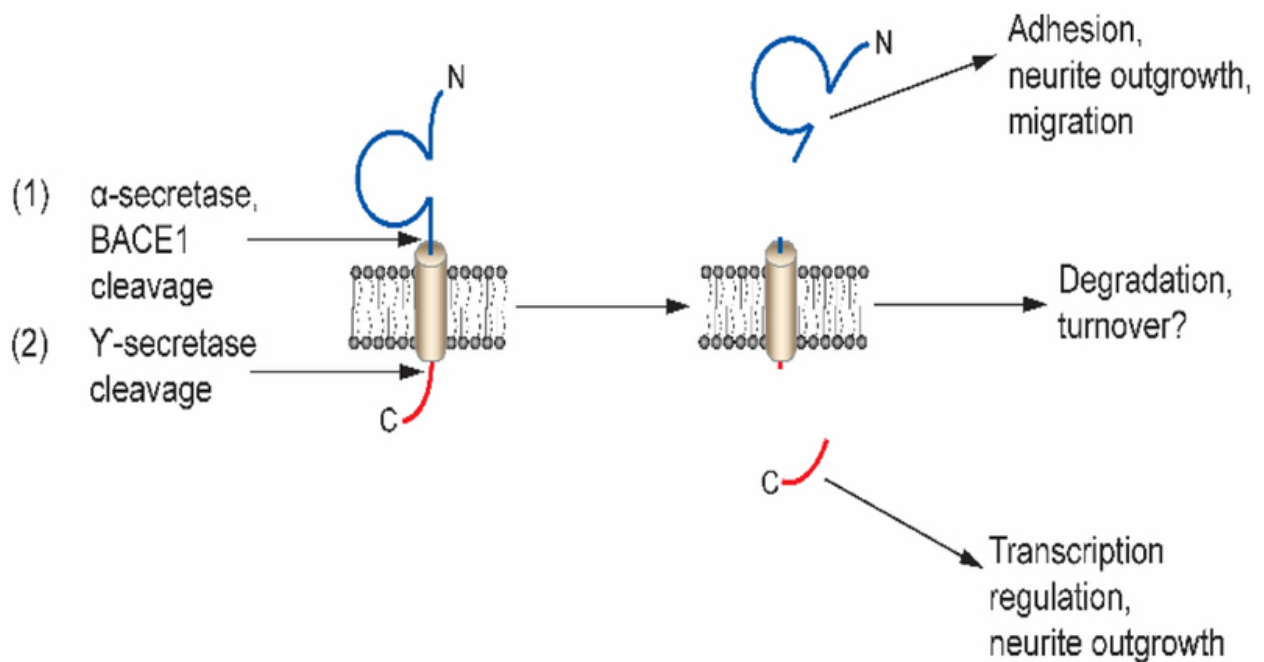
Figure 1.4: β subunits are sequentially cleaved by α-secretase and/or the β-site amyloid precursor protein-cleaving enzyme 1 (BACE1) and subsequently by γ-secretase in the lumen of the membrane. Sequential cleavage generates a soluble extracellular N-terminal domain and intracellular C-terminal domain (Kim, Ingano et al. 2005, Wong, Sakurai et al. 2005). The soluble N-terminal domain participates in cell adhesion and migration, while the intracellular domain modulates neurite outgrowth and, in the case of β2, regulates VGSC gene transcription in vitro (Davis, Chen et al. 2004, Kim, Ingano et al. 2005, Kim, Carey et al. 2007, Miyazaki, Oyama et al. 2007). Figure reproduced from (Brackenbury and Isom 2011).

β1/β1B-mediated cell adhesive activity has been implicated in neuronal development in vivo. In the *Scn1b*-null mouse, there are fewer optic nerve nodes of Ranvier. At the ultrastructural level, optic nerve, spinal cord, and sciatic nerve nodes have abnormal architecture (Chen, Westenbroek et al. 2004). *Scn1b*-null mice also have defects in neuronal pathfinding and fasciculation in multiple brain regions. In normal cerebellum, CGN axons project from the granule layer to the molecular layer, where they form parallel fibers. In the *Scn1b*-null mouse, CGN axons are defasiculated, forming a disrupted molecular layer. Abnormal pathfinding and defasiculation are also observed in the *Scn1b*-null corticospinal tract and hippocampus. In a related model, dendritic arborization of pyramidal neurons in subiculum is reduced in *Scn1b*-C121W mutant animals (Reid, Leaw et al. 2014). The *Scn2b*- and *Scn3b*-null mouse models do not have an apparent neurological phenotype, although *Scn2b*-null mice have increased seizure susceptibility and altered pain sensation (Chen, Bharucha et al. 2002) (Lopez-Santiago, Pertin et al. 2006, Hakim, Gurung et al. 2008, Hakim, Brice et al. 2010) (O'Malley and Isom 2015). CNS abnormalities in the *Scn4b*-null mouse model were recently described. *Scn4b*-null mice display deficits in balance and motor coordination and resurgent sodium current in null Purkinje neurons was reduced by approximately 50 percent. This was further validated using in vivo short hairpin RNA knockdown of β4 in adult Purkinje neurons (Ransdell, Dranoff et al. 2017). Overexpression of the β4 subunit in Neuro2a cells results in increased neurite outgrowth, dendrite formation, and filopodia-like protrusions, suggesting a role for β4 in neuronal pathfinding and migration (Oyama, Miyazaki et al. 2006).

The role of β subunits in pathophysiology

20

Cancer

VGSC β subunits are expressed in prostate, breast, lung, and cervical cancers. This expression is subunit specific and varies by cancer type (Brackenbury 2012). β1 is found in breast, prostate, and cervical cancers, while β2 has been detected in breast and prostate cancers, and β3 in prostate and lung cancers (Chioni, Brackenbury et al. 2009) (Diss, Fraser et al. 2008) (Hernandez-Plata, Ortiz et al. 2012) (Jansson, Lynch et al. 2012) (Roger, Rollin et al. 2007).

β1 and β2 expression levels correspond with metastatic potential in prostate cancer cells (Chioni, Brackenbury et al. 2009) (Jansson, Lynch et al. 2012). Experiments performed in vitro with breast cancer cells have shown that β1 expression enhances cell-cell and cell-substrate adhesion and decreases cell migration (Chioni, Brackenbury et al. 2009). On the other hand, data suggest that β1 contributes to cell invasion during metastasis in breast cancer cells (Chioni, Brackenbury et al. 2009). Overexpression of β1 increases vascular endothelial growth factor secretion and angiogenesis, and decreases apoptosis in endothelial cells (Andrikopoulos, Fraser et al. 2011). β1 overexpression in an orthotopic mouse model of breast cancer increases tumor growth and metastasis (Nelson, Millican-Slater et al. 2014). In the well-defined prostate cancer cell line, LNCaP, β2 overexpression increases cell length, but reduces cell volume, which may result in increased cellular motility and invasion. In a wound healing assay, cells overexpressing β2 migrate farther than controls. To the contrary, over-expression of β2 decreases tumor formation and growth after tumor implantation into nude mice. Furthermore, β2 over-expression enhances invasion and growth on laminin (Jansson, Lynch et al. 2012).

21

Unlike β1 and β2, β3 is postulated to function as a tumor suppressor because its amino acid sequence contains two p53 response elements. In p53-null mouse embryo fibroblasts, *Scn3b* is increased after andriamycin treatment and β3 expression induces p53-dependent apoptosis (Adachi, Toyota et al. 2004). Less is known about the expression of β4 in cancer, although β4 expression levels are lower in cervical and prostate cancer cells in comparison to noncancerous cells (Diss, Fraser et al. 2008) (Hernandez-Plata, Ortiz et al. 2012). β4 co-expression with Nav1.5 has also been shown to play a role in CD4^{+} T cell development (Lo, Donermeyer et al. 2012). These data suggesting roles for VGSC β subunits in cancer indicate that these molecules are important to the functioning of non-excitable, in addition to excitable, cells.

Cardiac arrhythmia

The VGSC β subunits are expressed in the human heart and conduction system. Here, *SCN1B* is expressed at the highest levels in atria and endocardium, while *SCN2B* and *SCN3B* are expressed throughout the human heart (Gaborit, Le Bouter et al. 2007). In mouse ventricular cardiomyocytes, β2, β4, and tyrosine-phosphorylated β1 subunits are expressed at the intercalated disc along with Nav1.5, the predominant heart α subunit, (Maier, Westenbroek et al. 2004) (Malhotra, Thyagarajan et al. 2004). At t-tubules of ventricular cardiomyocytes, β2, β3, and non-phosphorylated β1 are co-expressed with Nav1.1, Nav1.3, and Nav1.6 α subunits (Dhar Malhotra, Chen et al. 2001) (Maier, Westenbroek et al. 2004) (Malhotra, Thyagarajan et al. 2004). Cardiac VGSC β subunits are critical for action potential upstroke, conduction velocity, and excitation-contraction coupling,

suggesting that abnormal expression of β subunits may contribute to cardiac disease states (Remme and Bezzina 2010).

Mutations in genes encoding VGSC β subunits are linked to multiple types of cardiac disease (Bao and Isom), including long QT syndrome (LQTS) (Medeiros-Domingo, Kaku et al. 2007) (Riuro, Campuzano et al. 2014), a ventricular arrhythmia in which there is delayed action potential repolarization, resulting in prolongation of the QT interval on the electrocardiogram. LQTS causes an increased risk of ventricular fibrillation (VF) and sudden cardiac death (Alders and Christiaans 1993). There is now an extensive list of LQTS mutations, including mutations in ion channel genes (Nakano and Shimizu 2016) (Tester and Ackerman 2014). Two mutations, resulting in gain-of-function activity, have been identified in *SCN1B* and *SCN4B*, respectively (Medeiros-Domingo, Kaku et al. 2007) (Nakano and Shimizu 2016) (Riuro, Campuzano et al. 2014), including β1B p.P213T, which results in increased late sodium current and action potential duration, shifted window current, and decreased rate of slow inactivation, and β4 p.L179F, which results in a positive shift in sodium current inactivation causing abnormal action potential repolarization (Riuro, Campuzano et al. 2014) (Medeiros-Domingo, Kaku et al. 2007).

Multiple mutations in *SCN1B* have also been linked to Brugada syndrome (BrS) (Holst, Saber et al. 2012) (Hu, Barajas-Martinez et al. 2012) (Watanabe, Koopmann et al. 2008) (Yuan, Koivumaki et al. 2014). BrS patients have an increased risk of sudden cardiac death due to VF (Watanabe, Koopmann et al. 2008). *SCN1B* mutations are associated with reductions in Nav1.5-generated sodium current density, hyperpolarized voltage-dependence of sodium current

inactivation, and/or alterations in the rate of recovery from inactivation (Watanabe, Koopmann et al. 2008). A missense mutation in *SCN2B*, p.D211G, has been linked to BrS and results in reduced sodium current density by decreasing Nav1.5 cell surface expression (Riuro, Beltran-Alvarez et al. 2013). Mutations in all four of the VGSC β subunit genes are linked to atrial fibrillation (AF) (Li, Wang et al. 2013) (Olesen, Jespersen et al. 2011) (Wang, Yang et al. 2010) (Watanabe, Darbar et al. 2009).

Mouse models lacking individual β subunits show the important roles of these subunits in cardiac function. Cardiac function in *Scn1b*-null mice is altered, even after blocking autonomic input. These animals exhibit action potential depolarization and prolonged QT intervals, suggesting a LQTS phenotype. *Scn1b*-null ventricular myocytes have increased transient and persistent sodium current in comparison to wild-type animals, and an increase in Nav1.5 transcript and protein levels (Lopez-Santiago, Meadows et al. 2007)l. Scn1b-null mice also show increased TTX-sensitive sodium current in the ventricular myocyte midsection, concurrent with increased *Scn3a* mRNA levels. Cardiac-specific Scn1b-null mice also display increased *Scn3a* mRNA, lengthened action potential repolarization, delayed after repolarizations and Ca^{2+} transients, and frequent spontaneous release of Ca^{2+}. Alterations in Ca^{2+} levels were blocked by TTX (Lin, O'Malley et al. 2014). *Scn2b*-null mice exhibit a mixed, Brugada-atrial fibrillation like phenotype. *Scn2b*-null ventricular myocytes have alterations in sodium and potassium current densities, particularly in the right ventricular outflow tract. Similar to *Scn2b*-null brain, total levels of Nav1.5 protein were found to be similar to those from wild-type animals, supporting the hypothesis that a main function of β2 in the ventricle is to chaperone VGSC α subunits to the cell surface without changing overall

channel expression. In contract, *Scn2b*-null atria had normal levels of sodium and potassium currents but increased levels of fibrosis. Lastly, *Scn2b*-null hearts display increased susceptibility to atrial fibrillation and repolarization dispersion compared to wild-type animals (Bao, Willis et al. 2016). *Scn3b*-null mice also show cardiac dysfunction. In both atria and ventricles, *Scn3b*-null mice display an increased susceptibility to arrhythmia, reduced peak sodium current, conduction abnormalities that are similar to Brugada syndrome models, bradycardia, AV block, and deficits in sinoatrial node recovery (Hakim, Gurung et al. 2008). The role of β4 in cardiac function has yet to be reported using the null mouse model.

Epilepsy

Many mutations in VGSC genes have been linked to epilepsies, including *SCN1B* (Kaplan, Isom et al. 2016). There has as yet been no explicit neurological phenotype associated with *SCN3B* and no epilepsy phenotype linked to *SCN4B*. The mutation *SCN1B* p.C121W, identified in a patient with Generalized Epilepsy with Febrile Seizures plus (GEFS+), was one of the first epilepsy mutations ever identified (Wallace, Wang et al. 1998). GEFS+ patients initially experience febrile seizures, which then progress to persistent afebrile seizures (Wallace, Wang et al. 1998). The heterozygous p.C121W knock-in mouse has been shown to model the GEFS+ phenotype (Wimmer, Reid et al. 2010). The p.C121W mutation disrupts a key disulfide bond in the Ig loop (McCormick, Isom et al. 1998) (Wallace, Wang et al. 1998). Although p.C121W traffics appropriately to the plasma membrane and its co-expression increases VGSC α subunit cell surface levels in culture, it is unable to participate in trans-homophilic cell adhesion or modulate sodium

25

current in vitro (Meadows, Malhotra et al. 2002). Studies of p.C121W subcellular localization in cultured neurons showed that, unlike wildtype β1, mutant subunits do not traffic to specialized axonal subdomains including the AIS and nodes of Ranvier. Phenotypically, p.C121W homozygous mice model Dravet syndrome, displaying brain-region specific hyperexcitability, reduced dendritic arborization of pyramidal neurons in the subiculum, and an increased susceptibility to febrile and spontaneous seizures (Wimmer, Reid et al. 2010). Animals that are heterozygous for this mutation are more susceptible to hyperthermia-induced seizures than $Scn1b^{+/-}$ or $Scn1b^{+/+}$ animals. Even though β1-C121W is localized to the cell surface of neurons in vivo, they are incompletely glycosylated and do not interact with α subunits (Kruger and Isom 2016). Additional GEFS+ mutations in *SCN1B*, p.R85C and p.R85H, have also been studied in heterologous cells in vitro (Xu, Thomas et al. 2007). Both mutants have decreased expression compared to wild-type and are unable to modulate α subunits. Although of the two, only p.R85H has been shown to reach the plasma membrane (Patino, Claes et al. 2009) (Xu, Thomas et al. 2007).

The *Scn1b*-null mouse line is a model of Dravet Syndrome (DS), and mutations in *Scn1b* are linked to DS (Chen, Westenbroek et al. 2004) (Patino, Claes et al. 2009), a severe and intractable pediatric epileptic encephalopathy that typically presents within the first year of life with myoclonic seizures that can change etiology over time. DS patients also suffer from a variety of comorbidities including ataxia, behavioral and developmental delay, and a high risk of sudden unexpected death in epilepsy, or SUDEP (Gataullina and Dulac 2017). DS mutations in *SCN1B* are homozygous recessive. The first DS mutation identified in *SCN1B* was p.R125C. This mutation has abnormal

trafficking and does not reach the cell surface in vitro, resulting in a functional null phenotype (Patino, Claes et al. 2009). An additional *SCN1B* DS mutations, p.I106F, was later identified, although the mechanism underlying this mutation remains unknown (Ogiwara, Nakayama et al. 2012). Scn1b-null mice further validate the role of β1 in DS. These animals have frequent spontaneous seizures and abnormal neuronal excitability and development, consistent with that observed in DS patients (Chen, Westenbroek et al. 2004). In addition, *Scn1b*-null mice die at ~P 21, and are thus a SUDEP model.

Heterozygous mutations in *SCN1B* have been linked to a variety of other epilepsies. These include p.R85C, p.R85H, p.R125L, and an in-frame deletion mutation (Fendri-Kriaa, Kammoun et al. 2011) (Scheffer, Harkin et al. 2007) (Wallace, Wang et al. 1998). One mutation that is specific to the developmentally regulated splice variant, β1B, has also been identified, p.G257R, and is linked to idiopathic epilepsy in multiple pedigrees. In vitro, this mutation also has defects in membrane trafficking (Patino, Brackenbury et al. 2011). Except for this mutation specific to β1B, all epilepsy-linked mutations in *SCN1B* code for amino acids in the Ig loop domain, suggesting the clinical relevance of cell adhesion in the pathogenesis of epilepsy.

Scn2b-null mice express approximately half of normal levels of cell surface TTX-sensitive VGSCs in brain. These animals are also more prone to pharmacologically induced seizures compared to wild-type animals (Chen, Bharucha et al. 2002). Additionally, a polymorphism in *SCN2B* (rs2298771) has been associated with idiopathic epilepsy (Baum, Haerian et al. 2014). In conclusion, the β1 and β2 subunits play critical roles in epilepsy.

Neurodegenerative disorders

β subunits have been implicated in neurodegenerative disorders including amyotrophic lateral sclerosis (ALS), Alzheimer's Disease (AD), Huntington's disease (HD), Multiple Sclerosis (MS), and Parkinson's disease (PD) (Calhoun and Isom 2014) (O'Malley and Isom 2015). ALS is characterized by the degeneration of motor neurons in the spinal cord, motor cortex, and brainstem (Al-Chalabi, van den Berg et al. 2017). Differential gene expression of *Scn1b* and *Scn3b* have been observed in the Sod1 mouse model of ALS. Scn1b mRNA and protein are decreased, while there is increased *Scn3b* mRNA and protein in ventral dorsal horn. Neuronal hyperexcitability is found in ALS, thus, alterations in the expression of *Scn1b* and *Scn3b*, as well as the changes reported in the expression of Nav1.6, may explain hyperexcitability in ALS patients (Nutini, Spalloni et al. 2011).

Like that of the Amyloid Precursor Protein (APP), most famously known for its potential implications in AD, β subunits are substrates for sequential cleavage by β-site APP cleaving enzyme-1 (BACE1) and γ-secretase, potentially linking the β subunits to AD (Wong, Sakurai et al. 2005). In AD pathology, APP is initially cleaved on the extracellular portion of the membrane by BACE1 and then subsequently cleaved in the lumen of the membrane by γ-secretase, generating the amyloid β (Aβ) peptide. Aβ then accumulates and forms amyloid plaques. BACE1 is ubiquitously expressed throughout the body, but is expressed at highest levels in the pancreas and brain (Cole and Vassar 2007). The expression of BACE1 increases with age in the cortex of AD patients (Evin, Barakat et al. 2010). Interestingly, AD patients are at increased risk of seizures,

further supporting a potential role of VGSCs in AD (Pandis and Scarmeas 2012). BACE1 cleavage of β2 reverses normal β2 modulation of VGSC β subunits. In BACE1-null mice, decreased cleavage of β2 (or possibly other BACE1 substrates, including other VGSC β subunits) may contribute to the increased neuronal excitability observed in AD patients (Kim, Gersbacher et al. 2011). In addition, *SCN3B* mRNA is lower in AD brains with neurofibrillary tangles (NFTs), another pathological issue displayed in some AD cases, suggesting β subunits may be implicated in the formation of NFTs and hyperexcitability in AD (Dunckley, Beach et al. 2006).

β2 and β4 have been linked to HD, a genetic, neurodegenerative disease that affects motor coordination and mental ability. Ultimately, many of these patients lose their ability to walk and/or talk. In HD patient postmortem brain samples, *SCN4B* is downregulated in the striatum. This is mimicked in mouse models, where it has been shown to occur prior to loss of motor coordination. In vitro, β4 overexpression is implicated in neuronal development, suggesting that in HD, β4 dysregulation may contribute to neural degeneration. A decrease in β2 expression is also observed in the same mouse model of HD, but later in the pathogenesis of disease than observed for *Scn4b* (Oyama, Miyazaki et al. 2006).

Although *Scn2b*-null mice have normal myelination, at least in the optic nerve, deletion of *Scn2b* is neuroprotective in the Experimental Allergic Encephalomyelitis (EAE) model of MS. Interestingly, *Scn2b* deletion in the EAE mouse model leads to decreased axonal degeneration, fewer demyelinated and dysmyelinated axons, reduced phenotypic severity, and increased survival (O'Malley, Shreiner et al. 2009). β2 may also be implicated in MS through sequential cleavage by

BACE1 and γ-secretase. In cerebrospinal fluid from MS patients, there is decreased BACE1 activity and this biomarker in MS is linked to a more severe and prolonged disease state. Throughout MS progression, BACE1 expression continues to decline (Mattsson, Axelsson et al. 2009).

VGSC β1 subunits are also implicated in maintaining normal myelination. *Scn1b*-null mice phenotypically display abnormal optic nerve myelination, spinal cord dysmyelination, increased axonal degeneration, fewer optic nerve nodes of Ranvier, and defects in nodal ultrastructure in both the central and peripheral nervous systems. Loss of β1 expression, and thus adhesion, at nodes of Ranvier leads to abnormalities in the formation of paranodal junctions, suggesting β1 contributes to myelination (Chen, Westenbroek et al. 2004).

Increased expression and glycosylation of the VGSC β4 subunit compared to wild-type animals has been identified in a mouse model of PD. Studies of neurite outgrowth in response to expression of WT vs. mutant β4 that could not be glycosylated showed that neurite outgrowth was accelerated, with an increased level of filopdia-like protrusions. Thus, the glycosylation state of β4 may be critical for neuronal morphology and may be involved in PD pathogenesis (Zhou, Zhang et al. 2012). Overall, β subunits contribute to myelination and neurodegenerative disease states through a variety of mechanisms.

Neuropathic pain

A variety of factors can cause neuropathic pain, including genetic mutations and nerve injury. This leads to defects in nociception, the neuronal pathways implicated in sensing noxious stimuli. The

VGSC β subunits are expressed in dorsal root ganglion (DRG) neurons and peripheral nerves, suggesting potential roles for these proteins in neuropathic pain (Lopez-Santiago, Pertin et al. 2006). Behavioral pain phenotypes are difficult, if not impossible, to study in *Scn1b*-null mice due to their severe seizures and early post-natal death (Chen, Westenbroek et al. 2004). In spite of this, *Scn1b*-null DRG neurons are hyperexcitable, suggesting that these mice may have some form of allodynia (Lopez-Santiago, Brackenbury et al. 2011). On the other hand, *Scn1b* mRNA levels are increased in a model of chronic constrictive nerve injury, complicating the interpretation of the role of β1 in neuropathic pain (Blackburn-Munro and Fleetwood-Walker 1999).

Studies examining the role of β2 in neuropathic pain have also led to conflicting results. While *Scn2b*-null mice are less sensitive than wild-type littermates in models of inflammatory and neuropathic pain, β2 protein levels are increased in injured and non-injured wild-type neurons in spared nerve injury and spinal nerve ligation models in rat (Lopez-Santiago, Pertin et al. 2006) (Pertin, Ji et al. 2005). The latter occurs without a corresponding increase in mRNA levels (Pertin, Ji et al. 2005). Lastly, *Scn2b* mRNA levels are downregulated in cervical sensory ganglia after avulsion injury, but increased in a model of chronic constrictive nerve injury (Blackburn-Munro and Fleetwood-Walker 1999) (Coward, Jowett et al. 2001).

Scn3b mRNA expression is increased in multiple pain models, including in small C-fibers, in a chronic constrictive injury model in rats, in Aδ fibers in the streptozotocin model of diabetic neuropathy in rat, in the small and medium fibers in the sciatic nerve transection model, and finally, in the spared nerve injury model of neuropathic pain suggesting *Scn3b* may play a role in

modulating pain (Shah, Stevens et al. 2000, Shah, Stevens et al. 2001) (Takahashi, Kikuchi et al. 2003).

Although there are little data to directly implicate β4 in pain, the C-terminal portion of β4 plays a role in generating resurgent sodium current in DRG neurons (Grieco, Malhotra et al. 2005). Paroxysmal Extreme Pain Disorder (PEPD) is an inherited neuropathic pain syndrome linked to gain-of-function mutations in *SCN9A*, encoding Nav1.7. When PEPD-linked Nav1.7 mutants are co-expressed with the C-terminal β4 peptide, differential enhancement of resurgent current is observed, suggesting a potential role for β4 in pain (Theile, Jarecki et al. 2011). In all, the β subunits contribute to pain phenotypes in a cell-type and subunit-specific manner.

Sudden Infant Death Syndrome (SIDS) and Sudden unexpected death in epilepsy (SUDEP)

Sudden Infant Death Syndrome, or SIDS, is the unexpected death of a child up to one year of age where a clear cause of death cannot be identified via autopsy (Krous, Beckwith et al. 2004). The mechanism of SIDS remains to be elucidated, but one out of ten cases is associated with cardiac ion channel gene mutations, including in genes encoding the β subunits (Van Norstrand and Ackerman 2009). p.V36M and p.V54G mutations in *SCN3B* and p.S206L in *SCN4B* have been linked to SIDS (Tan, Pundi et al. 2010). Importantly, p.V36M in *SCN3B* has also been linked to idiopathic ventricular fibrillation, a potential fatal cardiac arrhythmia, and p.S206L in *SCN4B* also leads to abnormal excitability in rat ventricular myocytes (Tan, Pundi et al. 2010) (Valdivia, Medeiros-Domingo et al. 2010). There has been one instance of SIDS in a child with a p.R214Q in β1B, which has also been associated with Brugada Syndrome (Hu, Barajas-Martinez et al.

2012). β1B modulates Nav1.5 function, potentially providing an underlying mechanism for *SCN1B* linked cardiac dysfunction (Patino, Brackenbury et al. 2011). To date, no mutations in *SCN2B* have been linked to SIDS.

Some ion channel genes that have been linked to SIDS have also been linked to Sudden Unexpected Death in EPilepsy (SUDEP). SUDEP is defined as the sudden and unexpected death of a person with epilepsy without any identifiable cause of death during autopsy (Nashef, So et al. 2012). SUDEP occurs in up to 17% of epileptic patients and those diagnosed with Dravet syndrome (DS) are at an especially high risk for SUDEP (Ficker, So et al. 1998). Seizures that are difficult to treat by pharmacological intervention are also associated with increased SUDEP risk (Hesdorffer, Tomson et al. 2012). Currently, there are no reliable biomarkers for SUDEP, but it is likely that death is initiated by dysfunction in multiple organ systems, including autonomic dysfunction, cardiac arrhythmia, central or obstructive apnea, hypoventilation, and pulmonary edema (Surges and Sander 2012). Several types of cardiac events are known to occur during or after seizure activity in epilepsy patients. These include asystole, atrial fibrillation, bradycardia, tachycardia, and T-wave alterations (Jansen and Lagae 2010). Epileptic activity may affect the autonomic nervous system, which is known to be a critical regulator of cardiac function. Dysregulation of the autonomic nervous system and spreading depression to the brain stem centers during an epileptic event can result in fatal cardiac abnormalities (Jansen and Lagae 2010) (Massey, Sowers et al. 2014) (Surges and Sander 2012).

Multiple DS and epilepsy animal models also serve as models for SUDEP, including the previously discussed *Scn1b*-null mouse line (Chen, Westenbroek et al. 2004). Additional models include Scn1a$^{+/-}$ mice, which model the haploinsufficiency observed in most DS patients, and the *Kcna1*-null mouse line, which deletes the voltage-gated potassium channel Kv1.1 (Glasscock, Yoo et al. 2010) (Oakley, Kalume et al. 2011). Intriguingly, each of these SUDEP models presents with different cardiac alterations that may mechanistically contribute to SUDEP. *Scn1b*-null mice display increased cardiac sodium current and prolonged QT and RR intervals. *Scn1b*-null mice treated with atropine or propranolol do not show differences in QT interval compared to vehicle treated animals, indicating the cardiac phenotype may not be a result of an abnormal autonomic activity (Lopez-Santiago, Meadows et al. 2007). *Scn1a*$^{+/-}$ mice also display increased cardiac sodium current, but additionally have bradycardia, focal discharges, a variable RR interval, and bundle branch block (Auerbach, Jones et al. 2013) (Kalume, Westenbroek et al. 2013). *Kcna1*-null mice display a cardiac phenotype as well, including atrioventricular (AV) block, bradycardia, premature ventricular contractions and altered heart rate variability (Glasscock, Yoo et al. 2010). Contrary to *Scn1b*-null mice, treatment of *Scn1a*$^{+/-}$ and *Kcna1*-null animals with atropine reverses AV block, suggesting parasympathetic hyperexcitability in these models (Glasscock, Yoo et al. 2010) (Kalume, Westenbroek et al. 2013). In summary, studies with animal models and patient mutations provide evidence that β subunits are likely key regulators in the pathogenesis of SIDS and SUDEP, although additional work must be completed to further understand and ultimately prevent SIDS and SUDEP events.
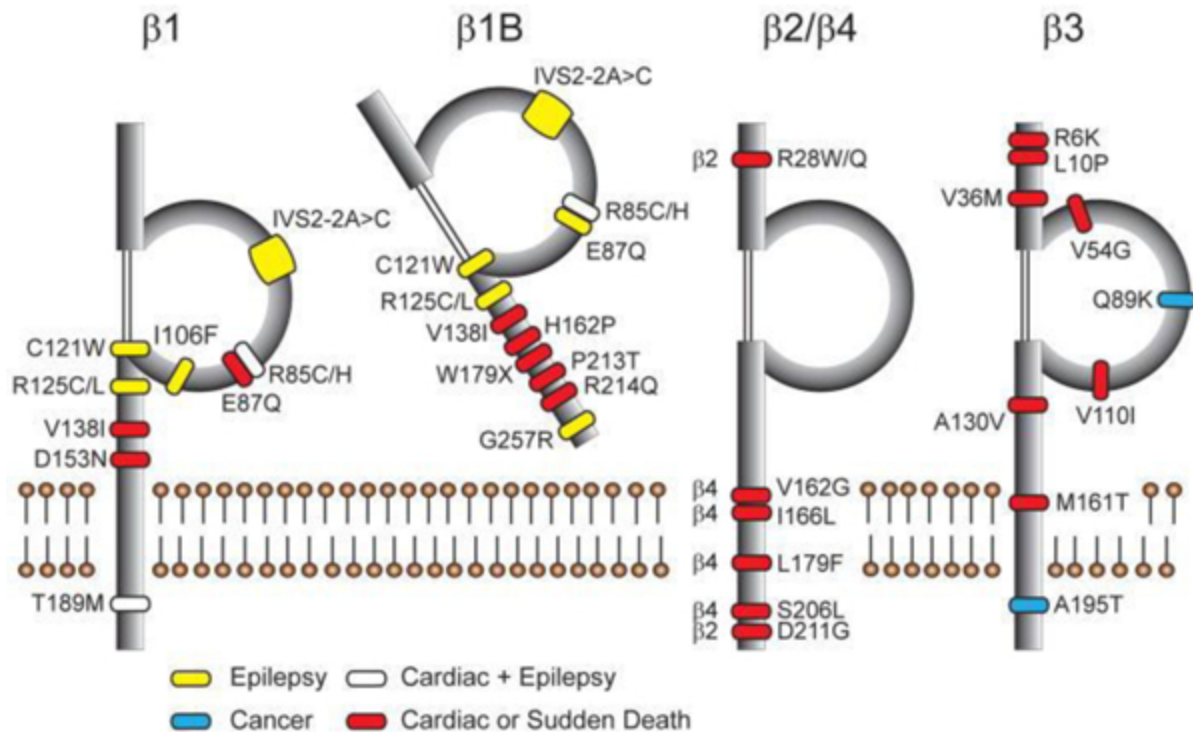
Figure 1.5: Disease-linked β subunit mutations. Figure reproduced from (O'Malley and Isom 2015).

Regulated Intramembrane Proteolysis (RIP)

Transmembrane spanning β subunits are substrates for sequential cleavage by BACE1 and γ-secretase, a process also referred to as Regulated Intramembrane Proteolysis (RIP) (Fig. 1.6). RIP of transmembrane-spanning proteins has been identified over the last 20 years as an essential cellular process which is conserved from mammalian cells down to unicellular organisms (Lal and Caplan 2011). Like more classic examples of transmembrane signaling, such as receptor-dependent signaling, RIP permits transmission of information across cellular compartments (Lal and Caplan 2011). The family of proteases that catalyze RIP are integral membrane proteins called intramembrane Cleaving Proteases (iCLiPs) (Wolfe, De Los Angeles et al. 1999). iCLiP catalytic residues are located within the hydrophobic environment of the membrane. This group of proteins can be divided into three conserved families: aspartyl proteases, zinc metalloproteinase site-2 proteases, and serine proteases (Lemberg and Freeman 2007, Spasic and Annaert 2008). For many iCLiPs, initial cleavage of the substrate by an ectodomain sheddase, or secretase, is required. Ectodomain shedding occurs at a peptide bond near the transmembrane surface. Ectodomain shedding is carried out by either proteases of the integrin and metalloprotease (ADAM) family, matrix metalloproteases, or the aspartyl proteases, β-site APP cleaving enzymes (BACE) (Lal and Caplan 2011). Initial cleavage by an ectodomain sheddase is required to prime the substrate for subsequent cleavage by an iCLiP. Sequential cleavage by first, an ectodomain sheddase, and subsequently by an iCLiP, results in the generation of a liberated protein domain (LPD) capable of intercellular signaling (Haapasalo and Kovacs 2011, Lal and Caplan 2011). Susbstrate LPDs

generated by these sequential cleavage events may signal within the nucleus, cytosol, or extracellular space depending on the particular characteristics and orientation in the membrane of each individual substrate LPD (Haapasalo and Kovacs 2011, Lal and Caplan 2011). Here, we will focus on ectodomain sheddase, BACE1, and iCLiP, γ-secretase, as these enzymes were identified to sequentially process VGSC β subunits (Wong, Sakurai et al. 2005).
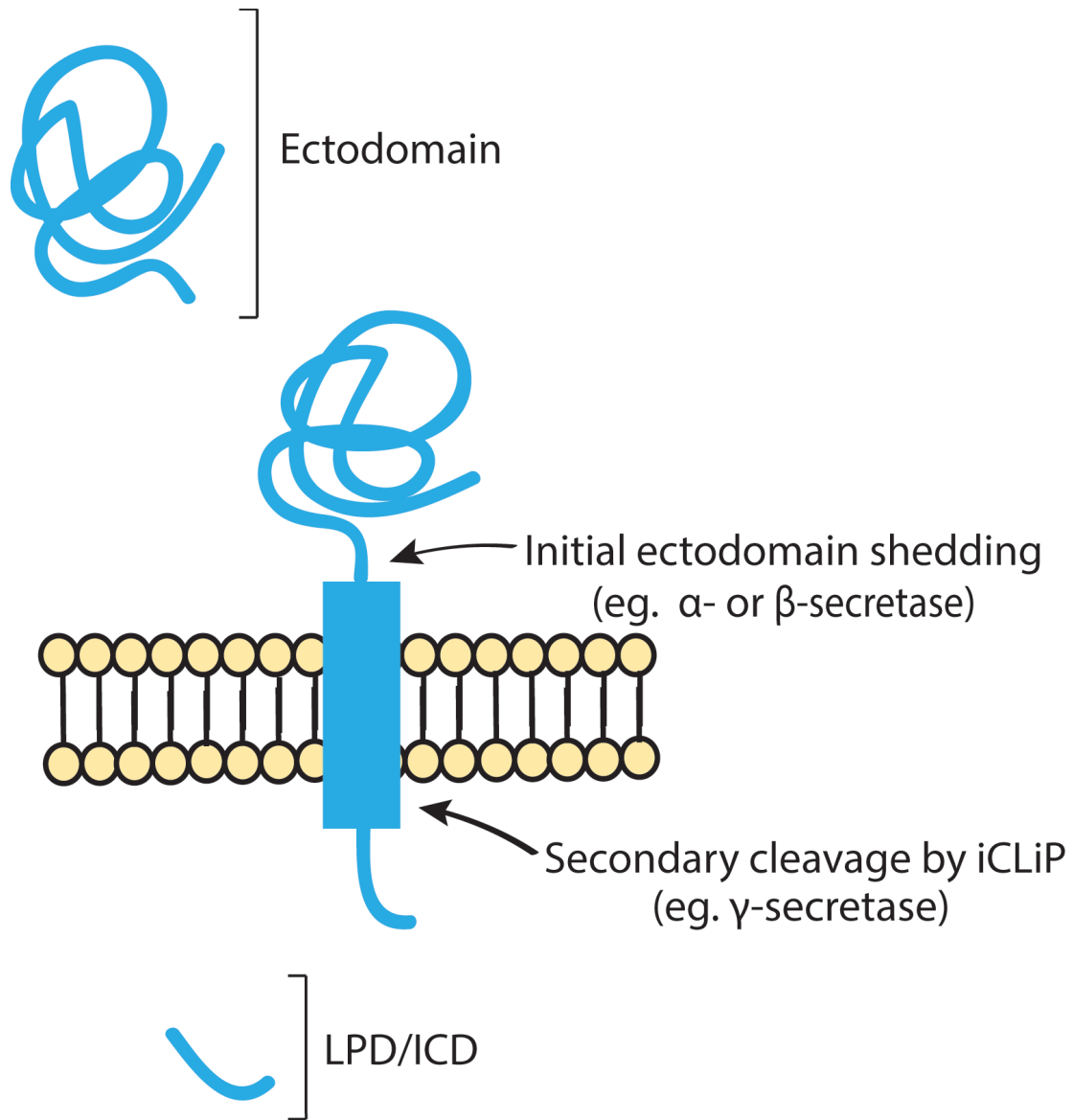
Figure 1.6: Cartoon diagram of RIP.

BACE1

Ectodomain shedding cleaves membrane protein substrates near or within the transmembrane domain, releasing a soluble extracellular domain (ectodomain) from a fragment that remains in the membrane (Lichtenthaler, Lemberg et al. 2018). The freed ectodomain often signals to other nearby cells. For many substrates of sheddase, or secretase, activity, the remaining fragment is further proteolytically processed by an iCLiP (Lichtenthaler, Haass et al. 2011, Lichtenthaler, Lemberg et al. 2018). BACE1 is a type-I transmembrane aspartyl-protease that assembles as a homodimer and functions as an ectodomain sheddase, or secretase (Vassar, Bennett et al. 1999, Hemming, Elias et al. 2009). Originally identified as the enzyme responsible for processing APP to generate Aβ, proteomic studies have now identified greater than 40 substrates of BACE1, many of which are involved in contact-dependent intracellular communication or serve as receptors (Vassar, Bennett et al. 1999, Hemming, Elias et al. 2009). Thus far, all known BACE1 substrates are transmembrane proteins, the vast majority of which are of type-I topology. BACE1 has loose substrate specificity that does not obey strict cleavage recognition motifs. Many of the identified substrates are yet to be examined under physiological conditions and the functional consequence of their cleavage by BACE1 remains undetermined. Of the sheddase substrates that have been studied, shedding can have multiple biological outputs. These include providing a mechanism to terminate the function of a full-length membrane protein, to release a biologically active substrate ectodomain to activate a membrane protein, or to induce further processing by an iCLiP (Hemming, Elias et al. 2009, Lichtenthaler, Lemberg et al. 2018).

BACE1 enzymatic activity plays important roles in numerous physiological functions (Yan 2017). These include astrogenesis (Hu, He et al. 2013), neurogenesis (Morrison, Perez et al. 2000, Breunig, Silbereis et al. 2007, Hu, He et al. 2013), myelination and remyelination (Hu, Hicks et al. 2006, Willem, Garratt et al. 2006, Hu, Fan et al. 2016), neuronal excitability (Wong, Sakurai et al. 2005, Kim, Carey et al. 2007, Sachse, Kim et al. 2013, Agsten, Hessler et al. 2015), muscle spindle activity (Cheret, Willem et al. 2013), axonal growth and neuronal migration (Rajapaksha, Eimer et al. 2011, Cao, Rickenbacher et al. 2012, Hitt, Riordan et al. 2012, Barao, Gartner et al. 2015), and synaptic function (Wang, Song et al. 2008, Mei and Nave 2014, Wang, Megill et al. 2014, Yan, Fan et al. 2016). Unsurprisingly, dysregulation or loss of BACE1 leads to aberrant progression of the aforementioned physiological processes, which may contribute to BACE1-linked disease onset and/or progression, such as Alzheimer's disease (AD). In addition to AD, BACE1 activity is linked to epilepsy and retinopathy. BACE1-null mice display spontaneous convulsive seizure activity. Epileptic activity begins early in life in BACE1-null mice and becomes more frequent with age (Kobayashi, Zeller et al. 2008, Hitt, Jaramillo et al. 2010, Hu, Zhou et al. 2010). Although the mechanism of how BACE1 deletion leads to seizure activity is unknown, cleavage of ion-channel subunits by BACE1 may contribute (Wong, Sakurai et al. 2005, Kim, Carey et al. 2007, Kim, Gersbacher et al. 2011, Sachse, Kim et al. 2013, Agsten, Hessler et al. 2015). Additional work has linked BACE1 activity to retinopathy, although conflicting results have been reported. BACE1 deletion in mice, as well as the administration of multiple BACE1 inhibitors, cause retinal thinning (Cai, Qi et al. 2012, Fielden, Werner et al. 2015). Some studies have linked BACE1 to retinal thinning via a mechanism mediated by vascular endothelial growth

factor receptor (VEGFR1) cleavage (Fielden, Werner et al. 2015). More recent work has shown that retinopathy from BACE1 inhibition is due to off-target inhibition of cathepsin D (Zuhl, Nolan et al. 2016). Furthermore, BACE1-null rats and some lines of BACE1-null mice do not show a retinopathy phenotype (Fielden, Werner et al. 2015). Additional work must be completed to determine whether BACE1 is directly implicated in these physiological processes and disease states or if aberrant processing of specific BACE1 substrates is the causative mechanism.

γ-secretase

γ-secretase comprises a protein complex of presenilin-1 (PS1) or presenilin-2 (PS2), nicastrin, anterior pharynx defective-1 (Aph-1), and presenilin enhancer-2 (Pen-2). These four proteins (in 1:1:1:1 stoichiometry) are necessary and sufficient to form functional γ-secretase (Edbauer, Winkler et al. 2003, Selkoe and Wolfe 2007, Spasic and Annaert 2008). PS contains the aspartyl-protease catalytic site of γ-secretase. The precise contributions of the remaining three components of the γ-secretase complex to function are still under debate, but aid in forming the mature enzyme (Haapasalo and Kovacs 2011). Substrates of γ-secretase, although diverse in structure, localization, and function, share some uniting characteristics. Most γ-secretase substrates are type-I transmembrane proteins with a large ectodomain that often contains CAM-like domains (Haapasalo and Kovacs 2011). Furthermore, the substrates typically contain a single-pass transmembrane domain and a cytoplasmic C-terminus that can mediate intracellular signaling (Haapasalo and Kovacs 2011). γ-secretase substrate proteins tend to function in cell signaling related to cell fate determination, adhesion, migration, neurite outgrowth, axon guidance, or the

formation and/or maintenance of synapses (Spasic and Annaert 2008). γ-secretase preferentially cleaves membrane-bound protein stubs generated after ectodomain shedding of the full-length substrate by an α- and/or β-secretase. Initial ectodomain shedding may occur constitutively or when induced by a stimulus (Haapasalo and Kovacs 2011). Although γ-secretase cleavage is not dependent on a specific amino acid sequence, cleavage occurs at or near the boundary of the transmembrane and cytoplasmic domains, typically flanking a stretch of hydrophobic amino acid sequence rich in positively charged residues (Spasic and Annaert 2008). Rather than sequence-specificity, it appears that substrate recognition is dependent on the conformational state of the transmembrane domain. Ultimately, cleavage by γ-secretase releases the intracellular domain (ICD) of the substrate protein. Of the studied substrate ICDs, several translocate to the nucleus where they are thought to play a role in modulating transcription. Generation of the ICD can be prevented by inhibition of γ-secretase by pharmacological inhibitors or lack of functional γ-secretase, resulting in an accumulation of the substrate C-terminal fragment left in the membrane after ectodomain shedding (Haapasalo and Kovacs 2011). Substrate ICDs are highly labile and often accumulate in the presence of protease inhibitors, suggesting the proteasome, at least in part, contributes to ICD degradation (Kopan and Ilagan 2004, Lal and Caplan 2011).

γ-secretase activity is implicated in a number of physiological processes, including maintenance and proliferation of neural stem cells, regulation of cell fate, regulation of cell death, axon guidance, neurite outgrowth, cell adhesion, spine maturation, synaptogenesis, angiogenesis, and tumorigenesis (Paris, Quadros et al. 2005, Haapasalo and Kovacs 2011). Many of these are

mediated through γ-secretase cleavage of its numerous substrates (Haapasalo and Kovacs 2011).

Due to its important and wide-spanning roles in biological processes, variants in γ-secretase itself

or its substrates are associated with pathophysiological conditions. Most widely known, variants

in *PSEN,* which encodes the catalytic subunit of γ-secretase, are linked to Familial Alzhiemer's

Disease (FAD) (Wolfe 2019). FAD-linked *PSEN* variants increase the ratio of Aβ towards the

amyloidogenic form, Aβ42, or increase the total amount of total Aβ produced (Chavez-Gutierrez,

Bammens et al. 2012). Work examining the genetic basis of Hidradenitis Suppurativa (HS), a

debilitating and chronic inflammatory skin condition, identified heterozygous variants in γ-

secretase genes, *PSEN1, PSENEN,* and *NCSTN,* in a small set of HS patients. The resulting variant

mRNAs, although not examined experimentally, are predicted to undergo nonsense-mediated

decay (Pink, Simpson et al. 2013). Variants in Notch, a well characterized γ-secretase substrate,

have been linked to T-cell lymphoblast and leukemia (TLL) (Aster, Blacklow et al. 2011). These

variants can alter Notch processing by γ-secretase or lead to nuclear accumulation of the Notch-

ICD (NICD) generated by RIP (Chadwick, Zeef et al. 2009, Aster, Blacklow et al. 2011, Bray and

Gomez-Lamarca 2018). Other substrate variants have not been examined, but, like BACE1,

dysregulation of substrate cleavage by γ-secretase may lead to abnormal function and

subsequently, disease.

Conclusion

In conclusion, VGSC β subunits play critical roles in modulating the gating, localization, and kinetics of the VGSC pore as well as modulate the activities of some potassium channels (O'Malley and Isom 2015). In addition, these non-pore-forming proteins function as CAMs and signaling molecules in both excitable and non-excitable cell types (O'Malley and Isom 2015). Their importance as CAMs is implicated in neurite outgrowth, axonal pathfinding and fasciculation, and migration in cancerous cells (Malhotra, Kazen-Gillespie et al. 2000, Brackenbury, Calhoun et al. 2010, Brackenbury and Isom 2011, Brackenbury 2012). β subunits are also substrates for sequential cleavage by BACE and γ-secretase (Wong, Sakurai et al. 2005). Variants in the genes encoding β subunits are linked to a variety of devastating diseases, including epilepsy, SIDS and SUDEP, cancer, neuropathic pain, and some of the major neurodegenerative disorders (Fig. 1.5) (Calhoun and Isom 2014). Additional research needs to be completed in order to further understand the biology of these critical proteins and their potential as novel therapeutic targets for a wide variety of disease states. The overall goal of the work described in this thesis is to further understand the mechanisms regulating and downstream signaling of β1 processing by BACE1 and γ-secretase.

Chapter 2 VGSC β1 Subunit Processing by BACE1 and γ-secretase Regulates Excitability by Ion Channel Gene Transcription

Alexandra A. Bouza, Nnamdi Edokobi, Alexa M. Pinsky, James Offord, PhD, Lin Piao, MD, PhD, Anatoli N. Lopatin, PhD, Luis F. Lopez-Santiago, PhD, and Lori L. Isom, PhD

Summary

Loss-of-function variants in *SCN1B,* encoding voltage-gated sodium channel (VGSC) β1 subunits, are linked to human diseases that carry a high risk of sudden death, including epileptic encephalopathy and cardiac arrhythmia. β1 subunits modulate the cell-surface localization, gating, and kinetics of VGSC pore-forming α subunits. They also participate in cell-cell and cell-matrix adhesion, resulting in intracellular signal transduction, promotion of cell migration, calcium handling, and regulation of cell morphology. Here, we show that, in addition to their known functions in channel modulation and cell adhesion at the plasma membrane, β1 subunits are substrates for sequential regulated intramembrane proteolysis (RIP) by BACE1 and γ-secretase, resulting in the generation of a soluble intracellular domain (ICD) that is translocated to the nucleus. Using an unbiased, RNA-seq approach, we identified a subset of genes that are downregulated by β1-ICD overexpression in heterologous cells but upregulated in *Scn1b* null cardiac tissue which, by definition, lacks β1-ICD signaling, suggesting that the β1-ICD may normally function as a molecular break on gene transcription *in vivo*. We propose that human disease variants resulting in *SCN1B* loss-of-function cause transcriptional dysregulation that

contributes to altered excitability. These results provide important new insights into the mechanism of *SCN1B*-linked channelopathies, adding RIP-excitation coupling to the multi-functionality of VGSC β 1 subunits.

Introduction

Loss-of-function (LOF) variants in *SCN1B,* encoding voltage-gated sodium channel (VGSC) β1 subunits, are linked to human diseases that carry a high risk of sudden death, including early infantile epileptic encephalopathy type 52 (EIEE52, OMIM 617350), Brugada Syndrome 5 (OMIM 612838), and Atrial Fibrillation Familial 13 (OMIM 615377). β1 subunits are type one transmembrane proteins containing a single, extracellular V-type immunoglobulin (Ig) domain, making them part of the Ig-superfamily of cell adhesion molecules (CAMs) (O'Malley and Isom 2015, Bouza and Isom 2018). β1 subunits are multifunctional proteins. In addition to their canonical roles in modulating the cell-surface localization, gating, and kinetics of VGSC pore-forming, α subunits (Isom, De Jongh et al. 1992, Isom, Scheuer et al. 1995), β1 subunits modulate voltage-gated potassium currents and participate in cell-cell and cell-matrix adhesion as CAMs (Isom and Catterall 1996, Malhotra, Kazen-Gillespie et al. 2000, Deschenes and Tomaselli 2002, Nguyen, Miyazaki et al. 2012). *Scn1b* null mice, which model EIEE52 and have cardiac arrhythmia, have cell type specific alterations in sodium current (Lopez-Santiago, Meadows et al. 2007, Brackenbury, Calhoun et al. 2010, Lopez-Santiago, Brackenbury et al. 2011, Lin, O'Malley et al. 2015), multiple deficits in neuronal migration and pathfinding in the cerebellum (Brackenbury, Yuan et al. 2013), fewer nodes of Ranvier in the optic nerve (Chen, Westenbroek et al. 2004), aberrant neuronal pathfinding and fasciculation in the corticospinal tract (Brackenbury, Davis et al. 2008), delayed maturation of GABAergic signaling in brain (Yuan, O'Malley et al. 2019), abnormal formation of cardiac intercalated discs (Veeraraghavan, Hoeker

et al. 2018), and altered calcium signaling in cardiac ventricular myocytes (Lin, O'Malley et al. 2015). Finally, VGSC β1 subunits are essential for life: *Scn1b* null mice have severe seizures, ataxia, and cardiac arrhythmia, with 100% mortality by postnatal day (P) 21 (Chen, Westenbroek et al. 2004, Lopez-Santiago, Meadows et al. 2007).

Previous work by others showed that β1 subunits undergo regulated intramembrane proteolysis (RIP) through sequential cleavage by the β-site Amyloid Precursor Protein (APP) cleaving enzyme-1 (BACE1) and γ-secretase (Wong, Sakurai et al. 2005). Initial cleavage by BACE1 sheds the β1 Ig domain, which our laboratory previously showed functions as a ligand for cell adhesion, and leaves the β1-C-termnial fragment (β1-CTF) in the membrane (Davis, Chen et al. 2004, Patino, Brackenbury et al. 2011). Initial cleavage by BACE1 was reported to be the rate-limiting step in β1 RIP. γ-secretase subsequently cleaves the remaining β1-CTF in the lumen of the membrane, generating a soluble intracellular domain (β1-ICD) (Fig. 2.1B) (Wong, Sakurai et al. 2005).

Although typically studied as neuronal enzymes, BACE1 and γ-secretase are expressed ubiquitously throughout the body and have been shown to play important roles in other tissues. For example, in cardiac myocytes, KCNE1, which assembles with KCNQ1 channels to generate delayed-rectifier potassium current, is a BACE1 substrate (Sachse, Kim et al. 2013, Agsten, Hessler et al. 2015). Atrial cardiomyocytes isolated from *BACE1* null mice show a decrease in total steady-state potassium current (Agsten, Hessler et al. 2015). Lastly, presenilins, the catalytic component of the γ-secretase complex, have been implicated in degradation of the ryanodine

receptor in cardiomyocytes (Pedrozo, Torrealba et al. 2013). BACE1 and γ-secretase also play roles in cancer. For example, inhibitors of γ-secretase inhibit growth of human glioblastoma as well as human lung adenocarcinoma tumors xenografted into nude mice (Paris, Quadros et al. 2005, Li, Chen et al. 2011, Pedrozo, Torrealba et al. 2013, Sachse, Kim et al. 2013, Chen, Liu et al. 2016).

Evidence from other BACE1 and γ-secretase substrates suggests that ICDs generated by RIP are translocated to the cell nucleus where they modulate transcription (Kim, Carey et al. 2007, Haapasalo and Kovacs 2011). Based on this evidence, we proposed that the β1-ICD may participate in transcriptional regulation *in vivo* and that the absence of β1 intramembrane cleavage and downstream signaling may contribute to disease mechanisms in patients with LOF *SCN1B* variants. Thus, the goal of this study was to test the hypothesis that the β1-ICD couples membrane excitability as a VGSC subunit to transcriptional regulation (RIP-excitation coupling). Using an unbiased RNA-seq approach, we identified multiple gene pathways that are downregulated by β1-ICD overexpression in heterologous cells. Due to our previous work showing the important role of *Scn1b* in cardiac physiology, we also performed RNA-seq to examine gene expression profiling in mouse cardiac ventricle isolated from P10 *Scn1b* wild-type (WT) vs. *Scn1b* null animals, in which the β1-ICD signaling pathway is deleted. In general, we found that the gene groups that were downregulated by β1-ICD overexpression in heterologous cells were upregulated in *Scn1b* null cardiac ventricle, suggesting that the β1-ICD may normally act as molecular break on gene expression in heart. We showed that the observed transcriptional upregulation of potassium

channel gene expression translates to increased potassium currents in *Scn1b* null cardiac myocytes. Finally, we showed that calcium current is decreased in *Scn1b* null ventricular myocytes, consistent with alterations in calcium ion binding proteins and calcium channel modulatory proteins identified by RNA-seq experiments. Taken together, our work identifies a novel VGSC β1-mediated signal transduction cascade in heart with physiological implications for the regulation of normal development as well as pathology. The absence of β1 intramembrane cleavage and downstream signaling, as modeled by *Scn1b* null mice, may contribute to cardiac disease mechanisms in patients with *SCN1B* LOF variants.

Results

β1 is sequentially cleaved by BACE1 and γ-secretase in vitro.

We used stably transfected Chinese Hamster Lung (CHL) fibroblasts to confirm previous results identifying β1 as a substrate for RIP by BACE1 and γ-secretase, as well as to establish a model system to study downstream signaling from β1 cleavage (Fig. 2.1 A and B) (Wong, Sakurai et al. 2005). CHL cells are optimal for this work because they do not express endogenous VGSC β1 subunit mRNA (Isom, Scheuer et al. 1995), but do express low levels of both BACE1 and γ-secretase (Fig. 2.1C). We generated a bicistronic, full-length WT VGSC β1 subunit cDNA expression vector containing a C-terminal V5 epitope tag, a cleaving 2A sequence, and enhanced Green Fluorescent Protein (eGFP) to establish a stable β1-V5-2AeGFP-CHL cell line. Western blot analysis of cell lysates revealed an immunoreactive band at ~37 kDa, the expected molecular weight (MW) of full-length β1. An additional band was present at ~20 kDa, consistent with the previously identified apparent MW of the β1-CTF that remains in the membrane following initial cleavage by BACE1 (Fig. 2.1D) (Wong, Sakurai et al. 2005). To determine if the ~20 kDa fragment was the β1-CTF, β1-V5-2AeGFP-CHL cells were treated with vehicle (0.1% DMSO) or increasing concentrations (50 nM to 1000 nM) of the γ-secretase inhibitor, DAPT (Wong, Sakurai et al. 2005, Kim, Carey et al. 2007). If the ~20 kDa fragment were indeed the β1-CTF, DAPT would block the second cleavage event by γ-secretase leading to an accumulation of the intermediary cleavage product produced by BACE1, β1-CTF, in the membrane. DAPT treatment

resulted in a concentration-dependent accumulation of the 20 kDa fragment, suggesting that this band represented β1-CTF, which would have been subsequently processed by γ-secretase in the absence of drug (Fig. 2.1 E and F).

To determine if initial β1 cleavage was the result of BACE1 activity, rather than activity of another protease, e.g. an α-secretase, β1-V5-2AeGFP-CHL cells were treated with vehicle (0.1% DMSO), 1000 nM DAPT, or 200 nM of β-secretase inhibitor IV (BSI) (Kim, Carey et al. 2007), varying the order of addition. Treatment of cells with 200 nM BSI alone did not alter the level of β1-CTF, as assessed by western blot. Instead, treatment with DAPT was required to detect differences in the amount of β1-CTF generated. Co-administration of BSI plus DAPT resulted in a significant decrease in the level of β1-CTF generated in comparison to DAPT treatment alone. Treatment with DAPT seven hours prior to BSI treatment did not change the amount of β1-CTF generated. Taken together, these results suggest that RIP of β1 occurs sequentially, with initial cleavage by BACE1 (Fig. 2.1 G and H). The data presented in Fig. 2.1 strengthen previous evidence showing that β1 is a substrate for sequential cleavage by BACE1, which generates the β1-CTF, followed by γ-secretase, generating the β1-ICD.

A VGSC α subunit — Trans homophilic adhesion — Outside / Inside — Na+ — β1 — ICD — Fyn — BACE1 and γ-secretase — Differential localization & Neurite outgrowth — Transcription — Nucleus — ?

B BACE1 cleavage site (initial cleavage) — β1-CTF — γ-secretase cleavage site — β1-ICD — β1 — ICD

C Mouse heart / CHL — 70 kDa — IB: BACE1 — 55 kDa / 35 kDa / 25 kDa — FL Presenilin 1 — IB: Presenilin 1 — CTF Presenilin 1 — 15 kDa

D CHL / CHL β1 — 36 kDa — FL β1 — IB: β1-intra — β1-CTF — 17 kDa — 55 kDa — IB: α-tubulin

E WT β1: − + + + + + + ; DAPT (nM): − DMSO 50 100 200 500 1000 — 36 kDa — FL β1 — IB: V5 — 17 kDa — β1-CTF — 55 kDa — IB: α-tubulin

F Relative β1-CTF intensity (normalized to vehicle) — DMSO, 50 nM DAPT, 100 nM DAPT, 200 nM DAPT, 500 nM DAPT, 1000 nM DAPT — * — p=0.05

G UT / WTβ1 — 0.1% DMSO / 200 nM BSI / 1 uM DAPT — +1 +2 / +2 +1 — 36 kDa — FL β1 — IB: V5 — 17 kDa — β1-CTF — 90 kDa — IB: HSP90 — +1 drug added first — +2 drug added second

H Relative β1-CTF intensity (normalized to vehicle) — No Tx, 0.1% DMSO, BSI, DAPT, BSI first, DAPT first, BSI/DAPT — ** ** * ns ns *

53

Figure 2.1 β1 subunits are substrates for BACE1 and γ-secretase intramembrane cleavage. A. Cartoon diagram of the proposed β1-mediated signal transduction cascade. B. Schematic of β1 with BACE1 and γ-secretase cleavage sites. C. Chinese Hamster Lung (CHL) cells stably expressing WT β1-V5 also endogenously express BACE1 and presenilin-1, the catalytic subunit of γ-secretase. D. WT β1-V5 is cleaved by BACE1 and the β1-C-terminal fragment (β1-CTF) is found in the membrane fraction. E. Treatment with γ-secretase inhibitor, DAPT, leads to a concentration-dependent accumulation of β1-CTF. F. Quantification of E. Protein levels were normalized to the loading control and reported as fold change respective to the vehicle treated group. Significance (p-value <0.05) was determined using a one-way ANOVA between each treatment and the negative control (vehicle treatment). G. Scheduled treatments with DAPT and β-secretase inhibitor IV inhibit formation of respective cleavage products in a manner consistent with sequential cleavage. H. Quantification of G. Protein levels were normalized to the loading control and reported as fold change respective to the vehicle treated group. Significance (p-value <0.05) was determined using a one-way ANOVA between each treatment and the positive control (DAPT treatment alone). Data are represented as the mean ± SEM.

The β1 ICD localizes to the nucleus.

To determine if the β1-ICD localizes to the nucleus, similar to other substrates of intramembrane sequential BACE1 and γ-secretase cleavage, we cloned and transiently expressed WT β1-V5 or β1-ICD-V5 in CHL cells (Haapasalo and Kovacs 2011). Immunofluorescence staining with anti-V5 showed that, unlike full-length β1-V5, for which there was little nuclear staining, approximately 50% of the expressed β1-ICD-V5 localized to the nucleus of CHL cells, as quantified by Pearson's correlation coefficient for colocalization with DAPI (Fig. 2.2 A and B).
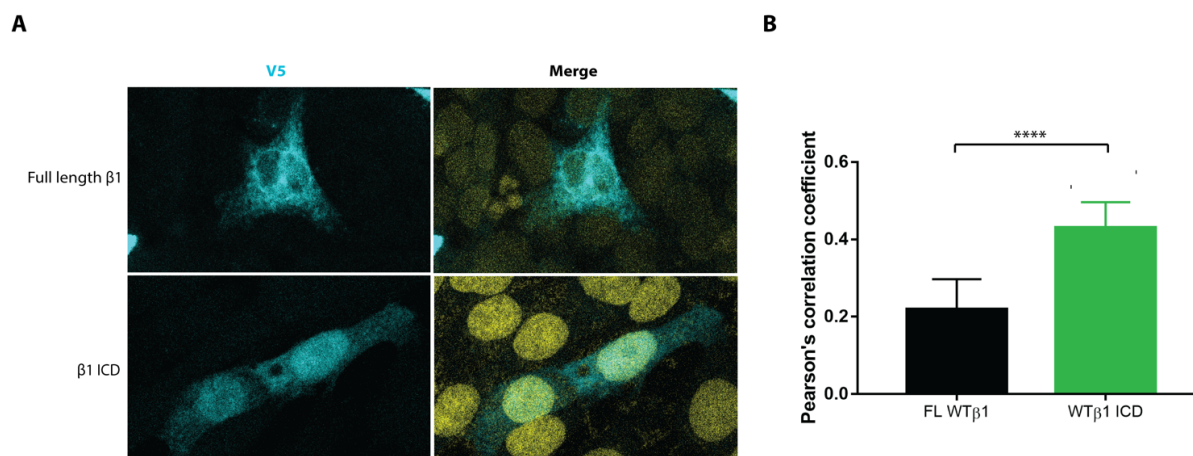
Figure 2.2: β1-ICD-V5 localizes to the nucleus. A. Full-length WT β1-V5 shows little to no nuclear localization, as determined by staining for the V5-epitope tag and DAPI. Strong colocalization is observed between staining for the V5-epitope tag of the β1-ICD and the nucleus (DAPI, yellow). B. Staining for the V5-epitope tag for β1-p.Y181A-V5, β1-p.Y181F-V5, and β1-p.Y181E-V5 colocalizes with the nucleus. C. Quantification of intensity of V5 and DAPI staining across the transfected cell. Average data from 11-17 cells per condition is shown. Data are represented as the mean ± SD.

β1-ICD overexpression in CHL cells leads to differential expression of VGSC genes.

After identifying the β1-ICD in the nucleus, a key question was to determine whether the β1-ICD can modulate transcription. To investigate this problem, we generated CHL cell lines which stably overexpressed either eGFP or β1-ICD-V52A-eGFP (Fig. 2.3 A and B). Paired-end RNA-Seq was performed on each cell line as fee-for-service at the University of Michigan Sequencing Core. Data were normalized and differential expression analysis was performed with DESeq2 as fee-for-service by the University of Michigan Bioinformatics Core. Samples grouped according to genotype by principal component analysis (PCA) (Supplemental Fig. 2.2A). 1,396 genes were found to be differentially expressed in the β1-ICD line compared to the eGFP-only control line. Interestingly, of the genes identified using this unbiased approach, three VGSC genes were identified as differentially expressed: *Scn3a* was downregulated in the β1-ICD overexpressing line compared to the control line, while both *Scn4a* and *Scn5a* were upregulated compared to the control line (Fig. 2.3C). RT-qPCR experiments confirmed these alterations in VGSC gene expression in the presence of the β1-ICD (Fig. 2.3D).

To ask whether the observed changes in VGSC transcription resulted in detectable changes in sodium current (I_{Na}), we overexpressed β1-ICD-V5-2A-eGFP or eGFP in Human Embryonic Kidney (HEK) cells using transient transfection and tested for I_{Na} using whole cell voltage clamp ~24 hours later (Fig. 2.4 β A). Four independent experiments were performed per condition. No

significant differences in I_{Na} density were observed in cells expressing the β1-ICD compared to control. We next transiently transfected cells that already expressed I_{Na}, HEK-Na$_v$1.5 cells, with eGFP (negative control), WT β1-V5-2A-eGFP (positive control), or β1-ICD-V5-2A-eGFP to ask whether β1-ICD expression could change I_{Na} density. eGFP positive cells were analyzed by whole cell patch clamp 24 hours post-transfection. Four independent experiments were performed per condition. Co-expression of the β1-ICD with Na$_v$1.5 did not significantly change I_{Na} density or the voltage-dependence of I_{Na} activation or inactivation compared to eGFP alone. Taken together, these results suggest that the combined β1-ICD-driven up- and down-regulation of VGSC α subunit gene expression may not be sufficient to change whole cells I_{Na} density in heterologous cells (Supplemental Fig. 2.1 B-E). Nevertheless, our previous *in vivo* work showing that *Scn1b* deletion results in upregulation of *Scn3a* and *Scn5a/*Nav1.5 expression and increased I_{Na} in cardiac myocytes is consistent with the idea that the β1-ICD regulates these genes (Lopez-Santiago, Meadows et al. 2007, Lin, O'Malley et al. 2015). However, the extent and direction of this regulation (up or down) may be cell type specific and/or developmentally regulated.

In addition to their nuclear functions, some ICDs play local roles at their site of cleavage (Lee and Ch'ng 2020). To test whether acute application of the β1-ICD could modulate I_{Na} directly, we applied a synthetic β1-ICD peptide (β1$_{183-218}$) through the patch pipet during whole cell voltage clamp recording of HEK-Nav1.5 cells. No significant differences in I_{Na} density or in the voltage-

dependence of activation or inactivation were observed with the addition of the peptide (Table 2.1

and 2.2).
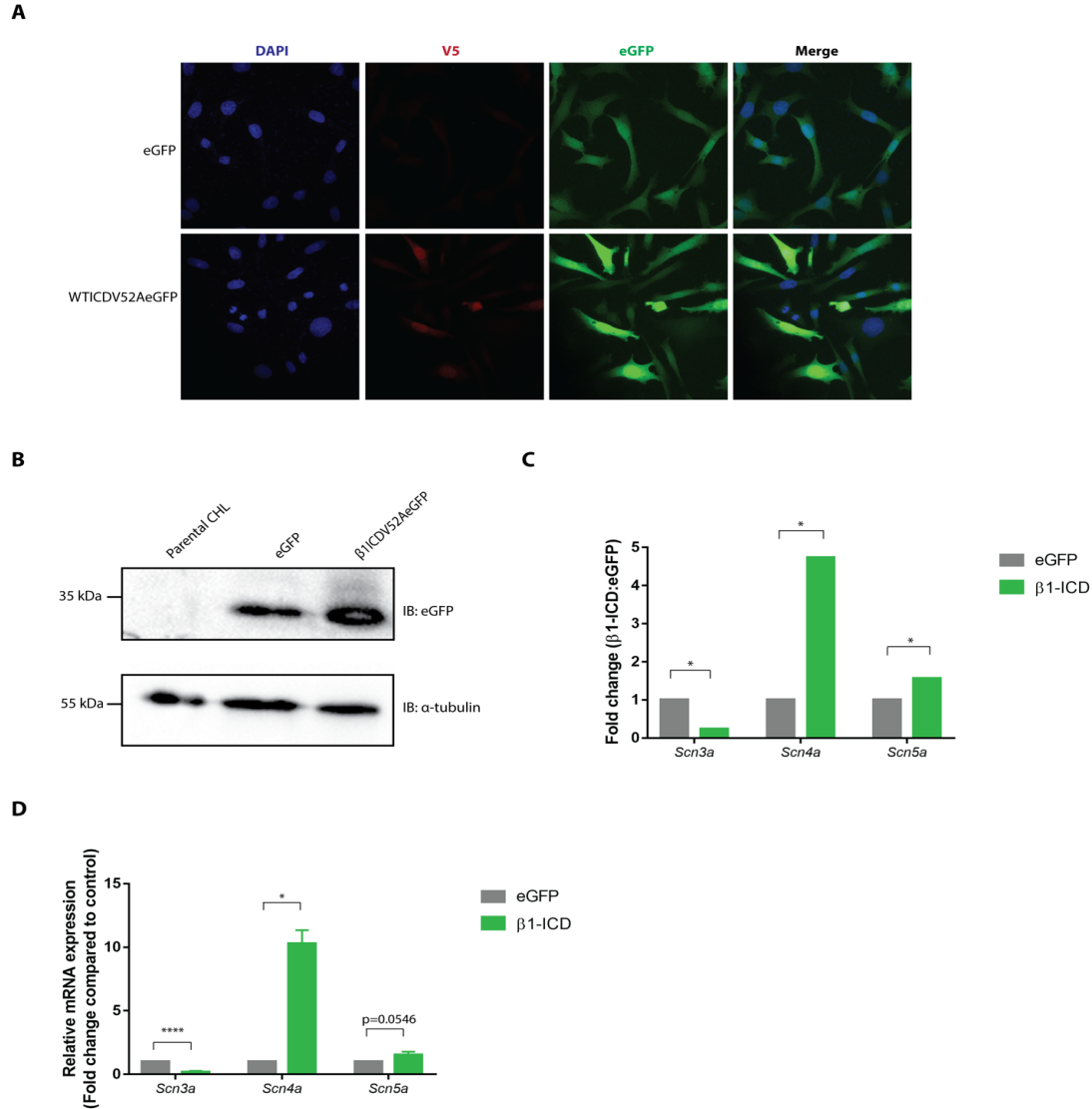
Figure 2.3: Expression of the β1-ICD alters VGSC gene expression. A. Immunocytochemistry for V5 for eGFP stable line and wild-type β1-ICDV52AeGFP stable line. DAPI in blue, eGFP in green, and V5 in red. B. Immunoblot (anti-GFP) of CHL cells stably overexpressing eGFP only or wild-type β1-ICD with a V5 epitope tag and a 2A-eGFP sequence on the 3' end. C. VGSC genes are differentially expressed in presence of β1-ICD compared to control. D. qPCR confirms some VGSC genes are differentially expressed in the presence of β1-ICD compared to control. Data represented as the mean ± SEM.
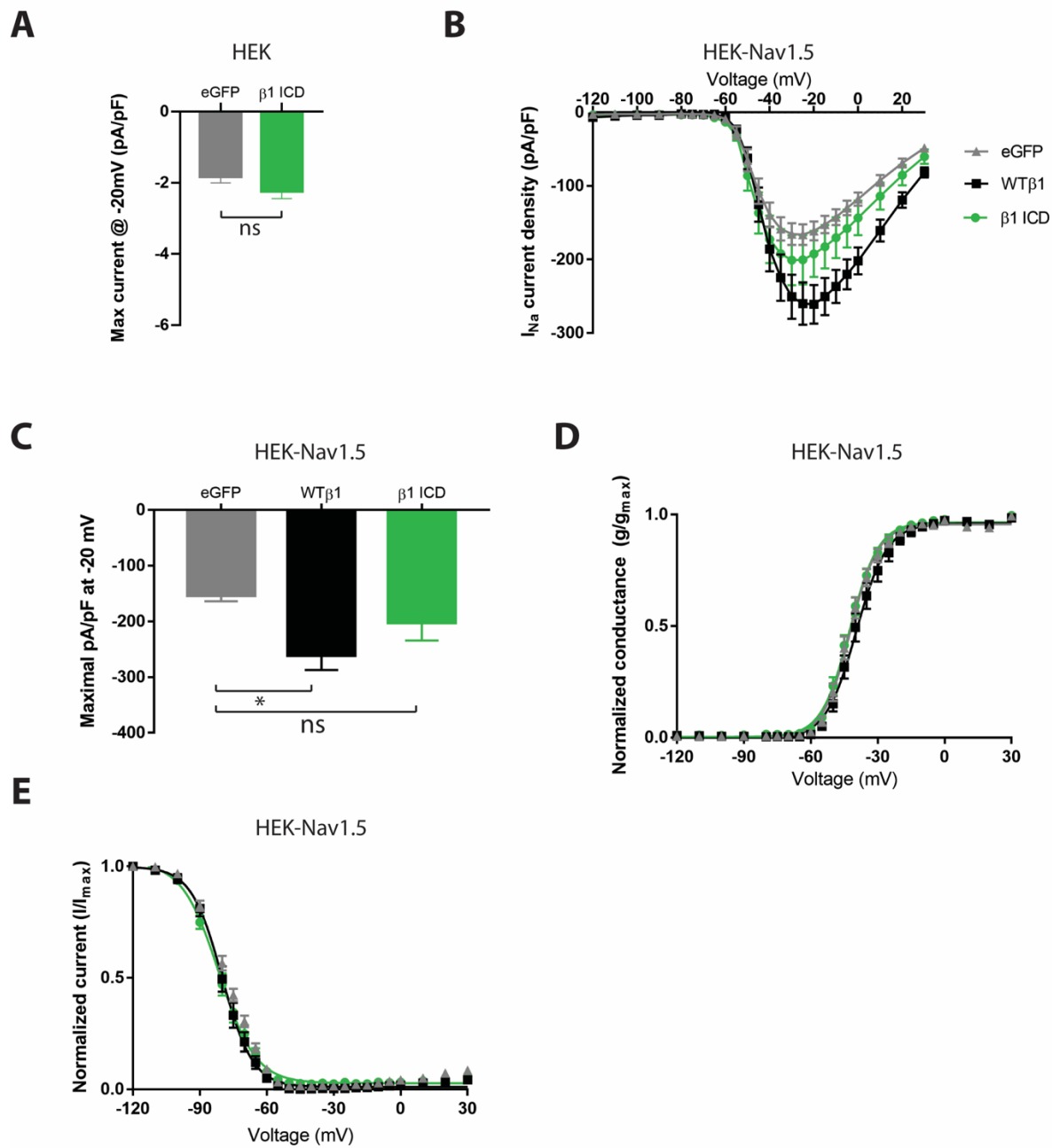
Supplemental Fig. 2.1: β1-ICD has no effect on sodium current in heterologous cells. A. Expression of βl-ICD-V5-2Ae-GFP does not increase INa density in parental HEK cells compared to control, eGFP-only. N=3, n=12-17 per condition. B. INa density is increased when

WT β1-V5-2A-eGFP is co-expressed with Nav1.5 compared to eGFP-only control. Co-expression with β1-ICD-V5-2A-eGFP does not increase INa density compared to eGFP-only control. C. Maximal current is increased when WT β1-V5-2A-eGFP, but not β1-ICD-V5-2A-eGFP, is co-expressed with Nav1.5 compared to eGFP control. D. Co-expression of WT β1-V5-2A-eGFP or β1-ICD-V5-2A-eGFP has no effect on the voltage-dependence of INa activation compared to eGFP control. E. Co-expression of WT β1-V5-2A-eGFP or β1-ICD-V5-2A-eGFP has no effect on the voltage-dependence of INa inactivation compared to eGFP control. N=3, n=10-24 per condition.

	Transient I_{Na} density (pA/pF)	Persistent I_{Na} density (pA/pF)
hNa$_v$1.5 alone	-156.8±30.2	-0.9±0.2
hNa$_v$1.5+ICB peptide	-177.6±29.5	-0.6±0.2

Table 2.1: βl-ICD peptide has no effect on Na$_v$1.5 transient or persistent sodium current density.

	Voltage dependence						
	Activation Curve			**Inactivation Curve**			**n**
	G$_{max}$ (nS)	***k (mV)***	**V$_{1/2}$ (mV)**	***h* (mV)**	**V$_{1/2}$ (mV)**	**C**	
hNa$_v$1.5 alone	1.95±0.42	6.56±0.47	-42.7±1.6	-9.25±0.42	-88.7±4.6	0.02±0.005	8
hNa$_v$1.5+ICD peptide	2.16±0.32	5.87±0.31	-44.2±1.1	-9.05±0.35	-85.9±2.2	0.02±0.003	10

Table 2.2: βl-ICD peptide has no effect on Na$_v$1.5 voltage-dependence of activation or inactivation.

Yin-Yang of gene expression changes

Gene Ontology (GO) analysis revealed groups of genes that were changed by overexpression of the β1-ICD via RNA seq (Fig. 2.4A and Supplemental Figure 2.3). The primary sets of genes differentially expressed included, but were not limited to, those involved in cell adhesion, the immune response, cellular proliferation, and calcium ion binding. (Fig. 2.4B, left). To determine whether the expression of any of these sets of genes was also modulated in an excitable tissue that is known to normally express *Scn1b*, and for which *Scn1b* LOF is critical to disease mechanisms, we performed a second RNA-Seq experiment from P10 *Scn1b* WT and null mouse cardiac ventricle (Fig. 2.4A). We chose P10 because this developmental time point is prior to disease onset in *Scn1b* null mice, and thus uncomplicated by possible secondary effects of epilepsy (Yuan, O'Malley et al. 2019). Paired-end RNA-Seq, normalization of data, and differential expression analysis with DESeq2 were performed as above. Samples grouped according to genotype by PCA (Supplemental Fig. 2.2B). 696 genes were found to be differentially expressed between *Scn1b* WT and null tissues. Although some of these changes in gene expression may be compensatory to deletion of the full-length β1 protein, rather than solely to the absence of the β1-ICD, we hypothesized that those which changed in a manner consistent with genes altered by overexpression of the β1-ICD may result from the loss of this novel signaling pathway. GO analysis revealed many similar groups of differentially expressed genes as in the CHL cell experiment, including genes in the immune response, proliferation, and calcium ion binding pathways (Fig. 2.4B, right). Importantly, in heterologous cells where the β1-ICD was overexpressed, the majority of these gene groups were downregulated. In contrast, where the β1-

64

ICD was deleted (*Scn1b* null cardiac tissue), these same gene groups were generally upregulated (Fig. 2.4C-G). Taken together, these data suggest that the β1-ICD may normally participate in gene suppression *in vivo*. In contrast to our previous work showing increased *Scn3a* and *Scn5a* expression at P14-17 in *Scn1b*-null hearts (Lopez-Santiago, Meadows et al. 2007, Lin, O'Malley et al. 2015), the present RNA-seq results showed no changes in VGSC gene expression at P10. Thus, *Scn1b* deletion may lead to developmentally regulated changes in VGSC α subunit expression in heart (Lopez-Santiago, Meadows et al. 2007, Lin, O'Malley et al. 2014).
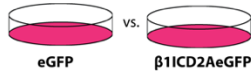
66
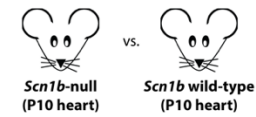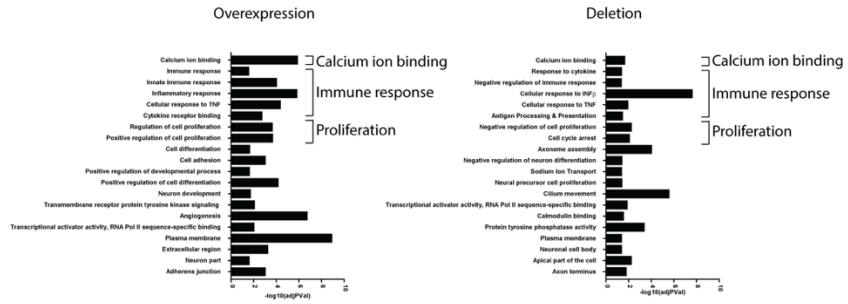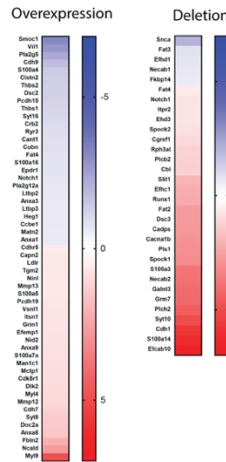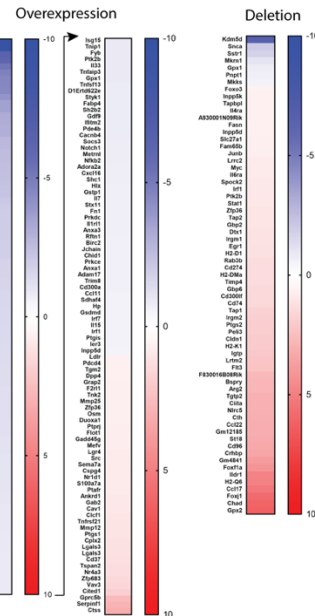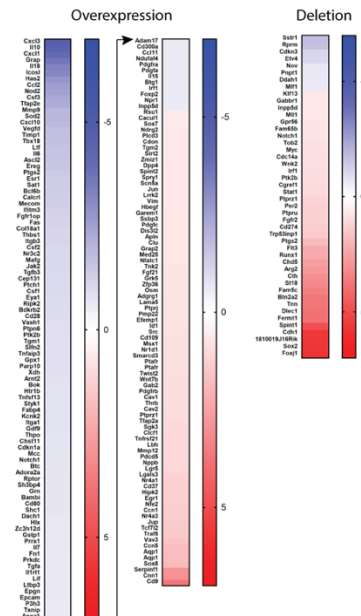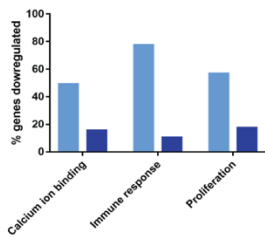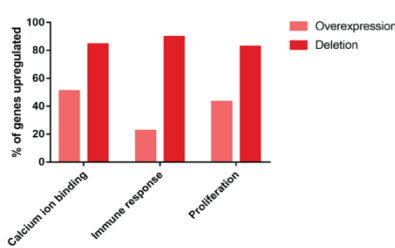
Figure 2.4: The β1-ICD modulates gene transcription in vitro and in vivo. A. Experimental design. B. Gene ontology (GO) groups overrepresented in analysis from CHL cells overexpressing the β1-ICD (left) and Scn1b null cardiac ventricle (right). C/D/E. Heat maps depicting genes altered in each RNA-seq related to calcium ion binding (C), the immune response (D), and proliferation (E). F. Percent of genes downregulated in each data set for calcium ion binding, immune response, and proliferation GO groups. G. Percent of genes upregulated in each data set for calcium ion binding, immune response, and proliferation GO groups.
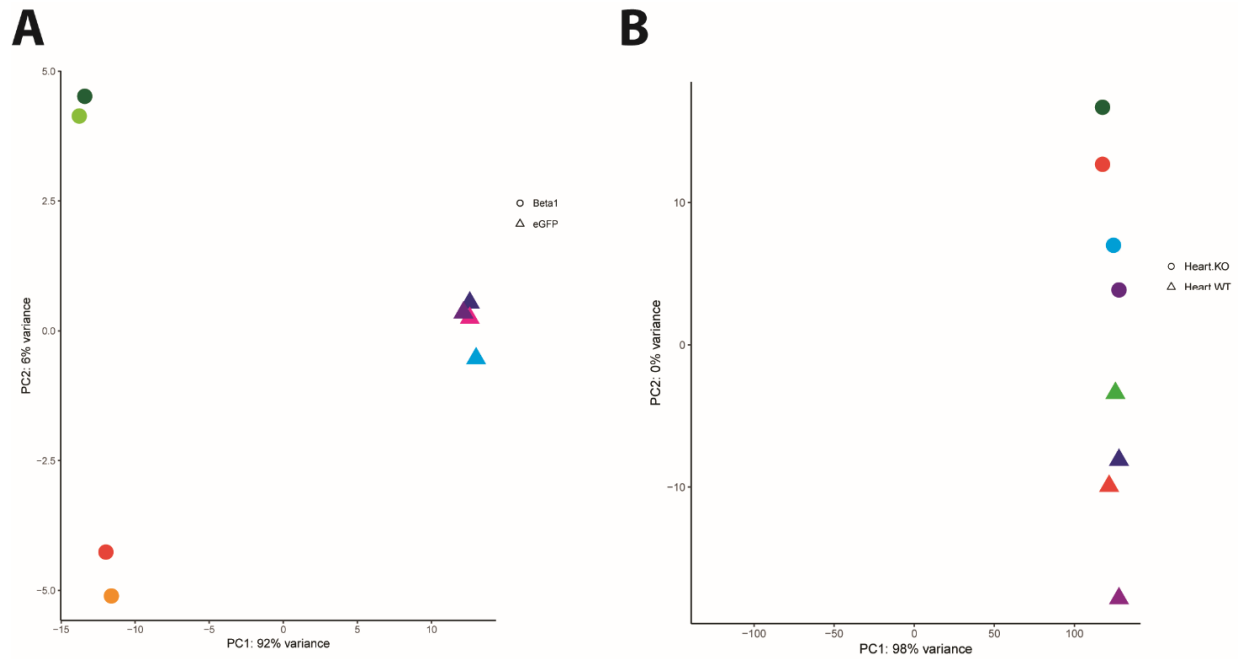
*Supplemental Fig. 2.2: Principal Component Analysis (PCA) for RNA-Seq experiments. **A.** CHL cells stably overexpressing eGFP only (▲) or β1-ICD-V5-2A-eGFP (●) samples bin according to genotype. **B.** Scn1b$^{+/+}$ (▲) and Scn1b$^{-/-}$ (●) P10 mouse cardiac ventricle bin according to genotype.*

Supplemental Fig. 2.3: ClueGO network analysis of RNA-seq data sets. A. ClueGO network analysis for Scn1b$^{+/+}$ vs. Scn1b$^{-/-}$ cardiac ventricle RNA-seq for GO groups with an adjusted p-value ≤ 0.05. B. ClueGO network analysis for CHL cells stably overexpressing eGFP or the β1-ICD and eGFP for GO groups with an adjusted p-value ≤ 0.0001.

Potassium currents are increased in Scn1b-null ventricular cardiac myocytes.

Over-expression of the β1-ICD in CHL cells resulted in changes in the expression of potassium channel genes compared to controls: downregulation of *Kcns3, and Kcnk2,* and upregulation of *Kcnk3*. In contrast, a set of potassium channel genes, *Kcnma1, Kcnmb4, Kcnk12, Kcnn1, Kcnd3, Kcnu1*, were upregulated in *Scn1b* null cardiac ventricular tissue, in which the β1-ICD signaling pathway is deleted (Fig. 2.5A and B). To investigate functional changes in potassium channel gene expression in *Scn1b* null cardiac ventricle, we recorded potassium currents in acutely dissociated ventricular cardiac myocytes from the left ventricular wall of P17 *Scn1b* WT and null mice.

A pre-pulse to -120 mV was required for this study since the voltage-dependence of steady state inactivation of the peak potassium current, and of most of the individual potassium current components, were significantly shifted to hyperpolarized potentials in myocytes isolated from P17 mice of both genotypes, compared to those previously reported in myocytes from adult mice (Zhou, Jeron et al. 1998, Xu, Guo et al. 1999). This may result from differences in myocyte preparation between laboratories or in the developmental stage of the cells and will be an interesting topic for future studies.

Whole-cell potassium currents were qualitatively similar in myocytes from *Scn1b* null and WT mice (Fig. 2.5C and D). Current amplitudes in myocytes from *Scn1b* null mice were smaller compared to those from WT animals, however, as observed previously during examination of I_{Na} (Lopez-Santiago, Meadows et al. 2007), *Scn1b* null myocytes had a significantly smaller

70

membrane capacitance (C_m) (WT, $C_m = 92.45 \pm 5.13$ pF, n = 17, and *Scn1b$^{-/-}$*, $C_m = 62.32 \pm 1.15$ pF, n =17 p < 0.001), resulting in increased potassium current densities of ~27% and ~53% for I_{peak} (Fig. 2.6A and Supplemental Table 2.3) and for I_{end} (Fig. 2.6B and Supplemental Table 2.3), respectively (Lopez-Santiago, Meadows et al. 2007). *Scn1b* deletion did not affect either the voltage-dependence or slope of inactivation of the peak current (Fig. 2.6C and Supplemental Table 2.3). For the voltage-dependence of inactivation of I_{end}, which is best described by the sum of two Boltzmann functions, *Scn1b* deletion resulted in a ~70% increase in the amplitude of the major component (A_1), while the minor component (A_2) was reduced by ~40% (Fig. 2.6D and Supplemental Table 2.4). $V_{1, 1/2}$ was unaffected, however $V_{2, 1/2}$ was shifted ~ +14 mV for *Scn1b* null myocytes compared to WT (Fig. 2.6D and Supplemental Table 2.4).

Detailed analysis of the decay phase of the potassium current revealed the presence of $I_{to\,f}$, $I_{to\,s}$, $I_{K\,slow}$, and I_{ss}. With the exception of $I_{to\,f}$, the current densities (at +60 mV, from -120 mV pre-pulse potential) of all other components were significantly increased in *Scn1b* null myocytes compared to WT (Fig. 2.7A). At strongly hyperpolarized membrane potentials (-120 to -90 mV) the availabilities of $I_{to\,s}$ (Fig. 2.7D), $I_{K\,slow}$ (Fig. 2.7E), and I_{ss} (Fig. 2.7F) were increased in *Scn1b* null myocytes, although for $I_{to\,s}$ this increase was not significant. In contrast, at hyperpolarized potentials $I_{to\,f}$ channels (Fig. 2.7C) exhibited similar availability, and at mildly depolarized potentials (-70 to -60 mV) availability was higher in myocytes from *Scn1b* null animals. While I_{end} also showed increased availability at hyperpolarized potentials (Fig. 2.7D), at -70 to -40 mV I_{end} availability in *Scn1b* null myocytes was less than that in WT animals (p = 0.05 to 0.1 at individual

membrane potentials). This difference was even more significant when I_{end} availability was averaged within this voltage range (WT $I_{end}= 10.3 \pm 0.8$ pA/pF, $Scn1b^{-/-}$ $I_{end}= 6.6 \pm 2.0$ pA/pF, p < 10^{-6}), with a ~36% loss in average availability following loss of *Scn1b* expression. *Scn1b* deletion resulted in a similar reduction of I_{ss} between -70 and -40 mV (Fig. 2.6F) (average I_{ss} at -70 to -50 mV reduced ~21%, p < 0.05). For the voltage-dependence of inactivation, both $I_{to\,f}$ (~+ 8 mV) and I_{ss} (~+10 mV) exhibited a significant depolarizing shift in response to *Scn1b* deletion. The slope (λ) for $I_{to\,f}$ increased approximately 2-fold while that of $I_{K\,slow}$ showed an approximate 50% increase (Supplemental Table 2.5). Additionally, decay of $I_{K\,slow}$ (at +60 mV) is slowed in *Scn1b* null myocytes (Fig. 2.7B).

A

CHL cells: overexpression

eGFP vs. β1ICD2AeGFP
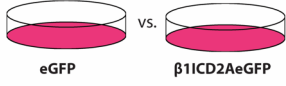
Mouse cardiac ventricle: deletion

Scn1b-null
(P10 heart)
vs.
Scn1b wild-type
(P10 heart)

B

ICD overpression
Scn1b deletion

Log2FC

Kcns3 Kcnk2 Kcnk3 Kcnma1 Kcnmb4 Kcnk12 Kcnn1 Kcnd3 Kcnu1

C

Scn1b(+/+)   *Scn1b(-/-)*

D

Scn1b(+/+)   *Scn1b(-/-)*
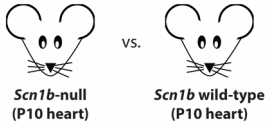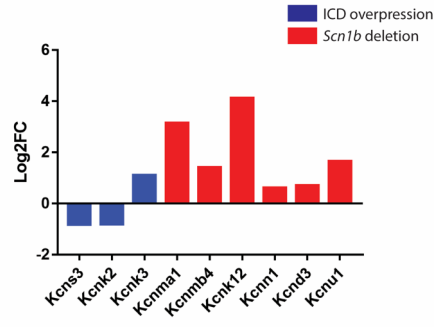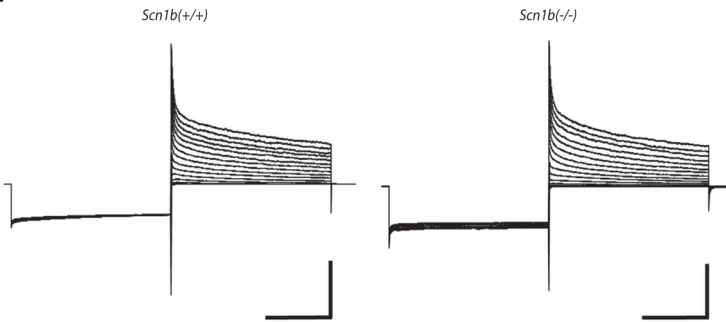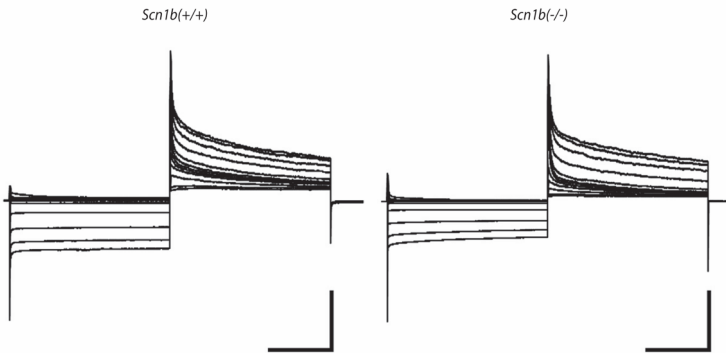
Figure 2.5: β1-ICD regulates potassium channel genes and potassium currents in cardiac ventricular myocytes. A. Experimental design of RNA-Seq experiments from CHL cells stably overexpressing the β1-ICD and from P10 Scn1b WT or Scn1b null mouse cardiac ventricle. B. RNA-seq showed that β1-ICD expression downregulates potassium channel genes, while Scn1b null mice show upregulated potassium channel gene expression in cardiac ventricle. C. Representative potassium currents recorded from ventricular myocytes obtained from WT and Scn1b null mice. To assess the I-V relationship 5 sec pulses were applied in +10 mV increments from -70 mV to +70 mV, following a 5 sec prepulse to -120 mV. D. Typical traces observed during investigation of voltage-dependence of steady-state inactivation. 5 sec conditioning pulses were applied in +10 mV increments from -120 to -10 mV followed by a 5 sec depolarization to +60 mV. Holding potential was -70 mV. Scale bars 5 nA and 2 sec.

	A (pA/pF)	V ½ (mV)	λ	C (pA/pF)
WT	87.6±6.0	-74.1±2.8	-0.06±0.00	3.4±0.6
Scn1b⁻/⁻	111.3±5.1**	-75.9±3.6	-0.06±0.00	5.2±1.0

*Table 2.3: Voltage-dependence of inactivation of peak potassium currents recorded from dissociated ventricular cardiomyocytes. C denotes the average pedestal current, while A describes the amplitude, and $V_{\frac{1}{2}}$ and λ the average half-voltage and slope values, respectively, of the voltage-dependence of inactivation of the peak (I_{peak}) potassium currents (see Fig. 7C) as described in Materials and Methods. Scn1b deletion results in a ~27% increase in A (I_{peak} amplitude) and ~53% increase in the pedestal current (C) amplitude but does not affect $V_{\frac{1}{2}}$ or λ. 15 myocytes were examined from each group. Myocytes were isolated from 3 WT and 2 $Scn1b^{-/-}$ mice. ** P < 0.01.*
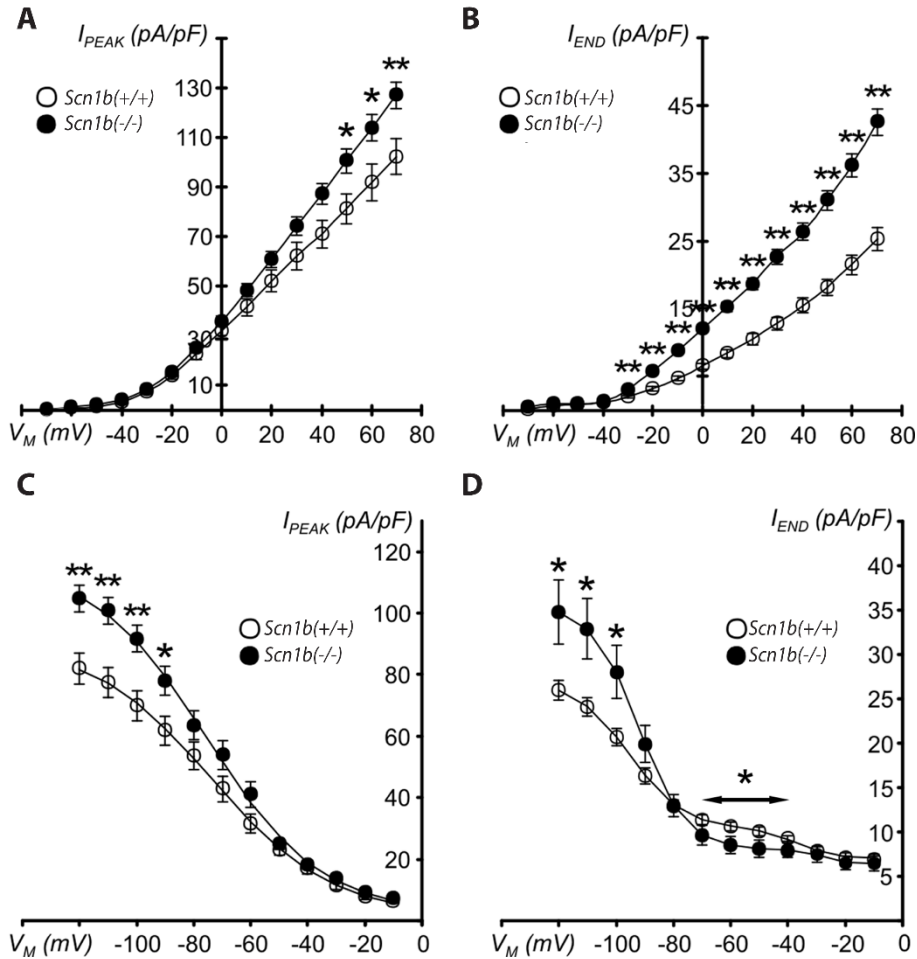
*Figure 2.6: Comparison of current density and voltage-dependence of inactivation of peak and end potassium currents. **A-B.** Scn1b deletion results in increased peak (I_{peak}) (A) and end (I_{end}) (B) potassium current densities at depolarized potentials. **C-D.** Availability of both I_{peak} (C) and I_{end} (D) current is increased at hyperpolarized potentials following Scn1b deletion, while I_{end} availability is decreased at more depolarized potentials (double-ended arrow). Voltage-dependence of inactivation for I_{peak} and I_{end} are described in Tables 1 and 2, respectively. *P ≤ 0.05 and **P ≤ 0.1.*

	A_1 (pA/pF)	$V_{1, ½}$ (mV)	λ_1	A_2 (pA/pF)	$V_{2, ½}$ (mV)	λ_2	C (pA/pF)
WT	16.2±1.1	-95.8±1.6	-0.13±0.01	4.0±0.3	-37.6±2.4	-0.23±0.05	6.8±0.4
$Scn1b^{-/-}$	27.3±2.9**	-92.6±1.4	-0.14±0.00	2.4±0.4**	-23.5±1.9**	-0.42±0.10	5.8±0.7

Table 2.4: Voltage-dependence of inactivation of end potassium currents. As described in Materials and Methods, the voltage-dependence of I_{end} is best described by the sum of two Boltzmann functions. A_1, $V_{1, ½}$, and λ_1 represent amplitude, half-voltage, and slope of the major component, respectively, while A_2, $V_{2, ½}$, and λ_2 represent the parameters of the minor component. C describes the average pedestal current (see Fig. 7D). Scn1b deletion increases the amplitude of the major component (A_1) by approximately 70% compared to current in myocytes from WT animals, while the amplitude of the minor component (A_2) shows a loss of ~40%. $V_{2, ½}$ is shifted by ~+ 14 mV. **P < 0.01.

A I (pA/pF)

B *Tau* (ms)

C Itof (pA/pF)

D Itos (pA/pF)

E Iks (pA/pF)

F Iss (pA/pF)
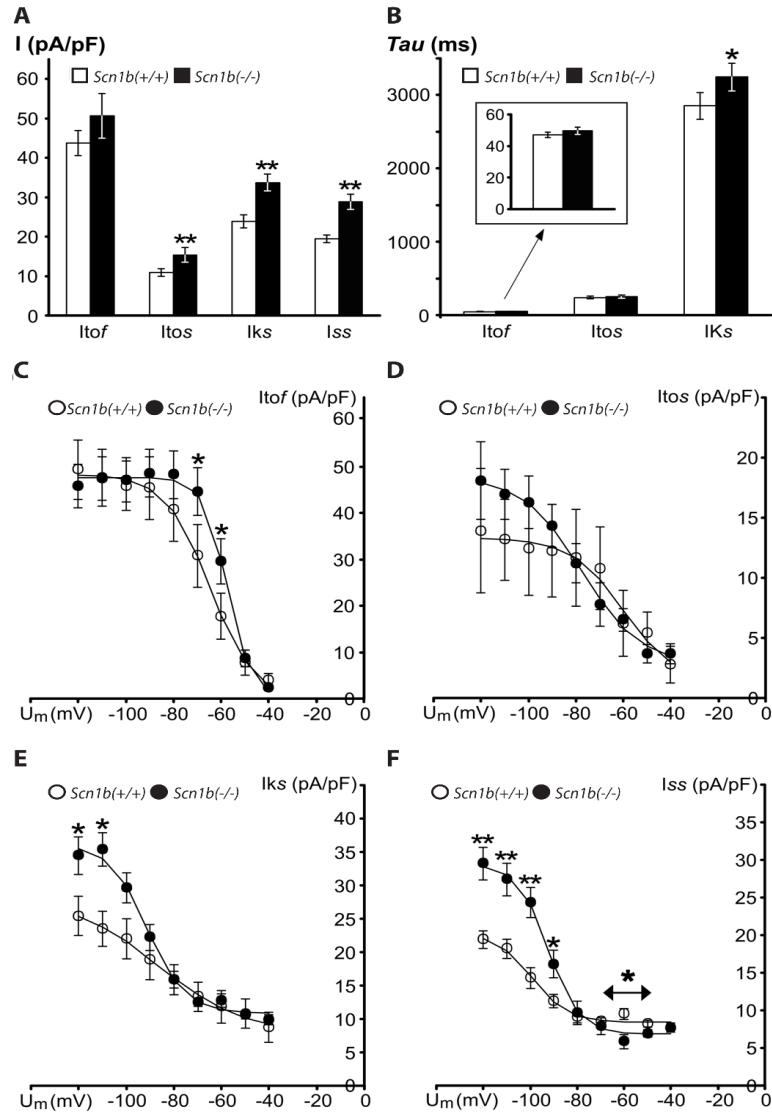
*Figure 2.7: Comparison of current density, rate of decay, and availability of individual components of the potassium current. A-B. Mean current density (A) and time-constant of current decay (B) measured at +60 mV for $I_{to\,f}$, $I_{to\,s}$, $I_{K\,slow}$, and I_{ss} currents in myocytes from WT (open columns) and $Scn1b^{-/-}$ (filled columns) mice. At +60 mV current density of $I_{to\,f}$ is unchanged (A) while that of $I_{to\,s}$, $I_{K\,slow}$, and I_{ss} is increased with Scn1b deletion. At +60 mV Scn1b deletion results in slower decay of $I_{K\,slow}$ (B) (inset, $I_{to\,f}$ data shown at higher magnification). C-F. Voltage-dependence of inactivation of $I_{to\,f}$ (C), $I_{to\,s}$ (D), $I_{K\,slow}$ (E), and I_{ss} (F) current in myocytes from WT (open circles) and $Scn1b^{-/-}$ (filled circles) mice. With Scn1b deletion, $I_{to\,s}$, $I_{K\,slow}$, and I_{ss} availability increases at hyperpolarized potentials, $I_{to\,f}$ availability increases at moderately depolarized potentials, while at depolarized potentials I_{ss} availability is decreased (double-ended arrow). Voltage-dependence of inactivation is described in Table 3. *$P \leq 0.05$ and **$P \leq 0.1$*

		A (pA/pF)	V½ (mV)	λ	C (pA/pF)	n
I_{tof}	WT	46.1±5.2	-67.1±2.4	-0.15±0.01	1.9±1.1	14
	$Scn1b^{-/-}$	47.9±4.7	-58.9±1.2**	-0.26±0.02**	2.1±0.4	14
I_{tos}	WT	13.0±6.2	-63.3±5.9	-0.20±0.12	0.5±2.2	3
	$Scn1b^{-/-}$	16.0±3.1	-74.4±7.3	-0.14±0.05	2.0±1.4	4
I_K slow	WT	19.0±2.4	-86.6±3.4	-0.08±0.01	10.3±3.3	5
	$Scn1b^{-/-}$	26.7±1.7*	-92.1±1.8	-0.12±0.01*	10.6±0.6	7
I_{ss}	WT	13.3±2.3	-101.5±0.8	-0.13±0.03	9.2±0.1	4
	$Scn1b^{-/-}$	23.1±2.6**	-91.1±3.2 *	-0.20±0.03	6.4±0.8*	5

*Table 2.5: Voltage-dependence of inactivation of $I_{to\,f}$, $I_{to\,s}$, $I_{K\,slow}$, and I_{ss}. A, $V_½$, λ, and C represent amplitude, half-voltage, slope and pedestal current, respectively, for $I_{to\,f}$ (see Fig. 8C), $I_{to\,s}$ (Fig. 8D), $I_{K\,slow}$ (Fig. 8E) and I_{ss} (Fig. 8F) as indicated in Materials and Methods. Both $I_{to\,f}$ and I_{ss} exhibited a shift in $V_½$ of ~+ 8 mV and ~+10 mV, respectively, on Scn1b deletion. $I_{to\,f}$ underwent an approximately 2-fold increase in slope while that of $I_{K\,slow}$ showed ~50% increase. **P < 0.01, *P < 0.05, n refers to the number of cells examined.*

Calcium currents are decreased in Scn1b null ventricular cardiac myocytes.

RNA-seq analysis of β1-ICD overexpression in CHL cells as well as of *Scn1b* null ventricular tissue showed alterations in the expression of genes encoding proteins known to modulate voltage-gated calcium channel (VGCC) activity. β1-ICD overexpression resulted in downregulated expression of the VGCC β4 subunit gene, *Cacnb4*. In contrast, P10 *Scn1b* null cardiac ventricle showed upregulation of the VGCC β1 subunit gene, *Cacna1b* (Supplemental Fig. 2.4)*. In general, β1-ICD overexpression led to decreased expression of calcium ion binding protein (CBP) genes, while *Scn1b* deletion led to increased expression of CBP genes (Fig. 2.4C). CBPs are complex regulators of VGCCs that can increase or decrease calcium current, depending on the particular CBP(s) at play (Nejatbakhsh and Feng 2011). To determine whether calcium handling was altered by *Scn1b* expression *in vivo*, we performed whole-cell voltage-clamp recording of L-type calcium current ($I_{Ca,L}$) and simultaneously added the calcium indicator, fluo-4, through the micropipette to record $I_{Ca,L}$-triggered calcium transients (Fig. 2.8A). Single ventricular cardiac myocytes were voltage-clamped and depolarized from a holding potential of -50 mV to +60 mV in 10 mV increments. At the same time, intracellular calcium dynamics were imaged by confocal microscopy, using the line-scan mode, at each depolarization voltage. During the imaging, 20 mM caffeine was rapidly perfused to determine sarcoplasmic reticulum calcium content at the peak of the caffeine-elicited calcium transient. Supplemental Fig. 2.5 shows that sarcoplasmic reticulum calcium content of cardiac myocytes was not different between genotypes. For calcium transients, the amplitude, time-to-peak, maximum rise rate, and full-duration at half-maximum were

analyzed. Fig. 2.8B shows that that $I_{Ca,L}$ is decreased in *Scn1b* null mouse ventricular myocytes compared to WT. In contrast, we found no differences in the calcium transient amplitude between genotypes (Fig. 2.8C). Finally, we calculated the excitation-contraction coupling gain (the amplification factor between calcium release from the sarcoplasmic reticulum via the ryanodine receptor and I_{Ca}), which is an indicator of intracellular Ca releasability, and found it to be increased in *Scn1b* null myocytes compared to WT (Fig. 2.8D).
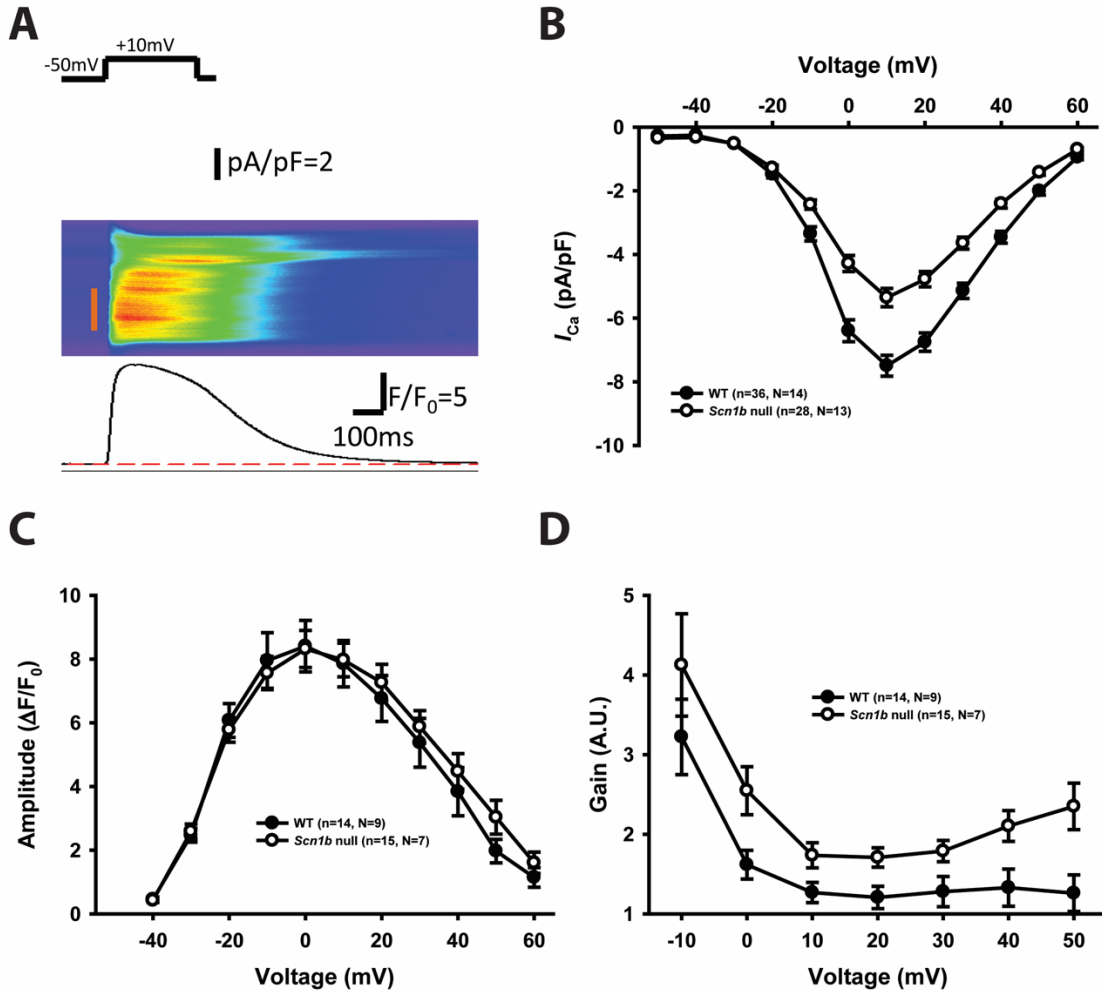
*Figure 2.8: Excitation-contraction (E-C) coupling in ventricular myocytes from P16-19 Scn1b null and WT mice. **A**. Representative example of E-C coupling recording. Top: I_{Ca} triggered by voltage-clamp depolarization; middle: whole cell Ca^{2+} transient; bottom: Ca^{2+} transient time profile. **B**. I-V curve shows decreased I_{Ca} in CMs from Scn1b null mice compared to WT. **C**. No change in Ca^{2+} transient amplitude between genotypes. **D**. E-C coupling gain (ratio between the Ca^{2+} transient amplitude and I_{Ca}) is decreased in Scn1b null myocytes compared to WT.*
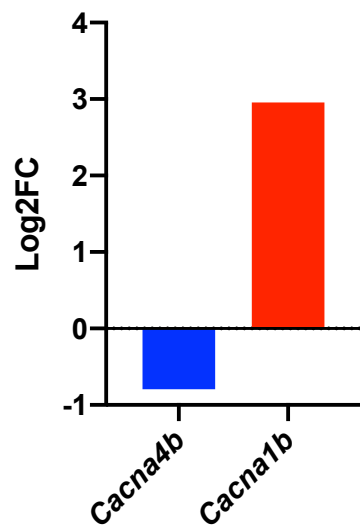
Supplemental Fig. 2.4: RNA-seq identifies changes in VGCC β subunit genes. Blue bar is from ICD overexpression experiment. Red bar is from Scn1b deletion.
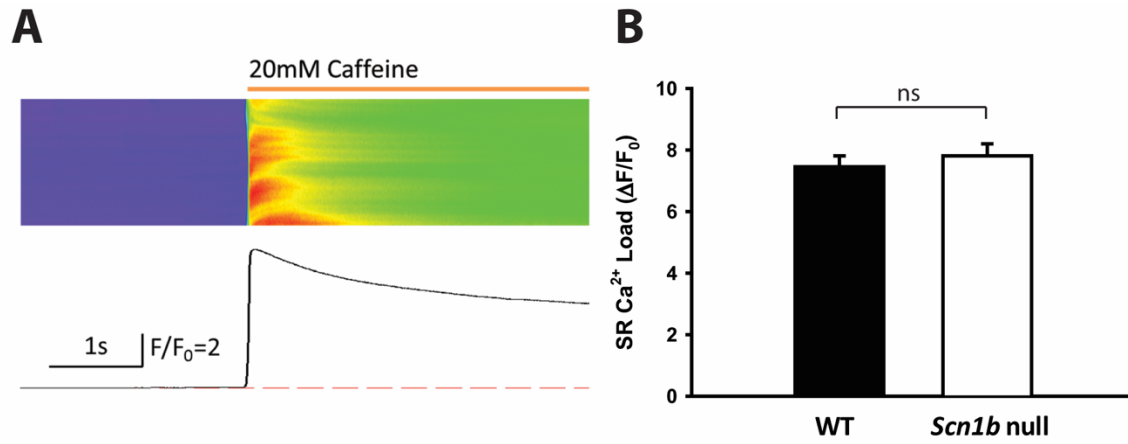
Supplemental Fig. 2.5: Sarcoplasmic reticulum calcium content of cardiac myocytes is not different between genotypes. A. Representative example of recorded sarcoplasmic reticulum calcium content. B. Sarcoplasmic reticulum (SR) calcium content in WT vs. Scn1b null cardiac myocytes.

Discussion

VGSC β1 subunits, encoded by *SCN1B*, play important roles in cardiac physiology. *SCN1B* variants are linked to human cardiac disease, including Brugada syndrome and atrial fibrillation, although recent work suggests that *SCN1B* may not be a monogenic cause of Brugada syndrome (Gray, Hasdemir et al. 2018). Our previous work showed that *Scn1b* null mouse ventricular cardiac myocytes have increased transient and persistent I_{Na}, action potential (AP) prolongation, prolonged calcium transients, and increased incidence of delayed afterdepolarizations (Lopez-Santiago, Meadows et al. 2007, Lin, O'Malley et al. 2015). *Scn5a*/Nav1.5 and *Scn3a* expression, as well as ^{3}H-saxitoxin binding, which measures levels of TTX-sensitive (TTX-S) VGSC expression, are increased in *Scn1b* null heart (Lopez-Santiago, Meadows et al. 2007, Lin, O'Malley et al. 2015). AP prolongation and aberrant calcium release in *Scn1b* null mice are TTX-S, implicating increased persistent I_{Na} via a TTX-S VGSC α subunit, perhaps Nav1.3, leading to activation of reverse Na/Ca exchange in the mechanism of arrhythmogenesis (Lin, O'Malley et al. 2015). *Scn1b* null mouse ventricles have abnormally formed intercalated discs that show perinexal de-adhesion, with significantly greater perinexal inter-membrane distances compared to WT littermates, due to the loss of β1-β1 homophilic cell adhesion (Veeraraghavan, Hoeker et al. 2018). Finally, *Scn1b* null mouse ECGs show prolonged QT intervals (Lopez-Santiago, Meadows et al. 2007).

RIP substrate are involved in a wide variety of biological processes. These include, but are not limited to, neurite outgrowth, cell adhesion, lipid metabolism, receptor protein tyrosine kinase signaling, axon guidance, calcium signaling, the immune response, and cellular proliferation (Haapasalo and Kovacs 2011). Some of these implications may be a result of transcriptional changes downstream of RIP from substrate-ICDs. Our work suggests that the β1-ICD regulates similar gene groups. Immune response, proliferation, potassium channel, and calcium ion binding genes are upregulated in *Scn1b* null mouse cardiac ventricle, while they are generally downregulated when the β1-ICD is overexpressed in CHL cells, suggesting that the β1-ICD may normally act as a transcriptional repressor in heart *in vivo*.

BACE1 null mice have brain region specific, developmentally regulated alterations in the expression levels of *Scn1a*, *Scn2a*, and *Scn8a*, as well as altered I_{Na} and neuronal activity (Hu, Zhou et al. 2010, Kim, Gersbacher et al. 2011). *BACE1* null atrial cardiomyocytes have decreased steady-state potassium current (Agsten, Hessler et al. 2015). Cardiomyocytes isolated from transgenic mice with inducible Notch-ICD (NICD) overexpression, which is generated by RIP, have prolonged AP duration, reduced upstroke amplitude, reduced rapidly activating voltage-gated potassium current, and reduced transient I_{Na} (Borghetti, Eisenberg et al. 2018). Treatment of cultured neonatal mouse myocytes with a γ-secretase inhibitor to decrease NICD production resulted in increased transcript levels of *Kcnip2*, encoding the potassium channel-interacting protein 2, KChIP2, and enhanced potassium current density (Borghetti, Eisenberg et al. 2018). In

other work, *Kcnip2* silencing in neonatal rat cardiac myocytes resulted in reduced levels of *Scn1b* and *Scn5*a mRNA (Deschenes, Armoundas et al. 2008). Taken together, these studies suggest that RIP substrates regulate sodium, potassium, and possibly other ion channel gene transcription. In support of this hypothesis, the present data show that VGSC β1 subunits undergo RIP through sequential intramembrane cleavage by BACE1 and γ-secretase, resulting in the generation of a soluble ICD that is translocated to the nucleus where it participates in transcriptional regulation of multiple gene families, including sodium and potassium channels (Summarized in Fig. 2.9). Using an unbiased, RNA-seq approach, we identified a subset of gene groups that are primarily downregulated when the β1-ICD is overexpressed in heterologous cells, but upregulated in *Scn1b* null cardiac tissue, suggesting that the β1-ICD may normally act as a molecular break on gene expression in heart *in vivo.* Consistent with the present RNA-seq results, our previous work showed increased I_{Na} in *Scn1b* null ventricular myocytes compared to WT (Lopez-Santiago, Meadows et al. 2007, Lin, O'Malley et al. 2015) and new data presented here show increased potassium currents and decreased calcium currents in *Scn1b* null myocytes compared to WT. While β1 subunits have been shown to facilitate sodium and potassium channel α subunit targeting to the plasma membrane (Marionneau, Carrasquillo et al. 2012, Calhoun and Isom 2014), this mechanism cannot explain the increased currents recorded in *Scn1b* null myocytes. To our knowledge, there is no evidence to date that VGSC β1 subunits affect VGCC α subunit targeting to the plasma membrane. Instead, our new data suggest the β1-ICD regulates the expression of a complex group of genes encoding proteins important in modulating VGCCs, including VGCC β subunits and CBPs. CBPs have been shown to both inactivate and facilitate ion conduction through

88

the channel pore (Nejatbakhsh and Feng 2011). The mechanism of decreased $I_{Ca,L}$ observed in *Scn1b* null ventricular myocytes is likely the result of complex gene regulation and will be the focus of future work. Taken together, this present study solidifies the critical, multi-functional roles of VGSC β1 subunits in cardiac physiology and adds RIP-excitation coupling to the complex list of β1 functionality.

Despite the identification of a growing list of RIP substrates, the factors that initiate RIP in specific cell types and subcellular domains are poorly understood. Neuronal activity and ligand binding have been shown to activate RIP at the synapse (Lee and Ch'ng 2020), but little is known about the initiation of RIP in heart. Our previous work showed that pretreatment with -secretase inhibitors blocked β1- β1 *trans* homophilic cell adhesion mediated neurite outgrowth (Brackenbury and Isom 2011), consistent with the idea that β1 binding to other β1 subunits on adjacent cells may initiate RIP. In ventricular myocytes, β1- β1 *trans* homophilic adhesion at the intercalated disk may provide a similar environment for RIP activation (Veeraraghavan, Hoeker et al. 2018). Substrate post-translational modification, such as ubiquitination and palmitoylation, and specific subcellular localization/co-compartmentalization have been shown to be critical factors in regulating BACE and γ-secretase cleavage (McCarthy, Coleman-Vaughan et al. 2017, Lee and Ch'ng 2020). While our previous work has shown that β1 subunits are post-translationally modified by glycosylation and tyrosine phosphorylation (Malhotra, Koopmann et al. 2002, Kruger, O'Malley et al. 2016), we have not yet investigated ubiquitination or palmitoylation.

Other ion channel proteins have been shown to participate in transcriptional regulation (Gomez-Ospina, Tsuruta et al. 2006, Kim, Carey et al. 2007, Schroder, Byse et al. 2009, Gomez-Ospina, Panagiotakos et al. 2013, Lu, Sirish et al. 2015). For example, the voltage-gated calcium channel $Ca_v1.2$ C-terminus contains a transcription factor, although the mechanism by which it is generated remains under debate. Some groups have shown that $Ca_v1.2$ encodes a transcription factor, CCAT, in its C-terminal region that is driven via a cryptic promoter located within exon 46. In contrast, others have shown the $Ca_v1.2$ C-terminus is a fragment generated by proteolysis. Regardless of its origin, evidence shows that the $Ca_v1.2$ C-terminus can localize to the nucleus and modulate transcription (Gomez-Ospina, Tsuruta et al. 2006, Schroder, Byse et al. 2009, Gomez-Ospina, Panagiotakos et al. 2013). Similar work on $Ca_v1.3$ demonstrated transcriptional activity of the protein's C-terminus (Lu, Sirish et al. 2015). Similar to β1, VGSC β2 subunits are also substrates of BACE1 and γ-secretase. In neuroblastoma cells, RIP generates a β2-ICD that can translocate to the nucleus and increase expression of *SCN1A*, which encodes the VGSC α subunit, $Na_v1.1$ (Kim, Carey et al. 2007).

Most BACE1 and γ-secretase substrate proteins are type-I transmembrane proteins with extracellular domains that often contain CAM-like loops. The released C-terminal domains have been shown to translocate to the nucleus where they participate in regulating genes that are involved in cell fate determination, adhesion, migration, neurite outgrowth, axon guidance, and/or synapse formation and maintenance (Haapasalo and Kovacs 2011, Pardossi-Piquard and Checler

90

2012). Because β1 is structurally and functionally similar to other BACE1 and γ-secretase substrates, we hypothesized that the β1-ICD generated by RIP may function in a similar manner (Isom, De Jongh et al. 1992, Isom and Catterall 1996, McCormick, Isom et al. 1998, Malhotra, Kazen-Gillespie et al. 2000, Davis, Chen et al. 2004, Brackenbury, Davis et al. 2008, Brackenbury, Calhoun et al. 2010). A large body of work has examined the transcriptional regulatory roles of the many substrate ICDs generated by BACE1 and γ-secretase (Haapasalo and Kovacs 2011). Notch-1, although initially cleaved by an α-secretase, is subsequently processed by γ-secretase, generating a NICD, which translocates to the nucleus to regulate transcription (Kopan, Nye et al. 1994, van Tetering and Vooijs 2011, Bray and Gomez-Lamarca 2018). The NICD associates with the DNA binding protein, CSL, and the transcriptional coactivator, Mastermind (MAM). The primary role of this assembled ternary complex is to activate transcription of Notch target genes (Bray and Gomez-Lamarca 2018). While the Notch activator complex is well conserved, the repressor complex is more diverse and the switch between activation and repression depends on the precise cellular context during the regulatory process (Contreras-Cornejo, Saucedo-Correa et al. 2016). This can be further complicated by cell-type specific effects on NICD-mediated transcriptional changes(Bray and Gomez-Lamarca 2018). The ICD generated by sequential cleavage of APP (AICD) by BACE1 and γ-secretase, AICD, forms a complex with the nuclear adaptor protein, Fe65, and the histone acetyltransferase, Tip60, to regulate transcription (Cao and Sudhof 2001). Subsequent studies have demonstrated that the AICD can function as a transcriptional activator or as a repressor, depending on the target gene (Kim, Kim et al. 2003, Cao and Sudhof 2004, von Rotz, Kohli et al. 2004, Ozaki, Li et al. 2006, Zhang, Wang et al. 2007).

VGSC β2 subunits are also substrates for intramembrane processing by BACE1 and γ-secretase (Kim, Mackenzie Ingano et al. 2005). Over-expression of the β2-ICD in SH-SY5Y cells increases expression of *SCN1A* (Kim, Carey et al. 2007). Complex formation of the β2-ICD with other DNA binding proteins has not been investigated. Because neither the β1-ICD nor the β2-ICD contain a DNA binding domain, they may require binding partner(s) to mediate their effects on gene expression, similar to NICD and AICD.

Variants in BACE1 and/or γ-secretase substrates, as well as variants in *PSEN1*, encoding the catalytic domain of γ-secretase, are linked to many pathophysiological conditions, including Alzheimer's disease, epileptic encephalopathy, cardiac disease, and cancer (Scheffer, Harkin et al. 2007, Watanabe, Koopmann et al. 2008, Patino, Claes et al. 2009, Aster, Blacklow et al. 2011, Li, Chen et al. 2011, Li, Wang et al. 2013, Kruger, O'Malley et al. 2016, Kelleher and Shen 2017). *SCN1B* variants, which are linked to epileptic encephalopathy and cardiac arrhythmia, may also be involved in cancer, especially through dysregulation of cell-cell or cell-matrix adhesion and transcriptional regulation. β1 overexpression *in vitro* induces the growth of neurite-like projections from cultured breast cancer cells (Brackenbury, Davis et al. 2008, Nelson, Millican-Slater et al. 2014). β1 subunits are expressed in breast, cervical, non-small cell lung, and prostate cancers (Brackenbury 2012) and their expression is upregulated in patient breast and prostate cancer samples (Diss, Fraser et al. 2008, Nelson, Millican-Slater et al. 2014). In prostate cancer, β1 expression correlates with metastatic strength (Diss, Fraser et al. 2008). Mouse xenografts of β1-

overexpressing MDA-MB-231 breast cancer cells promote primary tumor growth and metastasis compared to untransfected cells. Conversely, β1-overexpressing MDA-MB-231 cells display decreased motility and proliferation compared to the parental cell line in *in vitro* cultures (Nelson, Millican-Slater et al. 2014). Interestingly, knockdown of endogenous β1 subunits in MCF-7 breast cancer cells increases cell migration, while β1 expression inhibits cell motility in cervical cancer, suggesting that β1 expression may encourage tumor growth and metastasis (Chioni, Brackenbury et al. 2009, Sanchez-Sandoval and Gomora 2019). The present work suggests that transcriptional regulation via the cleaved β1-ICD may play a role in these cellular changes and that the presence of *SCN1B* variants may affect cancer outcomes. NICD dysregulation is similarly linked to disease. Variants in Notch receptor genes are linked to adult T cell acute lymphoblastic leukemia and lymphoma (T-LL). The most common type of Notch1 variants in human T-LL lead to ligand-independent metalloproteinase (α-secretase) cleavage (Aster, Blacklow et al. 2011). Activating Notch receptor variants can lead to nuclear accumulation of the NICD in T-LL. Here, nominated genes identified by overexpression of the β1-ICD in CHL cells and by *Scn1b* deletion suggest that β1-ICD-mediated gene transcription may regulate proliferation, calcium ion binding, and immune response genes *in vivo*. Each of these gene groups has direct relationships to *SCN1B*-linked disease states, including epileptic encephalopathy, cardiac arrhythmia, and cancer (Bouza and Isom 2018). Thus, we propose that dysregulation of the β1-ICD signaling pathway may contribute to β1-linked pathophysiology. In conclusion, our work adds to the multi-functionality of VGSC β1 subunits and provides novel insights into disease mechanisms linked to variants in *SCN1B*. Out work also

adds to the growing body of evidence suggesting that substrate ICDs generated by RIP are transcriptional regulators.
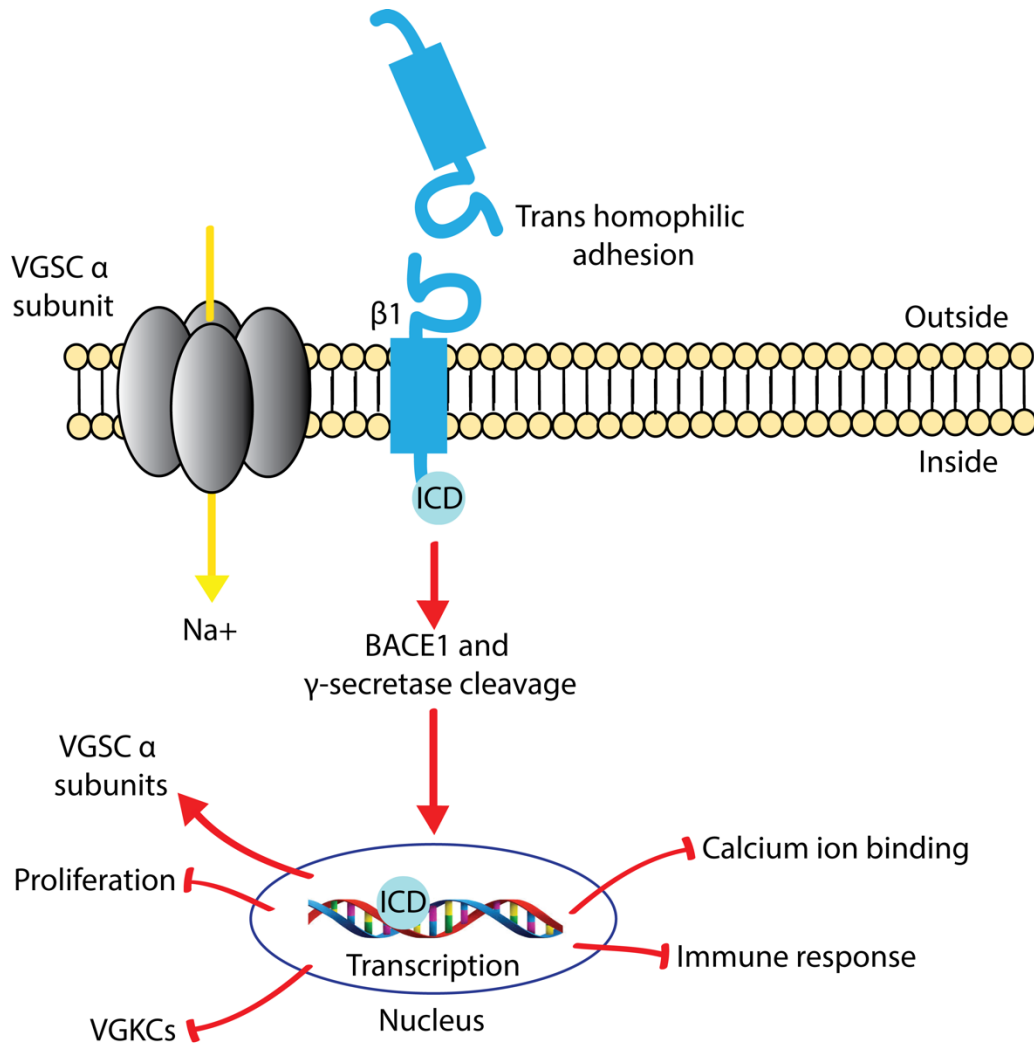
Figure 2.9: Cartoon diagram of β1-mediated signal transduction cascade.

Materials and Methods

Animals

$Scn1b^{+/+}$ and $Scn1b^{-/-}$ mice were generated from mating of $Scn1b^{+/-}$ mice congenic on the C57BL/6J background for over 20 N generations, as described(Yuan, O'Malley et al. 2019). Animals were housed in the Unit for Laboratory Animal Medicine at the University of Michigan. All procedures were performed in accordance with the NIH and the University of Michigan Institutional Animal Care and Use Committee (IACUC).

Antibodies

Primary antibodies used were: anti-$\beta 1_{intra}$ (1:1000 dilution), anti-V5 (1:1000 dilution, Invitrogen), anti-α-tubulin (1:1000 dilution, Cedar Lane) anti-presenilin-1 (1:200, APS18 Invitrogen), anti-BACE1 (1:1000, Invitrogen), or anti-HSP90 (1:1000 dilution, EnzoScientific). The specificity of anti-$\beta 1_{intra}$ has been shown previously by western blot. HRP-conjugated secondary antibodies were used in this study. Goat anti-rabbit or goat anti-mouse HRP-conjugated antibodies were diluted 1:1000 (anti-$\beta 1_{intra}$, anti-α-tubulin, anti-presenilin-1, anti-BACE1) or 1:10,000 (anti-V5 or anti-HSP90). Alexa Fluor 568 anti-mouse was used as a secondary (1:500 dilution) as a secondary antibody for anti-V5 in immunocytochemistry experiments.

Expression Vectors

A synthesis-optimized human WT β1-V5 cDNA was generated by gBLOCK from Integrated DNA technologies. The bicistronic cDNA construct included an in-frame β1 C-terminal V5 epitope tag followed by a self-cleaving 2A peptide and enhanced Green Fluorescent Protein (eGFP) to facilitate immune-detection of β1 as well as transfected cells by eGFP. β1-p.Y181A-V5, β1-p.Y181E-V5, and β1-p.Y181F-V5 were generated by site-directed mutagenesis using the WT β1-V5 cDNA construct in pENTR-SD/D TOPO as the template. The eGFP alone control and β1-V5-ICD-2A-eGFP constructs were generated by PCR from their respective full-length template cDNAs containing WT β1-V5, β1-p.Y181A-V5, β1-p.Y181E-V5, or β1-p.Y181F-V5. Using the Gateway cloning system, all constructs were moved from pENTR-SD/D-TOPO to pcDNAdest40 via LR Clonase reaction according to the manufacturers' protocol.

Cell lines

All CHL cells and HEK $Na_v1.5$ cells were maintained at 37°C with 5% CO_2 in Dulbecco's Modified Eagle Medium supplemented with 5% heat inactivated fetal bovine serum and penicillin/streptomycin. Stably transfected cell line media also included 600 µg/mL G418. To generate stable cell lines 1 µg of cDNAs were transfected with 5 µL of Lipofectamine 2000. 48 hours post transfection, cells were passed into fresh media containing 600 µg/mL G418. The cells were incubated for approximately one week or until eGFP positive cell colonies were visible. Individual colonies were isolated and grown until confluent and subsequently passaged for

biochemical characterization. Electrophysiological experiments used transient transfection. 1 μg of each cDNA was transfected with 5 μL of Lipofectamine 2000. Approximately 12 hours post-transfection cells were passaged onto glass cover slips for electrophysiological analysis. Electrophysiological recordings were taken approximately 24 hours post-final plating.

Measurement of sodium currents by whole-cell voltage clamp

Voltage-clamp recordings were performed at room temperature in the whole-cell configuration using a Multiclamp 700B amplifier and pClamp (versions 11, Molecular Devices, San Jose, CA) with 1.5–2.5 MΩ patch pipettes. Sodium currents were recorded in the presence of a bath solution containing (in mM): 120 NaCl, 1 $BaCl_2$, 2 $MgCl_2$, 0.2 $CdCl_2$, 1 $CaCl_2$, 10 HEPES, 20 TEA-Cl and 10 glucose (pH 7.35 with CsOH, Osmolarity: 300 – 305 mOsm). Fire-polished patch pipettes were filled with an internal solution containing (in mM): 1 NaCl, 150 N-methyl-D-glucamine, 10 EGTA, 2 $MgCl_2$, 40 HEPES, and 25 phosphocreatine-tris, 2 MgATP, 0.02 Na_2GTP, 0.1 Leupectin (pH 7.2 with H_2SO_4). Sodium current was recorded in response to a series of voltage steps between -100 and +30 mV in 5 mV increments, from a holding potential of -90 mV for 200 msec. A step back to -20 mV for 200 msec was used to determine the voltage-dependence of inactivation. Series resistance was compensated 40–65% and leak subtraction performed by application of a standard P/4 protocol. Normalized conductance and inactivation curves were generated as described previously.(Patino, Claes et al. 2009) Current densities were determined by dividing current

amplitude by the cell capacitance (Cm), as determined by application of +10 mV depolarizing test pulses.

Measurement of potassium currents by whole-cell voltage clamp

The bath solution contained in mM: 137 NaCl, 5.4 KCl, 1.5 CaCl$_2$, 0.5 MgCl$_2$, 10 HEPES, 0.16 NaH$_2$PO$_4$, 3 NaHCO$_3$, 0.002 nicardipine, 0.02 ouabain, pH 7.35 with NaOH. Nicardipine and ouabain were used to block L-type Ca^{2+} channels and Na/K pumps, respectively. Stock solutions for nicardipine (10 mM) and ouabain (20 mM) were prepared in DMSO and H$_2$O, respectively and diluted to the appropriate concentration in bath solution before use. Patch pipettes (2 - 3 MΩ) were filled with (in mM): 130 KCl, 2 K$_2$-ATP, 1 EGTA, 10 HEPES, pH 7.3 with KOH. Series resistance was routinely compensated to ~80% before the recordings. Holding potential was set to -70 mV and current traces filtered at 1 kHz. To assess voltage-dependence of activation, whole-cell outward potassium currents were recorded in response to 5 sec depolarizing voltage steps to potentials between -70 and +70 mV from a 5 sec -120 mV pre-pulse potential. To examine steady state inactivation, potassium currents were evoked during a 5 sec depolarization to +60 mV, after 5 sec pre-pulses to potentials between -120 to -10 mV in 10 mV increments at 15 sec inter-sweep intervals. The values of the I$_{peak}$ and I$_{end}$ ("end-current") were obtained at ~ 20 msec (variable) and 4.88 sec after the beginning of the depolarization, respectively.

The decay phases of the outward potassium currents were fit by the sum of three exponentials using the following expression: $I(t) = I_{to\ f} \times e^{-t/\tau f} + I_{to\ s} \times e^{-t/\tau s} + I_{K\ slow} \times e^{-t/\tau K\ slow} + I_{SS}$, where t is

time, τ_f, τ_s, and $\tau_{K\ slow}$ are the time constants of decay of $I_{to\ fast}$ ($I_{to\ f}$), $I_{to\ slow}$ ($I_{to\ s}$), and $I_{K\ slow}$. I_{ss} denotes the steady state current. Steady state inactivation curves for I_{peak}, I_{end}, $I_{to\ f}$, $I_{to\ s}$, $I_{K\ slow}$, and I_{ss} were fit using the following Boltzmann functions:

$$I = A/[1+\exp(-\lambda(V_m-V_{1/2}))], \text{ (single)}$$

$$I = \{A_1/[1+\exp(-\lambda_1(V_m-V^1_{1/2}))]\} + \{A_2/[1+\exp(-\lambda_2(V_m-V^2_{1/2}))]\}+C, \text{ (double)}$$

where A, A_1 and A_2 denote amplitudes; V_m is the pre-pulse voltage; $V_{1/2}$, $V^1_{1/2}$, and $V^2_{1/2}$ are the voltages of half-maximal inactivation; λ, λ_1, and λ_2 are the slope factors, and C is the "pedestal" current.

Measurements of calcium currents, calcium transients, and sarcoplasmic reticulum calcium content in cardiac myocytes

P16-19 mouse ventricular cardiac myocytes were isolated as previously described (Zhao, Valdivia et al. 2015). I_{Ca} and I_{Ca}-triggered whole cell calcium transients were recorded simultaneously as previously described (Zhao, Valdivia et al. 2015). Briefly, single ventricular myocytes were depolarized from a holding potential of -50mV to +60mV in 10mV increments for 300 ms. At the same time, intracellular calcium dynamics were imaged by confocal microscopy using the line-scan mode of a Nikon A1R microscope at each depolarization voltage. Sarcoplasmic reticulum calcium content was measured as previously described (Zhao, Guo et al. 2017). Briefly, single ventricular myocytes were loaded with fluo-4-AM (ThermoFisher Scientific) and imaged by

confocal microscopy in line-scan mode. 20 mM caffeine was rapidly perfused onto the cell. Sarcoplasmic reticulum calcium content was determined by the peak of the caffeine-elicited calcium transient.

Western blot analysis of cell lysates

Cell lysates were prepared either as described below for cleavage assays or surface biotinylation assays, as appropriate. Samples were mixed with loading buffer containing SDS, 5mM β-mercaptoethanol, and 1% dithiothreitol and heated for 10 min at 85°C. Proteins were separated by SDS-PAGE on 10, 12, or 15% polyacrylamide gels as indicated in the figure legends, transferred to nitrocellulose membrane overnight (16 h, 55 mA, 4°C), and probed with appropriate antibodies, as indicated in the figure legends. Incubations with anti-V5 or anti-$\beta 1_{intra}$ and their respective secondary antibodies were performed using a SnapID with 10-20 min incubations. Anti-α-tubulin and anti-HSP90 antibodies were incubated overnight at 4°C. Secondary antibodies for anti-α-tubulin and anti-HSP90 were incubated for 1 h at room temperature (RT). Immunoreactive bands were detected using West Femto chemiluminescent substrate (GE Health Sciences) and imaged using an iBrightFL1000 (Invitrogen). Immunoreactive signals from cleavage assays were quantified using ImageJ and normalized to the level of α-tubulin and then to the vehicle treated samples.

Cleavage assays

Stably transfected cells were grown until approximately 70% confluent in 100 mm tissue culture plates. Cells were treated with either vehicle (0.1% DMSO), varying concentrations of DAPT (Cayman Chemical) ranging from 50 nM to 1 μM, or 200 nM β-secretase inhibitor IV (Millipore), as indicated in the figure legends. 24 h post-treatment, cells were harvested, and membranes were prepared. Briefly, harvested cell pellets were resuspended in 50 mM Tris, pH 8.0 with Complete protease inhibitors, EDTA-Free (Roche). On ice, cells were broken with a dounce homogenizer and sonicated. Lysates were spun at 2,537xg for 10 min to remove nuclei and other large insoluble cell fragments. The supernatant was then removed spun at 80,000 x g for 15 min at 4°C. The supernatant was removed, and the membrane-containing pellets were resuspended in 133 μL of 50 mM Tris, pH 8.0 with Complete protease inhibitors, EDTA-Free (Roche) and sonicated on ice. Samples separated using 12% SDS-PAGE gels and western blots were performed as described above.

Immunocytochemistry and confocal microscopy

CHL cells were transiently transfected with cDNA constructs, as indicated in the figure legends, with Lipofectamine 2000. 24 h post transfection, cells were fixed with ice cold 100% methanol for 15 min then washed quickly 3x times with Dulbecco's Phosphate Buffered Saline (DPBS). Cells were blocked for approximately 1 h at RT in 90% DPBS, 10% goat serum, and 0.3% triton. Anti-V5 antibody was diluted 1:1000 in block (90% DPBS, 10% goat serum, and 0.3% triton) and

incubated with cells overnight at RT in a humidified chamber. Cells were washed three times for 10 min with DPBS. Cells were then incubated with secondary antibody for 2 h at RT in a humidified chamber. The secondary antibody, Alexa Fluor 568, was diluted 1:500 in block (90% DPBS, 10% goat serum, 0.3% triton x100). Cells were washed three times for 10 min with DPBS and allowed to dry. Cover slips were mounted with ProLong Gold (Invitrogen) with DAPI. Transfected cells were imaged while blinded at 63x on a Zeiss 880 confocal microscope in the University of Michigan Department of Pharmacology. Images were analyzed while blinded in ImageJ using plot profile.

RNA-Seq

RNA was isolated from CHL-eGFP, CHL-β1-ICD, or cardiac ventricle of P10 *Scn1b*$^{+/+}$ or *Scn1b*$^{-/-}$ mice using the Qiagen RNeasy Plus kit according to the manufacturer's instructions. Cells were lysed through a sterile, 18 gage hypodermic needle. As a fee for service, the University of Michigan Sequencing Core converted RNA to cDNA libraries using TrueSeq Kit (Illumina) and sequenced using Illumnia HiSeq4000 with 50 cycles of paired end sequencing. Chinese Hamster reference genome, CriGri_1.0, and mouse reference genome, UCSC mm10.fa, were used as the refence genome sequences. For the ICD RNA-Seq, eGFP and β1-ICD-V5-2A-eGFP transgenes were added to the reference. Quality of reads for each sample were assessed using FastQC (version v0.11.3). The University of Michigan Bioinformatics Core Facility completed DeSEQ2 analysis

as a fee for service. Genes and transcripts were considered differentially expressed if they met the following three criteria: test status = "OK", false discovery rate ≤ 0.05, and a fold change ≥ 1.5.

RT-qPCR

RNA was isolated from cardiac ventricles of P10 $Scn1b^{+/+}$ or $Scn1b^{-/-}$ mice or from CHL cells, as indicated in the figure legends, using the Qiagen RNeasy Plus kit according to the manufacturer's instructions. Cell or tissues were lysed through a sterile, 18 gage hypodermic needle or vortexed for 30 sec (heterologous cells). RNA was stored at -80°C until use. cDNA was generated from 1-2 μg of RNA using Reverse Transcriptase SuperScript III (RT SS III) and random primers (Invitrogen). Primers, dNTPs, and RNA were incubated at 65°C for 5 min. Salt buffers, RT SS III, and RNaseOUT were added and incubated at 25°C for 5 min, 50°C for 60 min, and then 75°C for 15 min. cDNA was diluted 1:3- to 1:5-fold in water. Comparative qPCR using SYBR Green (Applied Biosystems) and gene-specific primers (Integrated DNA Technologies) was completed. $\Delta\Delta Ct$ values were calculated by comparing genes of interest with GAPDH and normalizing to the control condition (WT or lipofectamine only treatment) to determine comparative gene expression. Data are presented as gene expression $\pm$SEM. Statistical significance (p-value <0.05) of comparisons between $Scn1b^{+/+}$ and $Scn1b^{-/-}$ mice were determined using Student's t-test. Statistical significance (p-value <0.05) of comparisons between lipofectamine treated, eGFP, and WT β1-ICD-V5 transfected cells were determined using one-way ANOVA for each examined gene.

Statistics

Statistical analysis for cleavage assay experiments were completed with n=3-4 for each experiment. The DAPT concentration response and -secretase inhibitor experiments were one-way ANOVA with multiple comparisons. Data are represented as the mean ± SEM. β1 mutant cleavage experiments were completed as unpaired t-tests between vehicle and DAPT treated groups. For the fyn kinase assay, three independent experiments were performed. Statistical significance was determined with Student's t-test. Data are represented as the mean ± SEM. Electrophysiology experiments had an n of 10-15 cells per condition for each experiment from a minimum of three independent transfections. The voltage-dependence of activation and inactivation were compared using nonlinear fit, maximum current was analyzed using one-way ANOVA with multiple comparisons, and current density was compared to the control, eGFP, with an unpaired t-test at each voltage-step. Analysis of co-localization between the β1-ICD constructs and nuclei, DAPI, were completed blinded using the ImageJ coloc2 package. Pearson's correlation coefficient for each cell (n=11-17 for each condition, from three independent transfections) was recorded. One-way ANOVA with multiple comparisons was completed. Data are represented as the mean ± SD. Differences were considered significant if the p-value was less than 0.05. University of Michigan Bioinformatics Core Facility completed DeSEQ2 analysis as a fee for service. The For each experiment, n=4 was used for each condition. Genes and transcripts were considered differentially expressed if they met the following three criteria: test status = "OK", false discovery rate ≤0.05, and a fold change ≥1.5.

Data availability

RNA-Seq data have been submitted to the repository at NCBI GEO. Accession numbers: GSE136927 and GSE136535

Chapter 3 VGSC β1 Palmitoylation Promotes its Plasma Membrane Localization

Alexandra A. Bouza*, Julie M. Philippe*, Nnamdi Edokobi, Alexa M. Pinsky, James Offord, PhD, Jeffrey D. Calhoun, PhD, Mariana Lopez-Floran, Luis F. Lopez-Santiago, PhD, Paul M. Jenkins, PhD, and Lori L. Isom, PhD

*These authors contributed equally to this work.

Summary

Voltage-gated sodium channel (VGSC) β1 subunits are multifunctional proteins that modulate VGSC α subunit biophysical properties and cell surface localization, as well as participate in cell-cell and cell-matrix adhesion, all with important implications for intracellular signal transduction, cell migration, and differentiation. Human loss-of-function variants in *SCN1B*, encoding the VGSC β1 subunits, are linked to severe diseases with high risk of sudden death, including epileptic encephalopathy and cardiac arrhythmia. We showed previously that β1 subunits are post-translationally modified by tyrosine phosphorylation. We also showed that β1 subunits undergo regulated intramembrane proteolysis (RIP) via the activity of BACE1 and γ-secretase, resulting in the generation of a soluble intracellular domain, β1-ICD, which modulates transcription. Here, we show that β1 subunits are phosphorylated by fyn kinase. In addition, we show that β1 subunits are *S*-palmitoylated. Mutation of a single residue in β1, cysteine (C) 162 to alanine (A), prevents

palmitoylation, reduces the level of β1 polypeptides at the plasma membrane, and results in a reduction in the extent of β1 RIP, suggesting that the plasma membrane is the site of β1 proteolytic processing. Treatment with the clathrin-mediated endocytosis inhibitor, Dyngo-4a, restores plasma membrane association of β1-p.C162A to WT levels. In spite of these observations, palmitoylation-null β1-p.C162A modulates sodium current and sorts to detergent-resistant membrane fractions normally. This is the first demonstration of *S*-palmitoylation of a VGSC β subunit, establishing precedence for this post-translational modification as a regulatory mechanism in VGSC function.

Introduction

Voltage gated sodium channels (VGSCs) are heterotrimeric protein complexes composed of one pore-forming α subunit and two non-pore forming β subunits (O'Malley and Isom 2015). VGSC β1 through β4 subunits contain a single, extracellular V-type immunoglobulin (Ig) domain and are thus members of the Ig superfamily of cell adhesion molecules (Ig-CAMs) (O'Malley and Isom 2015, Bouza and Isom 2018). β1 subunits are expressed in multiple tissues, including brain and heart, where they modulate the gating, kinetics, and plasma membrane localization of VGSC α subunits through non-covalent association (Isom, De Jongh et al. 1992, Isom, Ragsdale et al. 1995, Bouza and Isom 2018, Hull and Isom 2018). β1 subunits are multi-functional and play both conducting and non-conducting roles. In addition to modulating VGSCs, they contribute to voltage-gated potassium channel function, cell-cell and cell-matrix adhesion and cell migration, intracellular calcium signaling, neuronal pathfinding and fasciculation, neurite outgrowth, and cardiac intercalated disk formation (Malhotra, Kazen-Gillespie et al. 2000, Malhotra, Koopmann et al. 2002, Malhotra, Thyagarajan et al. 2004, Brackenbury, Davis et al. 2008, Brackenbury, Calhoun et al. 2010, Marionneau, Carrasquillo et al. 2012, Brackenbury, Yuan et al. 2013, Bouza and Isom 2018, Veeraraghavan, Hoeker et al. 2018). Concordant with their CAM function, β1-β1 *trans* homophilic cell adhesion *in vitro* results in outside-in signaling that includes ankyrin recruitment to points of cell-cell contact, which is terminated by β1 tyrosine phosphorylation (Malhotra, Kazen-Gillespie et al. 2000, Malhotra, Koopmann et al. 2002). In cultured cerebellar granule neurons, β1-β1 *trans* homophilic cell adhesion drives neurite extension through a

109

mechanism that includes *fyn* kinase (Brackenbury, Davis et al. 2008). β1 subunits form heterophilic partnerships with other CAMs, including contactin, N-cadherin, NrCAM, neurofascin, and VGSC β2 subunits, and associate with the extracellular matrix protein, tenascin-R, to modulate cell migration (Xiao, Ragsdale et al. 1999, McEwen and Isom 2004, McEwen, Meadows et al. 2004). Thus, β1 CAM activity is critical for neuronal development.

Human variants in VGSC genes are linked to the developmental and epileptic encephalopathies (DEEs) and to cardiac arrhythmia. Loss-of-function (LOF) variants in *SCN1B*, encoding β1, result in early infantile developmental and epileptic encephalopathy (EI-DEE) and Generalized Epilepsy with Febrile Seizures plus (Bouza and Isom 2018, Aeby, Sculier et al. 2019). *Scn1b*-null mice model EI-DEE, with severe spontaneous seizures of multiple etiologies, ataxia, and sudden death in the third week of life (Chen, Westenbroek et al. 2004). Consistent with loss of β1-mediated cell-cell and cell-matrix adhesion, *Scn1b*-null mice have neuronal pathfinding and fasciculation defects in brain (Brackenbury, Davis et al. 2008, Brackenbury, Yuan et al. 2013). *SCN1B* is expressed in heart in addition to brain. *Scn1b*-null mice have prolonged QT and RR intervals. *Scn1b*-null ventricular cardiomyocytes have increased sodium current, altered calcium handling, altered intercalated disc structure, and prolonged action potential duration (Lopez-Santiago, Meadows et al. 2007, Lin, O'Malley et al. 2015, Veeraraghavan, Hoeker et al. 2018). *SCN1B* variants are associated with human cardiac disease, including Brugada syndrome and atrial fibrillation (Watanabe, Koopmann et al. 2008, Watanabe, Darbar et al. 2009, Olesen, Holst et al. 2012, Ricci, Menegon et al. 2014, Gray, Hasdemir et al. 2018). Thus, *SCN1B* is essential for life.

110

β1 subunits undergo regulated intramembrane proteolysis (RIP) through the sequential activity of β-site Amyloid Precursor Protein (APP) cleaving enzyme-1 (BACE1) and γ-secretase (Wong, Sakurai et al. 2005, Bouza 2020). BACE1 cleavage, the rate-limiting step in this process, releases the extracellular β1 Ig domain, which functions as a CAM ligand to stimulate neurite outgrowth (Davis, Chen et al. 2004, Patino, Brackenbury et al. 2011). The remaining membrane-bound β1-C-terminal fragment (β1-CTF) is cleaved by γ-secretase in the lumen of the membrane, generating a soluble, intracellular domain, β1-ICD, that translocates to the nucleus to regulate transcription (Wong, Sakurai et al. 2005, Haapasalo and Kovacs 2011). Thus, β1 RIP plays important roles in neurite outgrowth, cell migration, cell adhesion, and transcription (Kim, Ingano et al. 2005, Brackenbury and Isom 2011).

BACE1- and γ-secretase-mediated processing of the well-studied RIP substrate, amyloid-β precursor protein (APP), is regulated by *S*-palmitoylation, the covalent addition of a 16-carbon fatty acid to cysteine residues via thioester bond formation (Bhattacharyya, Barren et al. 2013). Palmitoylation targets APP to its proper membrane domains, bringing it in close proximity to proteolytic enzymes for subsequent cleavage (Bhattacharyya, Barren et al. 2013). Here, we asked whether post-translational modification of β1 subunits by tyrosine phosphorylation or *S*-palmitoylation could regulate its plasma membrane localization and subsequent RIP. In contrast to β1-ankyrin association, for which β1 tyrosine phosphorylation is critical (Malhotra, Koopmann et al. 2002), we found that the tyrosine phosphorylation state of β1 has no effect on its membrane localization, intramembrane cleavage, or ability to modulate sodium current (I_{Na}). We report for

the first time that β1 subunits are *S*-palmitoylated in mouse brain. Using heterologous cells, we found that substitution of cysteine (C) residue 162 with alanine (A) abolishes β1 palmitoylation, decreases the fraction of β1 in the plasma membrane as assessed by surface biotinylation and immunocytochemistry, and thus reduces the level of β1 that is available for RIP. Treatment of cells with the clathrin-mediated endocytosis inhibitor, Dyngo-4a, restores β1-p.C162A to wild-type (WT) levels at the plasma membrane. Finally, we show that β1-mediated modulation of sodium current (I_{Na}) and β1 sorting to detergent-resistant membrane fractions do not depend on β1 palmitoylation. Taken together, our work suggests that multiple post-translational modification events regulate β1 function. Tyrosine phosphorylation regulates the association of β1 subunits with ankyrin but does not affect its plasma membrane localization. In contrast, S-palmitoylation regulates the cell-surface localization of β1 and consequently its extent of RIP, indicating that β1 cleavage occurs at the plasma membrane. This work provides novel insights into β1 subunit function that may aid in understanding the mechanism of *SCN1B*-associated pathophysiologies.

Results

β1 RIP occurs independently of β1 tyrosine phosphorylation.

β1 tyrosine residue (Y) 181, located in the intracellular domain, is important for β1-mediated downstream signaling (Malhotra, Koopmann et al. 2002) (Fig. 3.1A). In previous work, we used phosphorylation-null and phosphomimetic mutant constructs to show that phosphorylation of residue Y181 is a key regulatory mechanism for ankyrin binding (Malhotra, Koopmann et al. 2002). Our work in cerebellar granule neurons demonstrated that β1-β1 *trans* homophilic adhesion-mediated neurite outgrowth is inhibited by the administration of γ-secretase inhibitors and in neurons isolated from *fyn* null mice (Brackenbury, Davis et al. 2008, Brackenbury and Isom 2011). Taken together, these data suggested that β1-mediated neurite outgrowth requires association of the β1 intracellular domain with ankyrin, via residue Y181, which then triggers β1 RIP. Here, we tested the hypothesis that β1 tyrosine phosphorylation regulates cleavage using a multi-disciplinary approach.

We used a cell-free fyn kinase assay (Promega), in which ADP was measured via luciferase activity and positively correlated to kinase activity, to determine whether fyn directly phosphorylates a β1 peptide, QENASEYLAITC, at position Y181. Poly E_4Y_1 peptide was used as a positive control for fyn kinase activity (Fig. 3.1B). Inclusion of WT β1 peptide in the assay increased luciferase activity by approximately 3-fold over the no-substrate control. In contrast,

luciferase activity levels in the presence of Y181E β1 peptide (pYβ1) were not different from the no-substrate control. These data indicate that fyn kinase can directly phosphorylate β1 at the Y181 position (Fig. 3.1B).

To understand whether β1 phosphorylation at Y181 affects β1 RIP, we generated two phosphorylation-null, β1-p.Y181A-V5-2AeGFP and β1-p.Y181F-V5-2AeGFP, and one phosphomimetic, β1-p.Y181E-V5-2AeGFP mutant constructs. Chinese Hamster Lung (CHL) cell lines stably overexpressing each construct were generated, and plasma membrane localization of each mutant polypeptide was investigated using cell-surface biotinylation assays (29, 30). Similar to WT β1, all three β1 mutants were detected in the plasma membrane fraction (Fig. 3.1C). To determine if β1 phosphorylation at residue Y181 regulates BACE1- and γ-secretase-mediated cleavage of β1, each cell line was treated with vehicle (0.1% DMSO) or 1 μM DAPT, the γ-secretase inhibitor, and analyzed by western blot. Treatment with DAPT leads to an accumulation of the intermediary cleavage product, β1-CTF, generated by BACE1 cleavage (Bouza 2020). We found that levels of β1-CTF were generated similarly to WT in all three mutant lines and accumulated similarly to WT following treatment with DAPT, suggesting that neither BACE1 nor γ-secretase cleavage of β1 depends on its phosphorylation state (Fig. 3.1 D and E). These results also suggest that our previous work, demonstrating that γ-secretase inhibitors block β1-mediated neurite outgrowth (Brackenbury and Isom 2011), may have implicated other γ-secretase substrates.
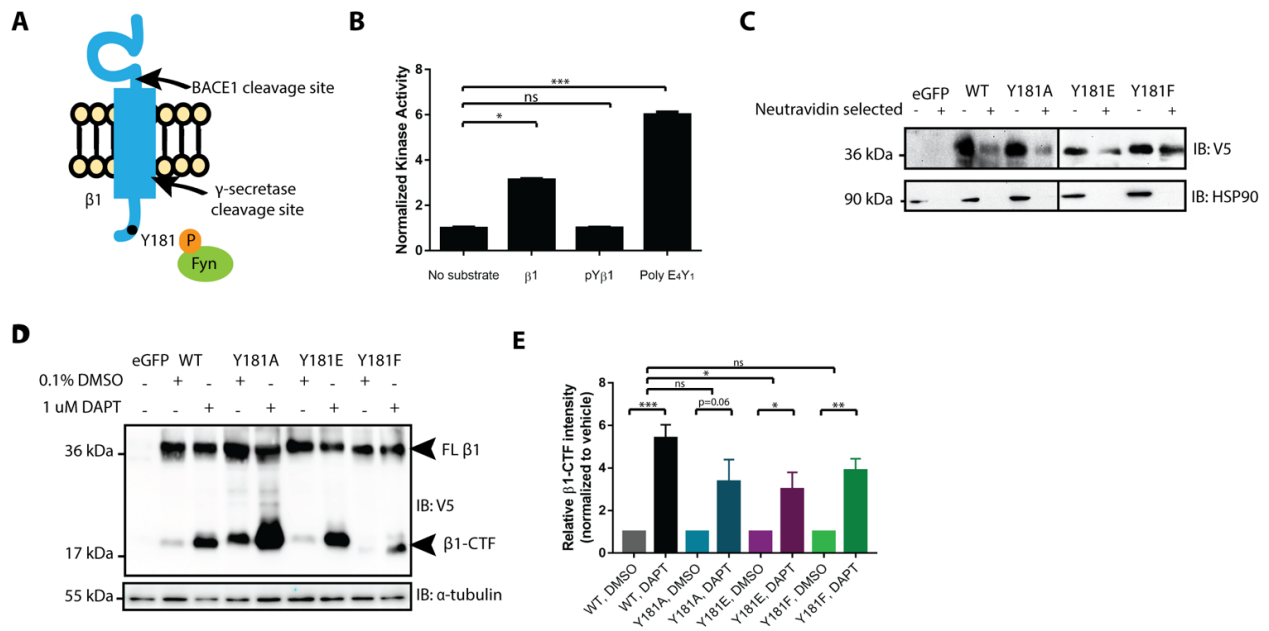
Figure 3.1: β1 phosphorylation at residue Y181 does not affect its RIP. A. Schematic of β1 identifying the location of the phosphorylation site, Y181, as well as BACE1 and γ-secretase cleavage sites. B. A β1 peptide (QENASEYLAITC) is directly phosphorylated at Y181 by fyn kinase in a cell-free assay. N=3. C. Cell surface biotinylation indicates that similar to WT β1-V5, β1-p.Y181A-V5, β1-p.Y181F-V5, and β1-p.Y181E-V5 are localized to the plasma membrane. N=3. D. WT β1-V5, β1-p.Y181A-V5, β1-p.Y181F-V5, and β1-p.Y181E-V5 are cleaved by BACE1 and γ-secretase. N=4. E. Quantification of D. Protein levels were normalized to the loading control and reported as fold change respective to the vehicle treated group. Significance (p-value <0.05) was determined using a one-way ANOVA.

β1 modulation of I_Na occurs independently of β1 tyrosine phosphorylation.

We next asked whether the phosphorylation state of residue Y181 affects the ability of β1 to modulate I_Na. Human Embryonic Kidney (HEK) cells stably expressing Na_v1.5 were transiently transfected with soluble enhanced Green Fluorescent Protein (eGFP), WT β1-V5-2AeGFP, β1-p.Y181A-V5-2AeGFP, β1-p.Y181F-V5-2AeGFP, or β1-p.Y181E-V5-2AeGFP. Inclusion of eGFP facilitated the identification of transfected cells for whole cell voltage patch clamp recordings. Co-expression of WT β1-V5-2AeGFP, β1-p.Y181A-V5-2AeGFP, or β1-p.Y181E-V5-2AeGFP with Na_v1.5 increased I_Na density compared to α alone (transfection of soluble eGFP), suggesting that the phosphorylation state of residue Y181 does not affect the ability of β1 to modulate I_Na density (Fig. 3.2 A and B). We observed no effects of any of the β1 constructs on the voltage-dependence of I_Na activation or inactivation compared to the eGFP control (Fig. 3.2 C and D). Interestingly, β1-p.Y181F-V5-2AeGFP, which was detected in the plasma membrane fraction biochemically, similar to WT β1, predicting its expression at the cell surface, had no effect on I_Na density. These results, showing that β1-p.Y181F localizes to the plasma membrane, functions as a homophilic CAM (Malhotra, Koopmann et al. 2002), and is post-translationally processed by BACE1 and γ-secretase, but does not modulate I_Na density (Fig. 3.2 A and B), is the first demonstration, to our knowledge, of the molecular separation of these β1-mediated effects.
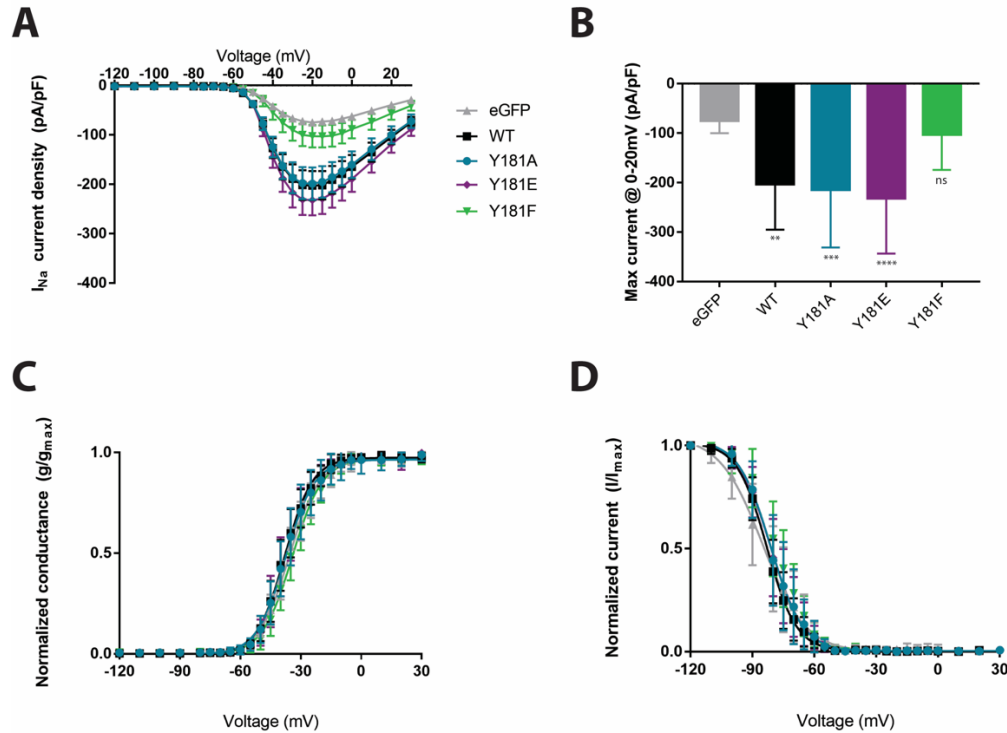
Figure 3.2: β1-mediated modulation of INa is not dependent on phosphorylation of residue Y181. A. I_{Na} density is increased when WT β1-V5, β1-p.Y181A-V5, or β1-p.Y181E-V5 is co-expressed with Na_v1.5. β1-p.Y181A-V5 and β1-p.Y181E-V5 increase I_{Na} density over α alone (eGFP). B. Maximal current is increased when WT β1-V5, β1-p.Y181A-V5, or β1-p.Y181F-V5 is co-expressed with Na_v1.5 compared to eGFP control. β1-p.Y181A-V5 and β1-p.Y181F-V5 increase maximal current to levels similar to WT β1-V5. β1-p.Y181F-V5 has no effect on maximal current compared to the eGFP control. C. Co-expression of WT or mutant β1-V5 subunits has no effect on the voltage-dependence of I_{Na} activation compared to eGFP control. D. Co-expression of WT or mutant β1-V5 subunits has no effect on the voltage-dependence of I_{Na} inactivation compared to eGFP control. N=3, n=10 per condition.

β1 is S-palmitoylated in vitro and in vivo.

APP is a type I transmembrane topology BACE1 substrate that results in the generation of Aβ peptides to form protein aggregates that can contribute to Alzheimer's disease pathogenesis (Cole and Vassar 2007). BACE1-mediated cleavage of APP is highly dependent on the proper localization of APP in lipid raft microdomains (Bhattacharyya, Barren et al. 2013). The post-translational lipid modification, *S*-palmitoylation, is required for proper targeting of APP to lipid rafts (Bhattacharyya, Barren et al. 2013). In lipid rafts, palmitoylated APP interacts with BACE1 for subsequent cleavage (Bhattacharyya, Barren et al. 2013). Given its similarity to APP, we asked whether β1 is also *S*-palmitoylated and, if so, whether *S*-palmitoylation regulates β1 subcellular localization and RIP. To assess steady-state palmitoylation of β1, we used the Acyl Resin Assisted Capture (Acyl RAC) assay, in which free cysteines are first blocked with the alkylating reagent methyl methanethiosulfonate (MMTS). Then, thioester bonds between the cysteine residue of the protein and the palmitate are cleaved using the reducing agent hydroxylamine (HA/NH$_2$OH), to liberate the previously palmitoylated cysteine residues. The liberated cysteines are selectively captured on activated thiol Sepharose beads and eluted, allowing for specific immunoblotting of palmitoylated proteins of interest (Forrester, Hess et al. 2011). We used endogenous flotillin-1, a known constitutively palmitoylated protein (Giri, Dixit et al. 2007), as a positive control for the Acyl RAC assay. In cells stably expressing WT β1-V5-2AeGFP, we observed that β1 is *S*-palmitoylated, as evidenced by hydroxylamine-dependent binding of β1-V5 to Sepharose beads (Fig. 3.3A).

We next asked whether β1 palmitoylation occurs *in vivo*. Using whole mouse brain lysates subjected to Acyl RAC, we observed β1 palmitoylation, as evidenced by hydroxylamine-dependent binding of endogenous β1 to Sepharose beads (Fig. 3.3B). These data demonstrate that β1 is *S*-palmitoylated *in vitro* as well as in mouse brain, providing feasibility for investigating the role of *S*-palmitoylation in β1 localization and proteolytic processing.
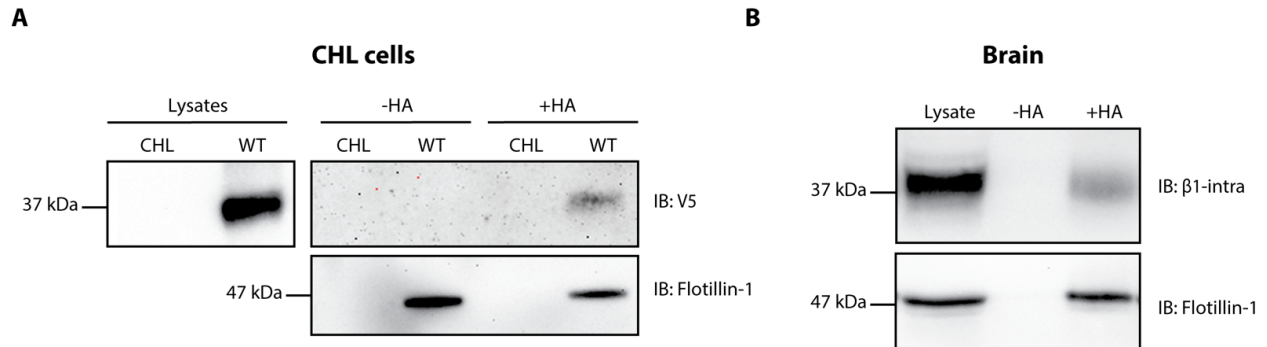
Figure 3.3: β1 is S-palmitoylated in CHL cells and in mouse brain. A. CHL cells stably expressing β1-V5-2AeGFP were processed for the Acyl-RAC assay to detect S-palmitoylation. S-palmitoylation of β1-V5 is detected in CHL cells using an antibody against V5, as shown by the anti-V5 signal in the +HA lane, compared to the expected absence of signal in the -HA lane. Flotillin-1 is used as a positive control for the Acyl-RAC assay. N=3. B. Whole mouse brain lysates were subjected to the Acyl-RAC assay to detect S-palmitoylation. S-palmitoylation of endogenous β1 is detected in whole mouse brains, using an antibody against the C-terminus of β1, as shown by the anti-β1 signal in the +HA lane, compared to the expected absence of signal in the -HA lane. N=3.

β1 is S-palmitoylated at cysteine residue 162.

To identify the palmitoylated cysteine residue(s) in β1, we first determined the number of palmitoylated sites on β1 using a mass-tag labeling technique, Acyl PolyEthylene Glycol exchange (Acyl PEG). In this assay, free cysteine residues are blocked with the alkylating reagent, N-ethyl maleimide. Palmitate groups linked to cysteine residues are subsequently cleaved with hydroxylamine and replaced with a 10 kDa PEG-maleimide group, resulting in a 10 kDa shift in the apparent molecular weight of the polypeptide for each palmitoylated cysteine residue, as detected by western blot (Percher, Ramakrishnan et al. 2016). CHL cells stably expressing WT β1-V5-2AeGFP were subjected to Acyl PEG. We observed a single 10 kDa shift in the apparent molecular weight of β1-V5, which occurred in a hydroxylamine specific manner, suggesting that β1 is singly palmitoylated (Fig. 4A). Based on homology models with the CAM myelin P0, which is *S*-palmitoylated at cysteine 153, we predicted that β1 would be palmitoylated at the homologous residue, cysteine 162 (Bharadwaj and Bizzozero 1995). Using site-directed mutagenesis, we engineered a cDNA construct in which β1 cysteine (C) residue 162 was converted to an alanine (A) and generated a stable β1-p.C162A-V5-2AeGFP CHL cell line. To test the effects of the C162A mutation on β1 palmitoylation, we subjected β1-p.C162A-V5-2AeGFP CHL cell lysates to both Acyl PEG and Acyl RAC. Using Acyl PEG, showed a hydroxylamine-dependent PEGylation-induced mass shift in WT β1-V5 but not in β1-p.C162A-V5, suggesting that β1-p.C162A-V5 cannot be palmitoylated (Fig. 3.4A). We confirmed these results by subjecting β1-p.C162A-V5-2AeGFP CHL cell lysates to Acyl RAC, where we observed virtually no

hydroxylamine-dependent signal for β1-p.C162A-V5, compared to WT β1-V5 (Fig. 3.4B). These results demonstrate that β1 is singly palmitoylated at cysteine 162 and that mutating this site to alanine completely abolishes β1 palmitoylation (Fig. 3.4C).
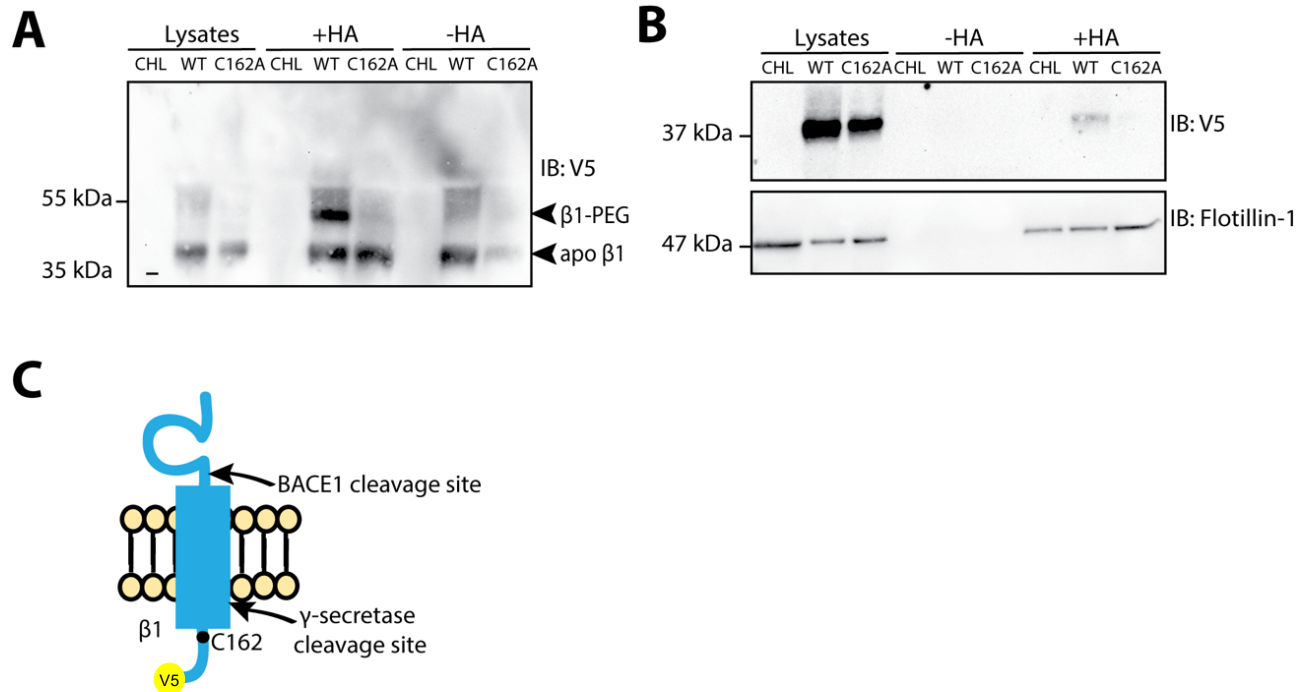
Figure 3.4: β1 is S-palmitoylated at cysteine 162. A. CHL cells stably expressing β1-V5-2AeGFP or β1-p.C162A-V5-2AeGFP were processed for the Acyl PEG assay to determine the number of palmitoylated cysteines on β1. A single 10 kDa shift in the apparent molecular weight of β1 was observed in a hydroxylamine-specific manner, using an antibody against V5. Compared to WT β1-V5, β1-p.C162A-V5 showed no hydroxylamine-dependent PEGylation-induced mass shift, suggesting loss of the palmitoylation site upon mutation of cysteine to alanine at β1 residue 162 of β1. N=3. B. CHL cells stably expressing β1-p.C162A-V5-2AeGFP were subjected to the Acyl-RAC assay to detect the effect of the mutation of β1 S-palmitoylation. S-palmitoylation of β1-p.C162A-V5 is not detected in CHL cells using an antibody against V5, as shown by the absence of anti-V5 signal in the +HA lane, compared to WT β1-V5. N=3. C. Cartoon diagram of β1 and its identified palmitoylation site.

β1 S-palmitoylation regulates its plasma membrane localization.

We asked whether palmitoylation regulates β1 association with the plasma membrane by comparing β1-p.C162A-V5 to WT β1-V5 in cell surface biotinylation assays. We found the level of β1-p.C162A-V5 polypeptide associated with the plasma membrane to be 63% less than WT (6%±4.05 for mutant versus 16%±2.249 for WT), as indicated by the reduced β1-p.C162A-V5 signal in the neutravidin-selected lane, compared to WT β1-V5 (Fig. 3.5 A and B). To further examine membrane localization of WT vs. palmitoylation-deficient β1, we performed immunocytochemistry followed by confocal microscopy. CHL cells stably transfected with WT β1-V5-2A-eGFP or β1-p.C162A-V5-2A-eGFP were stained with the plasma membrane marker, Wheat Germ Agglutinin (WGA) and an antibody directed against the V5-epitope tag to detect WT or mutant β1 (Fig. 3.5C). Colocalization maps were generated using ImageJ. Green signal indicates WGA signal only, red indicates V5 signal only, and white indicates colocalization between V5 signal and WGA. WT β1-V5 and WGA showed strong colocalization at the plasma membrane, as represented by the white arrows. In contrast, there was a marked reduction in the level of colocalization of the β1 palmitoylation-deficient mutant, β1-p.C162A-V5, and WGA (Fig. 3.5C, right-most column). These results suggest that *S*-palmitoylation promotes plasma membrane association of β1. However, in this overexpression system, only a small portion (~16%) of WT β1-V5 is localized to the plasma membrane. Using immunocytochemistry with antibodies directed against the endoplasmic reticulum marker, calnexin, and the V5-epitope tag, we determined that the majority of both WT β1-V5 and β1-p.C162A-V5 is localized to ER (Supplemental Fig. 3.1).
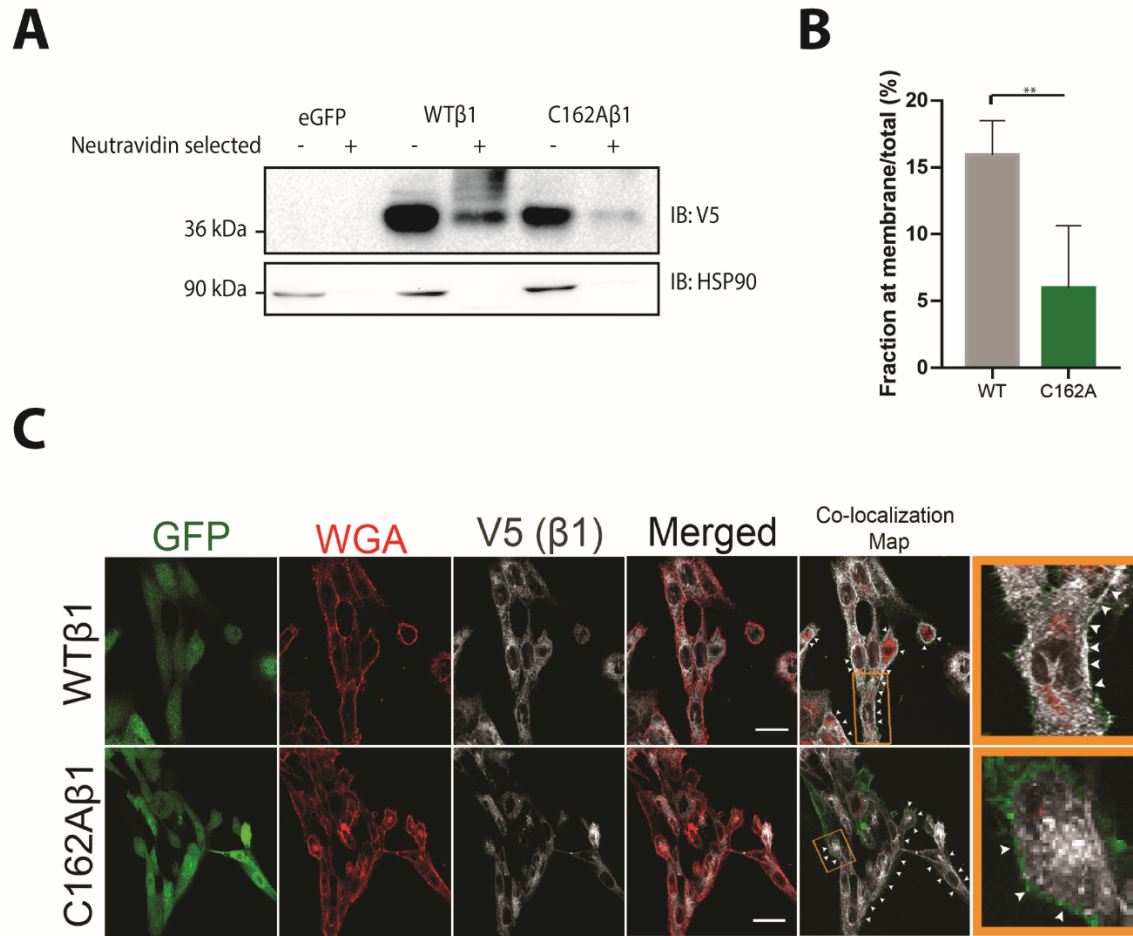
Figure 3.5: S-palmitoylation regulates plasma membrane localization of β1.CHL cells stably expressing β1-V5-2AeGFP or β1-p.C162A-V5-2AeGFP were processed for cell surface biotinylation assay. The level of β1-p.C162A-V5 protein in the biotinylated plasma membrane fraction was reduced compared to WT β1-V5, as evidenced by the lower anti-V5 signal in the neutravidin-selected lane. Soluble HSP90 was used as a negative control. N=4. B. Quantification of A. C. CHL cells stably expressing β1-V5-2AeGFP or β1-p.C162A-V5-2AeGFP were stained for the plasma membrane marker, Wheat Germ Agglutinin (WGA; red), and β1 (V5-epitope tag; white). Colocalization map shows WGA signal only in green, V5 signal only in red, and colocalization in white. WT β1 shows strong colocalization with WGA, while palmitoylation-deficient β1 does not. N=3.
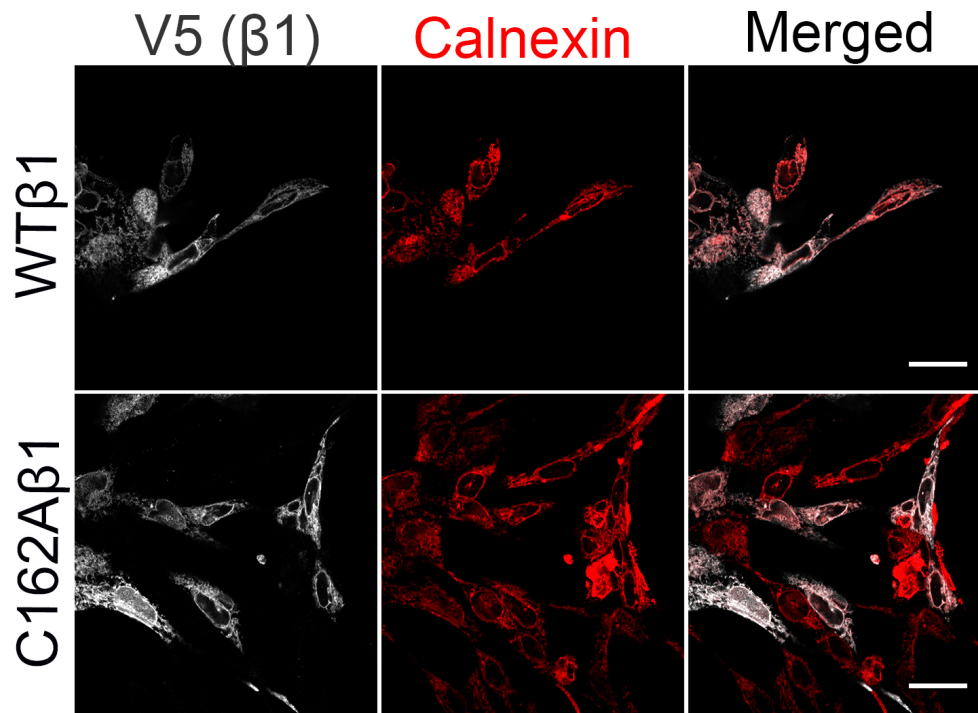
Supplemental Fig. 3.1: The majority of WT β1-V5 or β1-p.C162A-V5 subunits are localized to the ER in heterologous cells. CHL cells stably expressing β1-V5-2AeGFP or β1-p.C162A-V5-2AeGFP were stained for the ER marker, Calnexin (red), and β1 (V5-epitope tag; white).

S-palmitoylation regulates β1 endocytosis, but not sorting into detergent-resistant membranes

Palmitoylation has been shown to regulate the partitioning of certain proteins to cholesterol-rich lipid raft microdomains (Levental, Lingwood et al. 2010). We asked whether palmitoylation governed the localization of β1 to lipid rafts, similarly to what has been shown previously for APP (Bhattacharyya, Barren et al. 2013). β1 is known to localize to detergent-resistant membrane (DRM) fractions of mouse brain and primary neuronal cultures (Wong, Sakurai et al. 2005, Brackenbury, Davis et al. 2008). To verify the presence of β1 in DRM fractions in CHL cells stably expressing WT β1-V5, we prepared DRMs using density gradient centrifugation and analyzed them by western blot using anti-V5 antibody. We found that WT β1-V5 was present in both detergent-insoluble fractions, marked with flotillin-1, and in detergent-soluble fractions, marked with transferrin receptor, similar to previous results (Davis, Chen et al. 2004) (Fig. 3.6A). We observed no differences in this distribution for the palmitoylation-null mutant, β1-p.C162A-V5, as evidenced by the presence of anti-V5 signal in both flotillin-1-marked DRMs and transferrin receptor-marked non-lipid raft domains (Fig. 3.6A). These data suggest that, while palmitoylation of β1 is necessary for its proper association with the plasma membrane, it does not regulate the partitioning of β1 into lipid-raft domains.

Due to the observed reduction of β1-p.C162A at the plasma membrane, we compared the extent of WT β1 vs β1-p.C162A internalization through endocytosis. We treated CHL cells stably

127

expressing β1-V5-2A-eGFP or β1-p.C162A-V5-2A-eGFp with vehicle (0.1% DMSO) or 1 μM of the dynamin inhibitor, Dyngo-4a, and assessed the amount of β1-V5 vs. β1-p.C162A-V5 accumulation at the cell surface by biotinylation. Anti-HSP90 antibody was used as a negative control for the plasma membrane fraction and anti-transferrin receptor (TfR) antibody was used as a positive control for endocytosis inhibition with Dyngo-4a. We found that Dyngo-4a administration normalized the level of β1-p.C162A-V5 in the plasma membrane fraction to that of WT β1, implicating clathrin-dependent endocytosis in this process (Fig. 3.6B). This work adds new information to the VGSC field, showing that WT β1 subunits undergo endocytosis via a clathrin-dependent mechanism.
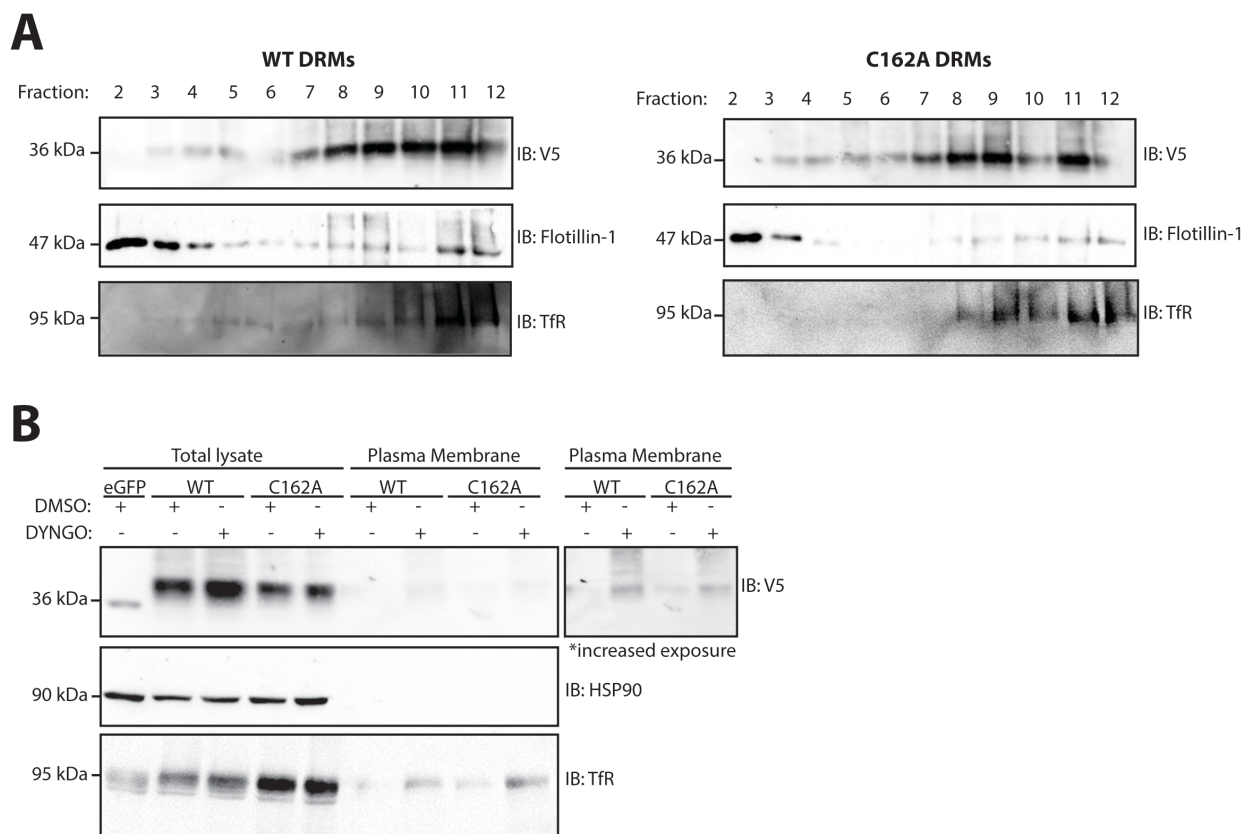
Figure 3.6: S-palmitoylation regulates β1 endocytosis, but not sorting into detergent-resistant membranes. A. CHL cells stably expressing β1-V5-2A-eGFP or β1-p.C162A-V5-2A-eGFP were processed for discontinuous flotation density gradients to investigate the role of palmitoylation in detergent-resistant membrane partitioning of β1. β1-p.C162A-V5 did not partition differently than WT β1-V5. Flotillin-1 was used as a marker for lipid rafts, whereas Transferrin Receptor (TfR) was used as a marker for non-raft domains. N=3. B. CHL cells stably expressing β1-V5-2A-eGFP or β1-p.C162A-V5-2A-eGFP were treated with vehicle (0.1% DMSO) or 1 μM Dyngo-4a and assessed by cell surface biotinylation. Dyngo-4a treatment restores the plasma membrane level of β1-p.C162A-V5 to that of WT β1. N=3.

The level of β1-p.C162A RIP is reduced compared to WT.

We hypothesized that reduction in plasma membrane localization of β1-p.C162A-V5 would reduce its level of RIP. To test this hypothesis, we treated stable β1-V5-2AeGFP or β1-p.C162A-V5-2AeGFP CHL cells with vehicle (0.1% DMSO) or 1 μM DAPT, and assessed formation of the ~20 kDa β1 intramembrane CTF by western blot analysis. As shown previously, inhibition of γ-secretase by DAPT results in β1-CTF accumulation in the presence of normally occurring BACE1 cleavage (Bouza 2020). If BACE1-mediated β1 cleavage is altered or reduced, DAPT administration results in reduced levels of β1-CTF accumulation, due to a reduction in available substrate for γ-secretase-mediated RIP. As expected, DAPT treatment of CHL cells stably expressing WT β1-V5 resulted in β1-CTF accumulation (Fig. 3.7A and B). In contrast, using the β1-p.C162A-V5 mutant construct as substrate resulted in an 80% loss in the level of cleavage product compared to WT (Fig. 3.7A and B). This result suggests that BACE1 cleaves the small fraction of β1-p.C162A-V5 that is localized to the plasma membrane, generating a reduced level of β1-CTF in response to DAPT treatment, compared to WT β1. These data demonstrate that β1 palmitoylation promotes β1 plasma membrane localization, which allows RIP to occur.
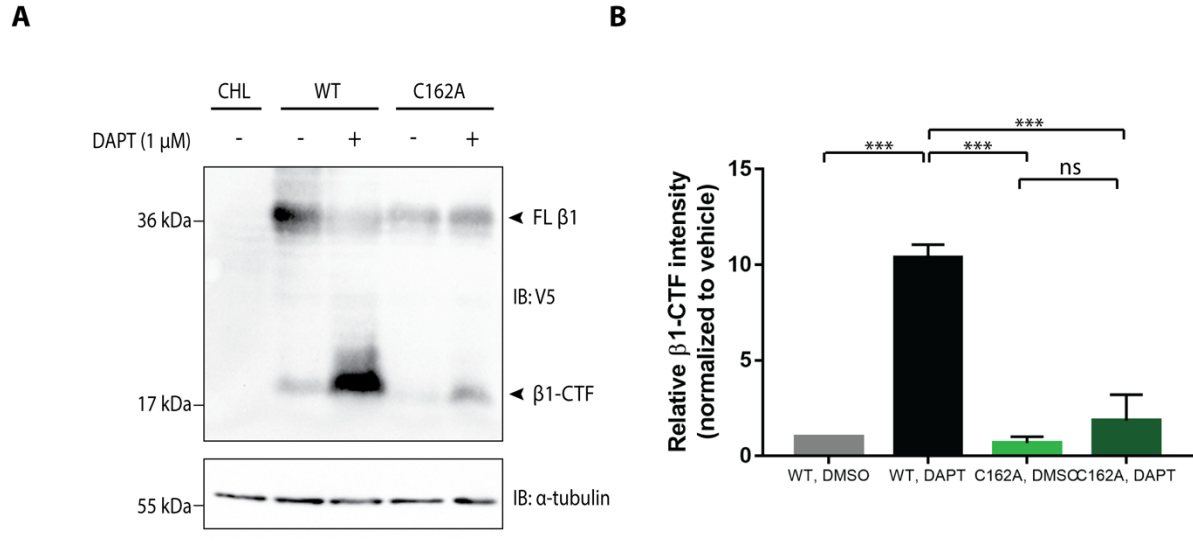
Figure 3.7: The absence of β1 S-palmitoylation at cysteine 162 reduces its intramembrane cleavage. A. CHL cells stably expressing β1-V5-2AeGFP or β1-p.C162A-V5-2AeGFP were treated with vehicle (0.1% DMSO) or 1 μM DAPT. Lysates were subjected to western blotting analysis to investigate the level of β1 cleavage. Compared to WT β1-V5, β1-p.C162A-V5, shows little to no cleavage product. N=3. B. Quantification of A. Protein levels were normalized to the loading control and reported as fold change respective to the vehicle treated group. Significance (p-value <0.05) was determined using a Student's t-test between vehicle and DAPT treated groups for each β1 construct.

β1 mediated modulation of I_{Na} is not affected by palmitoyalation

We next asked whether palmitoylation-deficient β1-p.C162A-V5 could modulate I_{Na}. WT β1-V5-2AeGFP, β1-p.C162A-V5-2AeGFP, or eGFP were transiently expressed in HEK cells stably overexpressing $Na_v1.5$. We found that WT β1-V5 and β1-p.C162A-V5 increased I_{Na} density to a similar extent, compared to the soluble eGFP control (Fig. 3.8A and B). We observed no effect of either β1 construct on the voltage-dependence of I_{Na} activation or inactivation (Fig. 3.8C and D). These data suggest that the small fraction of β1-p.C162A-V5 that remains properly localized to the plasma membrane (Fig. 3.5A and B) is sufficient to modulate I_{Na}.
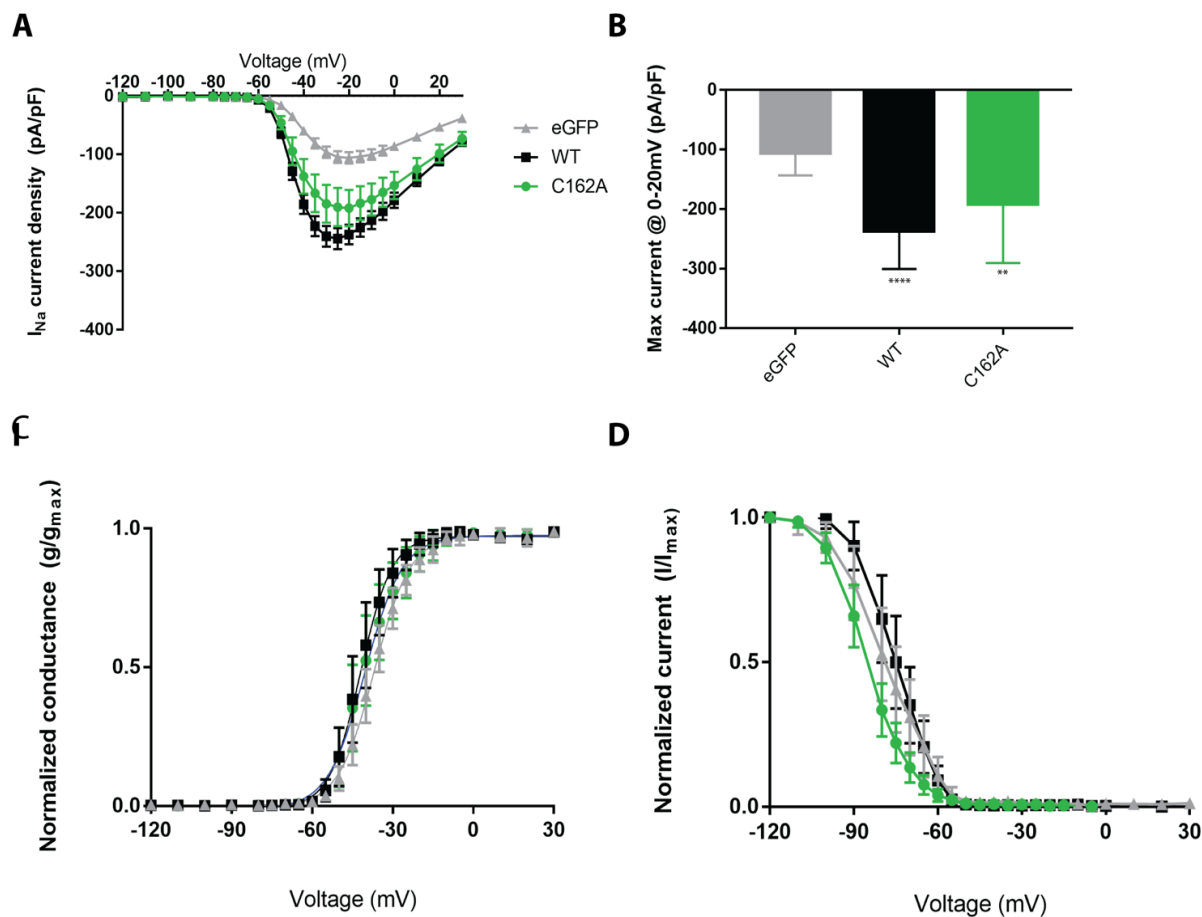
Figure 3.8: β1-mediated modulation of I_{Na} density is not dependent on S-palmitoylation of β1 at residue C162. A. I_{Na} density is increased when WT β1-V5 or β1-p.C162A-V5 is co-expressed with $Na_v1.5$ in HEK cells. B. Co-expression of WT β1-V5 or β1-p.C162A-V5 with $Na_v1.5$ increases maximal I_{Na} compared to eGFP control. C. Neither WT β1-V5 nor β1-p.C162A-V5 affects the voltage-dependence of I_{Na} activation compared to eGFP control. D. Neither WT β1-V5 nor β1-p.C162A-V5 affects the voltage-dependence of I_{Na} inactivation compared to eGFP control. N=3, n=10 per condition.

Discussion

VGSC β1 subunits are multi-functional. In addition modulation of the gating, kinetics, and localization properties of VGSC α subunits, β1 subunits function in cell adhesion, cell migration, calcium handling, modulation of potassium currents, neuronal pathfinding, fasciculation, and neurite outgrowth (Bouza and Isom 2018). Human *SCN1B* LOF variants are linked to EI-DEE and cardiac arrhythmia, often resulting in sudden death (Bouza and Isom 2018).

It's important to understand how β1 subunits are post-translationally processed. We showed previously that β1 is tyrosine phosphorylated. Here, we extend those findings to show that fyn kinase directly phosphorylates a β1 peptide. β1 subunits undergo RIP through the activity of BACE1 and γ-secretase (Wong, Sakurai et al. 2005, Bouza 2020). Initial cleavage of β1 by BACE1 sheds the β1 Ig ectodomain and leaves behind the β1 C-terminal fragment in the membrane, which undergoes subsequent cleavage by γ-secretase to generate a soluble intracellular domain (β1-ICD) (Wong, Sakurai et al. 2005). Recent work by our laboratory demonstrated that β1-ICD translocates to the nucleus, where it acts as a transcriptional regulator and modulates sodium, potassium, and calcium currents in mouse ventricular myocytes (Bouza 2020). Overexpression of β1-ICD resulted in the downregulation of genes related to proliferation, immune response, and sodium and potassium channels. In contrast, loss of β1-ICD in *Scn1b*-null mouse cardiac ventricular tissue

resulted in the upregulation of these gene groups, suggesting that the β1-ICD may act as a transcriptional repressor under normal physiological conditions.

Here, we demonstrate that β1 is lipid-modified by *S*-palmitoylation in the brain, that *S*-palmitoylation, but not tyrosine phosphorylation, regulates β1 RIP by facilitating β1 localization to the plasma membrane, and that β1 subunits undergo clathrin-mediated endocytosis. This work suggests that β1 must be associated with the plasma membrane for RIP to occur and that *S*-palmitoylation modulates β1 plasma membrane association and β1 endocytosis. Residue C162, at which β1 is palmitoylated, is conserved in VGSC β2 and β3 subunits, and thus may implicate palmitoylation as a similar regulatory mechanism in these proteins. Previous work has shown that palmitoylation of APP also promotes its RIP through its proper subcellular localization (Bhattacharyya, Barren et al. 2013). Although other RIP substrates, e.g. LRP1 and N-cadherin, have been shown to be palmitoylated, whether palmitoylation regulates their RIP in not known (Haapasalo and Kovacs 2011, Blanc, David et al. 2015).

S-palmitoylation is a reversible posttranslational modification, making it a highly dynamic and tunable process (El-Husseini Ael, Schnell et al. 2002, Noritake, Fukata et al. 2009, Brigidi, Sun et al. 2014, Brigidi, Santyr et al. 2015). Multiple palmitoyl acyltransferase enzymes, which mediate substrate palmitoylation, as well as protein thioesterases, which depalmitoylate substrates, are implicated in this process. The molecular identities of the enzymes that palmitoylate and

depalmitoylate β1 subunits are not known, but may be identified in the future to discover novel targets for *SCN1B*-linked pathophysiology. In addition, we do not know whether the level of β1 palmitoylation can be dynamically regulated by extracellular stimuli or by altered excitability, but this information will be important to elucidate as attempts to implicate this posttranslational processing in disease mechanisms move forward. It is possible that β1-mediated transcriptional regulation vai RIP can be manipulated via altering the level of β1 palmitoylation. Finally, the effects of *SCN1B* disease-linked variants on β1 subunit palmitoylation, RIP, and transcriptional regulation should be considered.

Materials and Methods

Cell culture

CHL stably expressing cell lines and HEK Na$_v$1.5 cells were sustained in Dulbecco's Modified Eagle Medium with 5% heat inactivated fetal bovine serum, penicillin/streptomycin, and 600 µg/mL at 37°C, 5% CO_2. Stable cell lines were created by transfecting parental CHL cells with 1 µg of cDNA with 5 µL of Lipofectamine 2000. 48 hours following transfection, cells were split into media containing 600 µg/mL G418 (Gibco). The cells were grown for approximately one week or until eGFP positive colonies were large enough to isolate. Individual colonies were selected and grown until confluent and characterized by western blot analysis. Patch clamp experiments used transient transfection of *SCN1B* cDNAs into HEK cells stably expressing Na$_v$1.5. 1 µg of cDNA was transfected with 5 µL of Lipofectamine 2000 (Invitrogen). Approximately 12 hours post-transfection cells were plated for electrophysiological recordings. Patch clamp was completed approximately 12 hours post final plating.

Antibodies

Primary antibodies used were: anti-β1$_{intra}$ (1:1000 dilution), anti-V5 (1:1000 dilution, Invitrogen), anti-α-tubulin (1:1000 dilution, Cedar Lane), anti-BACE1 (1:1000, Invitrogen), anti-HSP90 (1:1000 dilution, EnzoScientific), anti-TfR (1:1000 dilution, Thermo), and anti-Flotillin-1 (1:1000, Cell Signaling Technologies). The specificity of anti-β1$_{intra}$ has been shown previously by western

blot. HRP-conjugated secondary antibodies were used in this study. Goat anti-rabbit or goat anti-mouse HRP-conjugated antibodies were diluted 1:1000 (anti-β1$_{intra}$, anti-α-tubulin, anti-presenilin-1, anti-BACE1, anti-TfR) or 1:10,000 (anti-V5, anti-Flotillin-1 or anti-HSP90). Alexa Fluor 568 anti-mouse was used as a secondary (1:500 dilution) as a secondary antibody for anti-V5 in immunocytochemistry experiments.

Expression Vectors

A synthesis-optimized human WT β1-V5-2A-eGFP cDNA was generated by gBLOCK from Integrated DNA technologies. The bicistronic cDNA construct included an in-frame β1 C-terminal V5 epitope tag followed by a self-cleaving 2A peptide and enhanced Green Fluorescent Protein (eGFP) to facilitate immune-detection of β1 as well as transfected cells by eGFP. β1-p.C162A-V5-2A-eGFP, β1-p.Y181A-V5-2A-eGFP, β1-p.Y181E-V5-2A-eGFP, and β1-p.Y181F-V5-2A-eGFP were generated by site-directed mutagenesis using the WT β1-V5-2A-eGFP cDNA construct in pENTR-SD/D TOPO as the template. The eGFP alone control was generated by PCR from their respective full-length template cDNAs containing WT β1-V5-2A-eGFP. Using the Gateway cloning system, all constructs were moved from pENTR-SD/D-TOPO to pcDNAdest40 via LR Clonase reaction according to the manufacturers' protocol.

Measurement of sodium currents by whole-cell voltage clamp

Voltage-clamp recordings were performed at room temperature in the whole-cell configuration using an Axopatch 700B amplifier and pClamp (versions 11, Axon Instruments, Foster City, CA) with 1.5–2.5 MΩ patch pipettes. Sodium currents were recorded in the presence of a bath solution containing (in mM): 120 NaCl, 1 BaCl2, 2 MgCl2, 0.2 CdCl2, 1 CaCl2, 10 HEPES, 20 TEA-Cl and 10 glucose (pH 7.35 with CsOH, Osmolarity: 300 – 305 mOsm). Fire-polished patch pipettes were filled with an internal solution containing (in mM): 1 NaCl, 150 N-methyl-D-glucamine, 10 EGTA, 2 MgCl2, 40 HEPES, and 25 phosphocreatine-tris, 2 MgATP, 0.02 Na2GTP, 0.1 Leupectin (pH 7.2 with H2SO4). Sodium current was recorded in response to a series of voltage steps between -100 and +30 mV in 5 mV increments, from a holding potential of -90 mV for 200 msec. A step back to -20 mV for 200 msec was used to determine the voltage-dependence of inactivation. Series resistance was compensated 40–65% and leak subtraction performed by application of a standard P/4 protocol. Normalized conductance and inactivation curves were generated as described previously . Current densities were determined by dividing current amplitude by the cell capacitance (Cm), as determined by application of +10 mV depolarizing test pulses.

Western blot analysis of cell lysates

Cell lysates were prepared either as described below for cleavage assays, surface biotinylation assays or DRMs, as appropriate. Loading buffer containing SDS, 5mM β-mercaptoethanol, and 1% dithiothreitol was added to samples and heated for 10 min at 85°C. Protein lysates were

separated by SDS-PAGE on 10 or 12% Tris-Glycine polyacrylamide gels as indicated in the figure legends, transferred to nitrocellulose membrane overnight (16 h, 55 mA, 4°C), and probed with the needed antibodies, as indicated in the figure legends. Incubations with anti-V5 or anti-$\beta1_{intra}$ and their respective secondary antibodies were performed using a SnapID with 10-20 min incubations. Anti-α-tubulin, anti-TfR, anti-Flotillin-1, and anti-HSP90 antibodies were incubated overnight at 4°C. Secondary antibodies for anti-α-tubulin, anti-TfR, anti-Flotillin-1, and anti-HSP90 were incubated for 1 h at room temperature (RT). Immunoreactive bands were detected using West Femto chemiluminescent substrate (GE Health Sciences) and imaged using an iBrightFL1000 (Invitrogen). Immunoreactive signals from cleavage assays were quantified using ImageJ and normalized to the level of α-tubulin and subsequently to vehicle treated samples.

Cleavage assays

Stably transfected CHL cells were grown until approximately 70% confluent in 100 mm tissue culture plates. Cells were treated with either vehicle (0.1% DMSO) or 1 μM DAPT (Cayman Chemical), as indicated in the figure legends. After a 24 hour treatment, cells were harvested, and membranes were prepared. Briefly, cells pellets were harvested and resuspended in 50 mM Tris, pH 8.0 with Complete protease inhibitors, EDTA-Free (Roche). On ice, cells were homogenized 10 times with a dounce followed by sonication. To remove nuclei and insoluble material, lysates were spun at 2,537xg for 10 at 4°C. The supernatant was removed and spun at 80,000 x g for 15 min at 4°C. The supernatant was removed, and the membrane-containing pellets were resuspended

in 133 μL of 50 mM Tris, pH 8.0 with Complete protease inhibitors, EDTA-Free (Roche) and sonicated on ice to resuspend the membrane-containing pellets. Samples were heated at 85°C for 10 minutes and separated using 12% SDS-PAGE gels and western blots were performed as described above.

Surface biotinylation assays

Stably transfected cells were grown to 90%-100% confluence in 100 mm tissue culture plates. Cell surface proteins were biotinylated using the Cell Surface Protein Isolation Kit (Pierce) following the manufacturer's instructions and as previously described (Patino, Claes et al. 2009). All samples were heated at 85°C for 10 minutes and separated on 10% SDS-PAGE gels. Western blots were performed as described above. For endocytosis experiments, prior to cell surface biotinylation, cells were treated with vehicle (0.1% DMSO) or 1 μM Dyngo-4a for two hours in a 37°C incubator with 5% CO_2.

Detergent Resistant Membrane (DRM) preparations

10, 100mm dishes of CHL cells stably transfected with WT β1-V5-2AeGFP or p.C162A β1-V5-2AeGFP were grown to 90-100% confluent. As described previously (Reverter, Rentero et al. 2011), cells were washed and resuspended in 2.5 mL of HES buffer (20mM HEPES, 1mM EDTA, 250mM sucrose, pH7.4) supplemented with 1mM Na_3VO_4 and Complete Protease Inhibitors (Roche). Cells were homogenized by 10 passages through a 22 gauge needle and centrifuged at

245,000g for 90 minutes at 4°C. Membranes were resuspended with 10 passages through a 22 gauge needle in 2.5 mL of MBS buffer (25mM MES, 150mM NaCl, pH6.5) with 1% Triton X-100 and Complete Protease Inhibitors (Roche) and incubated for 20 minutes at 4°C. Homogenate was mixed with 2.5 mL of 90% sucrose. 5 mL of 35% sucrose and 2.5 mL of 5% sucrose were overlaid and samples were centrifuged at 200,000g in a swinging bucket rotor for 17 hours. 1 mL fractions were collected from top to bottom, heated at 85°C for 10 minutes with sample buffer, and subsequently analyzed by western blot.

Immunocytochemistry and confocal microscopy

Approximately 100,000 CHL cells stably expressing WT β1-V5-2AeGFP, p.C162A-V5-2AeGFP, or eGFP were plated on 10mm MatTek glass bottom dishes. 24 hours post plating, cells were incubated on ice for 15 minutes at 4°C before staining with wheat germ agglutinin (WGA) for 10 minutes at 4°C. Cells were washed 2x with PBS for 5 minutes at 4°C. For ER staining with the ER marker calnexin, cells were fixed with 100% methanol for 5 minutes, permeabilized with 0.1% triton in PBS for 5 minutes, and blocked with 1% BSA/10% goat serum/0.3M glycine in PBS containing 0.2% tween for 1 hour at room temperature. The cells were incubated with rabbit anti-calnexin antibody (Abcam ab22595) at 1:1000 and mouse anti-V5 (ThermoFisher??) at 1:1000, overnight at 4°C in a humidified chamber. After 3 consecutive 10min washes with PBS containing 0.2% tween, the cells were incubated with secondary antibody (goat anti rabbit 350 Alexa Fluor and donkey anti mouse 687 Alexa Fluor, diluted 1:250 in block buffer) for 1 hour at room

temperature. Cells were washed 3x for 10 minutes with PBS containing 0.2% tween before

mounting with Prolong Gold. For non-ER staining, following WGA staining, cells were fixed with

4% paraformaldehyde for 20 minutes, permeabilized with 0.2% triton in PBS for 10 minutes, and

blocked with 5% BSA in 0.1% tween in TBS for 1 hour at room temperature. Cells were then

incubated with mouse anti-V5 antibody diluted 1:1000 in block buffer, overnight at 4°C in a

humidified chamber. After 3 10 min washes with PBS containing 0.2% tween, cells were incubated

with secondary antibody (donkey anti mouse 687 Alexa Fluor, diluted 1:250 in block buffer) for

1 hour at room temperature. Cells were washed 3x for 10 minutes with PBS containing 0.2% tween

before mounting with Prolong Gold. Samples were imaged on a Zeiss LSM 880 with a 63x NA1.4

Oil/DIC Plan-Apochromat objective in airyscan mode. Excitation was accomplished using 405,

488, 561, and 633 nm lasers. All images were further processed in Adobe Photoshop CS6 software.

Acyl Resin Assisted Capture (Acyl RAC)

Stably transfected cells were grown until approximately 90% confluent in 100 mm tissue culture

plates. Cells were lysed in buffer containing 100 mM HEPES, 1 mM EDTA, 2.5% SDS, and 2%

methyl methanethiosulfonate (MMTS) (Sigma), adjusted to pH 7.5, sonicated, and left to rotate at

40°C overnight. Acetone precipitation was performed to remove MMTS: 3x volume of cold

acetone were used to precipitate the protein for 20 min at -20°C, before spinning down in standard

bench-top ultracentrifuge at 5000 x g for 1 min. The supernatant was discarded and the pellet was

washed 3x with 70% acetone, each time discarding the supernatant. Protein pellet was left to dry

in air and stored overnight at -20°C. Twelve hours later, protein was resuspended in 500 μL of "binding" buffer containing 100 mM HEPES, 1 mM EDTA, and 1% SDS, adjusted to pH 7.5, sonicated, and vigorously shook for 1 h, before splitting the protein sample into 3 1.5mL tubes, 1 with 40 μL for "unmanipulated" starting material, and 2 with 220 μL for the palmitoylation assay (one for +HA and one for -HA condition). A 1:1 slurry of pre-activated thiopropyl sepharose beads (GE) was prepared using binding buffer (50 mg beads = 250 μL of binding buffer). 50 μL of the activated bead slurry was added to each 220 μL lysate. 50 μL of freshly prepared 2 M hydroxylamine (HA) (Sigma), adjusted to pH 7.5, were then added to the lysate designated "+HA", while 50 μL of 2M NaCl were added to the sample designated "-HA". Hydroxylamine/bead/lysate mixtures were left to incubate at RT for 2.5 h, rotating. To wash out the hydroxylamine and NaCl, the beads were spun at 5000 x g for 1 min, and the supernatant was removed and discarded. Bead resin was washed 5x with 1 mL of binding buffer, each time spinning at 5000 x g for 1 min and discarding the supernatant to recover the beads. Palmitoylated proteins were eluted using 50 μL of 5x sample buffer supplemented with 100 mM DTT. Samples were heated at 65°C for 10 min, loaded on a 10% SDS-PAGE gel, and probed with anti-V5, using flotillin-1 as a positive control.

Acyl PolyEthylene Glycol (Acyl PEG)

Stably transfected cells were grown until approximately 90% confluent in 100 mm tissue culture plates. Cells were lysed with blocking buffer consisting of 100 mM HEPES, 150 mM NaCl, 5 mM EDTA, 2.5% SDS, and 200 mM tris(2-carboxyethyl)phosphine (TCEP) (Sigma), adjusted to pH

7.5, sonicated, and rotated at RT for 1 h. After 1 h, 12.5 μL of freshly prepared 1 M N-ethyl maleimide (NEM) (dissolved in ethanol) (Sigma) for 25 mM final NEM concentration were added to each lysate, with rotation overnight at room temperature. To scavenge the NEM, 12.5 μL of 2,3-dimethyl 1,3-butadiene (Sigma) were added to each sample and rotated vigorously for one hour at RT. 100 μL of chloroform were added to each sample, vortexed vigorously for 1 min, and centrifuged at max speed for 3 min to achieve phase separation. The supernatant on top of the resulting 'protein pancake' was split into 3 1.5 mL tubes: 1 containing 40 μL for "unmanipulated" starting material, 1 containing 100 μL designed for "+HA" condition, and 1 containing 100 μL designated for "-HA" condition. 20 μL of 2 M freshly prepared hydroxylamine (HA) (Sigma), adjusted to pH 7.5, were added to the lysate designated "+HA", while 20 μL of 2 M NaCl were added to the lysate designated "-HA". The HA/lysate mixture was incubated for 2 h at 40°C, rotating. The HA and NaCl were desalted using a pre-equilibrated 40K MWCO Zebaspin desalting column (Thermofisher). 10 μL of a freshly prepared 20 mM stock of 5 kDa mPEG-maleimide (Sigma) (dissolved in water) were added to each desalted lysate and incubated for 2 h at 40°C, rotating. 100 μL of 5x sample buffer supplemented with 100 mM DTT were added to stop the mPEG-maleimide alkylation reaction and heated for 10 min at 65°C. The samples were loaded on a 10% SDS-PAGE gel and probed with anti-V5.

Fyn kinase assay

Fyn kinase assay was performed according to manufacturer's recommendations (Fyn kinase assay kit, Promega). Reactions were performed in triplicate and each reaction contained 200 ng of active GST-tagged Fyn kinase, 50 uM Ultrapure ATP, 0.2 mg/mL peptide substrate, 50 μM DTT diluted in a standard kinase reaction buffer (contents of 5X buffer: 40 mM Tris pH 7.5, 20 mM MgCl2, 0.1 mg/mL BSA). β1 peptides corresponded to intracellular domain of β1 surrounding Y181 (amino acids 175 to 185; β1 peptide, QENASEYLAITC; pYβ1 peptide, QENASE[pY]LAITC). The Poly E 4 Y 1 peptide is a well-characterized substrate of fyn kinase. Kinase reactions lacking substrate were used to normalize the kinase activity in substrate containing reactions. Three independent experiments were performed. Statistical significance was determined with Student's t-test.

Statistics

Statistical analysis for cleavage assay experiments were completed with n=3-4 for each experiment. Data are represented as the mean ± SEM. β1 mutant cleavage experiments were completed as one-way ANOVA with multiple comparisons to WTβ1 treated with DAPT. For the fyn kinase assay, three independent experiments were performed. Statistical significance was determined with Student's t-test. Data are represented as the mean ± SEM. Electrophysiology experiments had an n of 10-15 cells per condition for each experiment. The voltage-dependence of activation and inactivation were compared using nonlinear fit, maximum current was analyzed

146

using one-way ANOVA with multiple comparisons, and current density was compared to the

control, eGFP, with an unpaired t-test at each voltage-step.

Chapter 4 Discussion and Future Directions

Alexandra A. Bouza, Siena Snyder, Gemma L. Carvill, PhD, and Lori L. Isom, PhD

Summary and Significance

Variants in *SCN1B,* which encodes β1, are linked to diseases with high risk of sudden death, including Early Infantile Epileptic Encephalopathy 52 (EIEE52, also called early infantile developmental and epileptic encepaholpathy) and Brugada Syndrome (Calhoun and Isom 2014, Bouza and Isom 2018). *Scn1b*-null mice are a model of EIEE52 and phenotypically present with spontaneous seizures and cardiac abnormalities as well as ataxia and failure-to-thrive (Chen, Westenbroek et al. 2004). Our research group is focused on understanding the roles of VGSC α and β subunits under normal physiological conditions and in pathology. My body of work has focused on VGSC β1 subunits, and how variants in *SCN1B* contribute to β1 dysfunction and ultimately, *SCN1B*-linked pathophysiology. My doctoral dissertation describes how I investigated the biochemical regulation and downstream signaling of VGSC β1 subunit processing by BACE1 and γ-secretase (Wong, Sakurai et al. 2005).

Using a cell culture method, we demonstrated that β1 is a substrate for sequential cleavage by BACE1 and γ-secretase. These sequential cleavage events generate a soluble peptide, the β1-ICD, which translocates to the nucleus where it can modulate transcription. Utilizing RNA-seq, we

identified gene ontology (GO) groups that were, in general, downregulated in response to β1-ICD overexpression in heterologous cells and, in general, upregulated in *Scn1b* null mouse cardiac ventricle, in which the β1-ICD was deleted. These results suggest that the β1-ICD may normally function as a molecular brake, both *in vitro* and *in vivo*. For example, in our experiments complementary changes in gene expression were observed for a group of voltage-gated potassium channel (VGKC) genes. Overexpression of the β1-ICD in cell culture resulted in decreases in VGKC mRNA, while *Scn1b* deletion in mouse cardiac ventricle led to increases in VKGC mRNA. Consistent with changes in gene expression, we observed increased potassium current in ventricular myocytes acutely isolated from *Scn1b*-null animals compared to wild-type. In addition to changes in VGKC gene expression, we found that heterologous overexpression of the β1-ICD resulted in increased VGSC α subunit mRNAs, although we were not able to detect changes in sodium current density. These data show β1 subunit processing by BACE1 and γ-secretase generates a novel, transcriptional modulator, β1-ICD, which ultimately contributes to regulating cellular excitability by altering transcription of VGKC genes. Finally, we showed that β1 palmitoylation, but not tyrosine phosphorylation, regulates β1 cell surface expression and thus β1 cleavage. Using a β1 palmitoylation-null mutant, β1-p.C162A, we found that cleavage is significantly reduced, suggesting that BACE1-mediated β1 cleavage occurs at the plasma membrane.

This body of work identified a novel, non-conducting role for VGSC β1 subunits as transcriptional modulators - which ultimately contributes to the regulation of cellular excitability. Understanding the basic biochemistry and signaling mechanisms of β1 is critical in learning how patient variants in *SCN1B* result in neurological and cardiac diseases. Further work elucidating this newly identified β1-mediated signaling pathway may reveal novel therapeutic targets.

Future Directions

Although this work identified a novel, non-canonical function for β1 as a transcriptional modulator, it also raised important new questions, e.g. What is the mechanism of β1-ICD translocation to the nucleus? How does the β1-ICD alter of gene expression? What are the effects of *SCN1B* disease-linked variants on β1 subunit processing by BACE1 and γ-secretase? In the following sections, we will discuss these future directions, provide a hypothesis, and suggest potential approaches for addressing these important questions.

Investigation of regulatory elements for β1 ectodomain shedding

Ectodomain shedding occurs primarily for type-I transmembrane proteins. Release of the substrate protein's ectodomain from the membrane results in altered protein function (Lichtenthaler, Lemberg et al. 2018). Ectodomain shedding occurs in all cellular organelles of the endocytic and secretory pathways as well as the plasma membrane, thus protein trafficking is one of the most

important regulatory mechanisms for ectodomain shedding (Lichtenthaler, Lemberg et al. 2018). Membrane-bound sheddases, such as BACE1, and their transmembrane substrates, must be trafficked to the same organelle in order for cleavage to occur (Lichtenthaler, Lemberg et al. 2018). The importance of trafficking as a regulatory mechanism for ectodomain shedding was originally shown for the substrate, SREBP, When cholesterol decreases, SREBP moves from the ER to the Golgi. In Golgi, SREBP is shed by S1P and then further processed by a site-2-protease (Rawson, Zelenski et al. 1997, Sakai, Rawson et al. 1998). Trafficking as a regulatory mechanism has also been demonstrated for APP (Haass, Hung et al. 1993, Koo and Squazzo 1994, Chyung and Selkoe 2003, Carey, Balcz et al. 2005, Bhattacharyya, Barren et al. 2013, Sannerud, Esselens et al. 2016). Palmitoylation of APP is critical for its exit from the ER. A palmitoylation-deficient APP mutant is retained in the ER is unable to be cleaved (Bhattacharyya, Barren et al. 2013). In chapter 3, we demonstrate a similar mechanism for regulating β1 cleavage. β1 is also post-translationally palmitoylated. Expression of a palmitoylation-deficient β1 mutant leads to decreased plasma membrane localization compared to wild-type and subsequently, less β1 is cleaved by BACE1.

Although protein trafficking is a highly important contributor to the regulation of ectodomain shedding, other factors such as, but not limited to, abundance of enzyme and substrate, lipid modulation, post-translational modification of the substrate, and ligand-dependent induction provide regulatory elements (Lichtenthaler, Lemberg et al. 2018). For example, substrate O-glycosylation of amino acid residues near the cleavage site controls ectodomain shedding by ADAM proteases. Substrate ubiquitination has been shown to induce intramembrane proteolysis

following initial shedding (Fleig, Bergbold et al. 2012, Goth, Halim et al. 2015). Most famously, ligands, Delta and Jagged, bind to the notch receptor and only upon ligand binding is notch processed by RIP (Kopan 2012). Interestingly, glycosylated notch receptors have a higher affinity for Delta than Jagged-type ligands (Hicks, Johnston et al. 2000). Future work fully elucidating the complex regulatory mechanisms for β1 RIP will be critical in developing interventions to selectively block β1 RIP, while leaving β1's other functions intact.

β1 is highly N-linked glycosylated, accounting for approximately one-third of its molecular weight (Brackenbury and Isom 2011). While the majority of glycosylation sites are located within the β1 Ig domain, a single site is located N-terminally adjacent to the predicted BACE1 cleavage site (Brackenbury and Isom 2011). We hypothesize that loss of glycosylation at this site may, like Notch and other ADAM protease substrates, contribute to regulating ectodomain shedding of β1. To test this hypothesis, each glycosylation site will need to be mutated and cleavage assessed. It is also possible that β1 ectodomain shedding by BACE1 occurs constitutively. Should manipulation of other known regulatory elements of ectodomain shedding, such as mutating the Ig domain to prevent ligand interaction or manipulating lipid composition and substrate glycosylation, have no effect, it may be that trafficking is the only regulatory component for β1 ectodomain shedding.

Determine the β1-ICD mechanism of nuclear entry and exit

Chapter 2 of this work has shown the β1-ICD localizes to the nucleus. To enter and exit the nucleus, proteins interact with nuclear transport receptors that enable passage through nuclear pore complexes (NPC)(Di Ventura and Kuhlman 2016). The NPC restricts entry of proteins through the pore, although proteins smaller than approximately 40 kDa can diffuse through the barrier. Proteins larger than 40 kDa necessitate nuclear transport receptors, which can act as importins, assisting proteins in entering the nucleus, or exportins, assisting proteins in exiting the nucleus (Di Ventura and Kuhlman 2016). The interaction between proteins and nuclear transport receptors is typically facilitated by short amino acid motifs called nuclear localization signals (NLS) or nuclear export signals (NES) (Gorlich, Henklein et al. 1996, Chook and Suel 2011, Gorlich and Kriwacki 2016). Nuclear entry and export are critical factors in regulating gene expression. In order to enable temporal regulation of gene expression, transcription factors and transcriptional coregulators are often retained in the cytoplasm until the proper stimuli initiate their translocation to the nucleus (Komeili and O'Shea 2000, Di Ventura and Kuhlman 2016). Cytoplasmic retention of transcription factors and transcriptional coregulators prevents their access to their binding partners, e.g. DNA, DNA binding proteins, and/or cofactors, and thus prevent their ability to modulate gene transcription (Komeili and O'Shea 2000). Proper nuclear export can be important in terminating a protein's nuclear action (Shank and Paschal 2005). Thus, it is critical to determine the mechanism of nuclear entry and export of the β1-ICD.

Interestingly, the β1-ICD contains neither a NLS nor a NES. Although the β1-ICD has a molecular weight less than 40 kDa and could enter the nucleus by diffusion through the NPC, we hypothesize that it enters and exits through a more regulated mechanism. Other known substrates of sequential cleavage that are small in size enter the nucleus by binding to a partner that does contain a NLS. For example, the ICD generated by sequential cleavage of APP, AICD, localizes to the nucleus only when it can bind to the adaptor protein, Fe65 (Cao and Sudhof 2001). Expression of a mutant version of APP that cannot bind Fe65 results in the loss of APP nuclear localization (Cao and Sudhof 2001). To address the question of how the β1-ICD enters and exits the nucleus, we performed an initial nomination of binding partners. Potential experimental approaches to address this question included yeast two hybrid screens, proteomics approaches, and bioinformatic approaches. Our lab decided to take this initial step using a proteomics approach. Using P18 mouse brain, we immunoprecipitated β1 and then performed liquid chromatography tandem mass spectrometry (LC-MS/MS) to identify the β1 interactome. We were surprised to find that β1 interacts specifically with the nuclear pore complex protein, Nup160. Furthermore, our data showed that β1 interacts with a singular importin, importin-9, and with a singular exportin, exportin-5. As full-length β1 does not localize to the nucleus, these data support the hypothesis that the β1-ICD enters and exits the nucleus via the NPC with assistance from the nuclear transport receptors, importin-9 and exportin-5, rather than by passive diffusion. Additional work to validate these interactions will be critical to test this working hypothesis. Not only do these interactions

154

need to be confirmed by co-immunoprecipitation, but also functional studies must be completed. If importin-9 is necessary for β1-ICD entry into the nucleus, knockdown or knockout of importin-9 should lead to the cytoplasmic accumulation of β1-ICD. Conversley, if exportin-5 is necessary for β1-ICD exit from the nucleus, knockdown or knockout of exportin-5 should lead to the nuclear accumulation of β1-ICD.

Determine the mechanism by which the β1-ICD modulates gene transcription

Chapter 2 demonstrates that expression of the β1-ICD leads to changes in gene expression, but the precise mechanism of how the β1-ICD drives differential gene expression remains unexplored. Many substrate-LPDs generated by RIP do not contain a DNA-binding domain (Lal and Caplan 2011). The β1-ICD falls in the majority in that it too lacks a DNA-binding domain. Other similar substrates of RIP with transcriptional modulatory function do so as coregulators (Cao and Sudhof 2001, Sardi, Murtie et al. 2006, Zhang, Wang et al. 2007, Haapasalo and Kovacs 2011, Bray and Gomez-Lamarca 2018). One example, APP, modulates transcription by binding with the adaptor protein, Fe65, and histone acetyltransferase, tip60. Tip60 functions in chromatin remodeling, DNA repair, and transcription (Cao and Sudhof 2001). Notch-1 is also processed by RIP, generating a Notch-ICD (NICD), which translocates to the nucleus to regulate transcription (Kopan, Nye et al. 1994, van Tetering and Vooijs 2011, Bray and Gomez-Lamarca 2018). The NICD associates with the DNA binding protein, CSL, and the transcriptional coactivator, Mastermind (MAM), to modulate gene transcription (Kopan 2012, Bray and Gomez-Lamarca 2018). Thus, we hypothesize

155

that the β1-ICD modulates transcription by acting as a coregulator, rather than as a canonical transcription factor directly binding to DNA.

To identify potential interacting partners that may function with the β1-ICD to regulate transcription, a bioinformatic or experimental approach could be used. Using gene expression data determining genes affected by expression of the β1-ICD, bioinformatic analysis could identify common promoters or DNA elements amongst those genes to nominate protein complexes that could alter expression of β1-ICD affected genes. Alternatively, experimental approaches such as yeast two hybrid or proteomics could be utilized to identify other members of a complex in which the β1-ICD modulates transcription. Based off our laboratory's proteomics data set on the β1-interactome, we hypothesize that the β1-ICD modulates gene expression through chromatin remodeling. β1 interacts with a core subunit of the PBAF complex (SWI/SNF-B), Smarcc2. The PBAF complex functions in chromatin remodeling (Yan, Cui et al. 2005). Interestingly, our data also show that β1 interacts with a variety of histones and histone modifying enzymes. Again, as full-length β1 does not localize to the nucleus, these data further support our hypothesis the β1-ICD localizes to the nucleus and modulates transcription.

Although we have exciting preliminary data, many additional experiments must be completed in order to test the hypothesis that the β1-ICD modulates transcription via chromatin remodeling. Initially, co-immunoprecipitations followed by western blot between the β1-ICD and those

proteins listed in Table 4.1 must be completed to validate the proteomics experiment. Should these binding partners be confirmed, interacting sites must be identified and mutants generated that specifically block interactions with each binding partner. Subsequent functional studies examining how preventing these interactions affect β1-ICD-mediated changes in gene transcription must be completed. Determining the exact mechanism by which the β1-ICD modulates transcription is critical to understanding how dysfunction of this signaling pathway in disease could be manipulated for therapeutic benefit.

Protein	Function
Histone H2AX	Replaces convention H2A in a subset of nucleosomes.
Histone H3.3C	Core component of nucleosome.
Histone H1.5	Binds to linker DNA between nucleosomes, forming the chromatin fiber.
Heterochromatin protein 1-binding protein 3	Component of heterochromatin that maintains heterochromatin integrity during G1/S progression.
Histone H2A type 2-A	Core component of nucleosome.
Transcriptional regulator ATRX	Involved in transcriptional regulation and chromatin remodeling.
DNA (cytosine-5)-methyltransferase 3A	Required for genome-wide de novo methylation. Essential for establishment of DNA methylation patterns during development.
Histone deacetylase complex subunit SAP18	Component of SIN3-repressing complex. Enhances ability of SIN3-HDAC1-mediated transcriptional repression.
SWI/SNF complex subunit SMARCC2	Involved in transcriptional activation and repression of select genes by chromatin remodeling.
Histone-lysine N-methyltransferase 2A	Histone methyltransferase that plays essential role in early development and hematopoiesis.
Histone-lysine N-methyltransferase EZH1	Polycomb group protein. Catalytic subunit of PRC2/EED-EZH1 complex which methylates Lys-27 of histone H3, leading to transcriptional repression of affected target gene.
Methylosome protein 50	Non-catalytic component of methylosome complex, which modifies specific arginines to dimethylarginines in several spliceosomal Sm proteins and histones.

Table 4.1: *β1 binding partners which may implicate the β1-ICD in chromatin remodeling as a mechanism by which it modulates transcription.*

Enrichment analysis using the Gene Ontology (GO) knowledgebase and KEGG pathways were also completed for the β1 IP-mass spectrometry experiment. Surprisingly, gene set enrichment analysis (GSEA) revealed that spliceosome proteins were over-represented in the dataset (Figure 4.1). Because we performed the immunoprecipitation experiment using a C-terminal anti-β1 antibody, all three species of β1, full-length β1, β1-CTF, and β1-ICD, were detectable. Because our results show that full-length β1 and the β1-CTF do not localize to the nucleus, we hypothesize that β1-ICD is the β1 species interacting with the spliceosome. Additional experiments must be completed in order to test this hypothesis. First, β1 interaction with the spliceosome need to be validated by co-IP followed by western blot from mouse brain. Subsequently, using a cell line which only expresses the β1-ICD, co-immunoprecipitation followed by western blot would allow us to determine if the β1-ICD, but not other β1 species, is able to bind to spliceosome components. Additional work is underway to determine if expression of the β1-ICD has an effect on isoform switching, further solidifying that the β1-ICD interacts with the spliceosome and has a functional effect on splicing. This may provide an additional mechanism by which the β1-ICD contributes to regulating gene expression.

Figure 4.1: Enrichment analysis of β1 interactome in mouse whole brain identifies spliceosome as major interacting partner. Enrichment groups shown in blue are related to splicing. A. Cellular component gene ontology groups enriched in data set. B. Biological function gene ontology groups enriched. C. Molecular function gene ontology group enriched in data set. D. KEGG pathways enriched. E. Cartoon diagram of splicing machinery and mechanism from iPathway guide.

160

Investigate cell-type specific alterations in gene transcription by the β1-ICD

In this work, we have examined the role of the β1-ICD in regulating gene expression in heterologous cells and in mouse cardiac ventricle, but β1 plays important roles in many tissue types (Calhoun and Isom 2014, Bouza and Isom 2017). Work from other well-studied substrates of RIP, which result in modulating gene expression, have shown cell-type specific effects. Cell-type specific effects of the NICD is arguably the most well characterized (Andersson, Sandberg et al. 2011). Although some conserved genes are modulated by NICD, genome-wide transcriptome studies in various cell-types have shown unique sets of NICD target genes in each individual cell type (Palomero, Lim et al. 2006, Weerkamp, Luis et al. 2006, Dohda, Maljukova et al. 2007, Buas, Kabak et al. 2009, Chadwick, Zeef et al. 2009, Mikhailik, Mazella et al. 2009, Main, Lee et al. 2010, Meier-Stiegen, Schwanbeck et al. 2010, Aoyagi-Ikeda, Maeno et al. 2011). The NICD driven changes in gene expression can also change under specific cellular contexts, such as the cell cycle, cell lineage progression, and differentiation (Kageyama, Ohtsuka et al. 2009, Das, Lanner et al. 2010, Radtke, Fasnacht et al. 2010). Due to the high expression of β1, BACE1, and γ-secretase in brain, examining β1-ICD driven changes in gene expression using genome-wide transcriptomics in neuronal tissue, taking into account specific brain regions, is critical (Vassar, Kovacs et al. 2009, Haapasalo and Kovacs 2011). Although these proteins are highly expressed and most well characterized in brain, they are found in many other tissue types. Work determining β1-ICD mediated gene expression in other tissues should also be pursued. More elaborate analysis of β1-ICD driven gene expression throughout development and differentiation, as well as cell

cycle in proliferating tissues, should be examined. This may have particular importance in *SCN1B*-linked disease states, which show onset during critical periods of development.

Determine the effect of disease-linked SCN1B variants on β1 cleavage and β1-ICD signaling

Patient variants in *SCN1B* are linked to disease states with high risk of sudden death (Calhoun and Isom 2014, Bouza and Isom 2017). *SCN1B* patient variants to date are LOF and unable to properly modulate the ion channel pore and/or function in cell adhesion (Patino, Claes et al. 2009, Kruger, O'Malley et al. 2016, Aeby, Sculier et al. 2019). The effect of these variants on β1 RIP is yet to be determined. Disease-linked variants in other RIP substrates lead to dysregulation of the RIP pathway, which is thought to mechanistically contribute to disease onset and/or progression. For example, variants in Notch receptor genes are linked to adult T cell acute lymphoblastic leukemia and lymphoma (T-LL) (Aster, Blacklow et al. 2011). The most common of these variants are found in the Notch1 gene and result in ligand-independent ectodomain shedding. Other variants, which activate the Notch receptor, can lead to NICD buildup in the nucleus in T-LL (Aster, Blacklow et al. 2011). Variants in APP also affect its processing by RIP and are linked to early onset familial Alzheimer's disease (FAD)(Weggen and Beher 2012). Nearly all FAD-linked APP variants are clustered around the BACE1 and γ-secretase cleavage sites and lead to increased Aβ production (Weggen and Beher 2012). Aβ is the primary constituent in two out of three of the hallmarks of AD, senile plaques and vascular amyloid (Weggen and Beher 2012). We hypothesize that patient variants in *SCN1B* may lead to aberrant processing of β1 by BACE1 and/or γ-secretase. In addition

to variants in other substrates that affect RIP, a Brugada Syndrome 5 patient variant in *SCN1B,* p.C162Y, it predicted to prevent β1 palmitoylation (ClinVar). In chapter 3, we showed that β1 palmitoylation regulates β1 localization at the plasma membrane, and consequently its cleavage. The majority of *SCN1B* patient variants are located in the protein's Ig domain (Bouza and Isom 2018). Although this is distal to the predicted β1 cleavage sites, variants in the Ig domain may affect BACE1 recognition of the substrate (Table 4.2) (Wong, Sakurai et al. 2005). Additional disease-linked variants are located near the predicted BACE1 and γ-secretase cleavage sites (Table 4.2). Future work should assess the effect of *SCN1B* disease-linked variants on cleavage and subsequent signaling. Dysregulation of β1 RIP may be an important contributor to *SCN1B*-linked disease onset and/or progression.

Variant	Protein coding mutation	Structural location of mutation
c.133C>T	p.R45C	Ig domain
c.C253>T	p.R85C	Ig domain
c.C319>A	p.I106F	Ig domain
c.C363>G	p.C121W	Ig domain
c.C373>T	p.R125C	Ig domain
c.G412>A	p.V138I	Near BACE1 predicted cleavage site
c.G415>A	p.V139I	Near BACE1 predicted cleavage site
c.G542>A	p.C162Y	β1 palmitoylation site

Table 4.2: Selection of SCN1B patient variants from ClinVar.

Overall Conclusions

In all, this thesis describes a novel, non-canonical role of the VGSC β1 subunit, when processed by BACE1 and γ-secretase, as a transcriptional modulator. Changes in gene expression driven by the β1-ICD lead to changes in cellular excitability. Thus this work provides a new mechanism to regulate excitability. β1 cleavage, like other substrates of RIP, is regulated in part by intracellular localization. When β1 cannot be palmitoylated, more protein is intracellularly retained. Consequently, less β1 is proteolytically processed. Furthermore, the identified β1-mediated signaling cascade may shed light on the mechanism by which differential gene expression occurs in the *Scn1b*-null mouse. Based on this work, we hypothesize that disease-linked variants in *SCN1B* may disrupt this signaling pathway, ultimately contributing to disease onset and/or progression. Future work will examine detailed mechanisms by which the β1-ICD modulates transcription, the effect of *SCN1B* variants on the identified pathway, and determine if targeting this pathway has therapeutic benefits for *SCN1B*-linked disease states.

Materials and Methods

Immunoprecipitation

P18 whole brain isolated from mice with an in-frame, C-terminal, V5-epitope tag knocked in to the *Scn1b* locus (β1V5 mice) were utilized. Brains were flash frozen in liquid nitrogen immediately upon removal , crushed with a mortar and pestle, and suspended in 400 μL of dilution buffer (60 mM Tris/HCl, 180mM NaCl, 6mM EDTA, 1% Triton X-100, pH 7.5). Samples were incubated on ice for 30 minutes and sonicated three times for ten pulses every 10 minutes during the 30 minute incubation for a total of three times. 50 μL of Protein G Sepharose per sample was washed three times in DPBS. Protein G Sepharose was resuspended in 400 μL of dilution buffer and incubated with antibody for 1 hour at 4°C. Control antibody, mouse IgG (Jackson Immuno Research Laboratories) was diluted 1:10 in molecular biology grade water and 1 μL was added to Protein G Sepharose. 1 μL of experimental antibody, mouse V5 (Invitrogen) was added to Protein G Sepharose. After 1 hour incubation, Protein G Sepharose was spun down at 2,500g for 1 minute and the supernatant was removed. 200 μL of brain lysate was added to each tube (mouse IgG, V5) and incubated at 4°C for 4 hours with shaking. Protein G Sepharose was spun down at 2,500g for 1 minute and supernatant was removed. Resin was subsequently was three times with 400 μL of washing solution (50mM Tris/HCl, 150mM NaCl, 0.02% SDS, 5mM EDTA, pH7.5) and a final time with washing solution with 0.1% Triton X-100. 30 μL of sample buffer was added to each sample and heated at 85 C for 5 minutes. Samples were stored at -80°C until use.

Mass Spectrometry and Proteomics Analysis

The sample was reduced with dithiothreitol, alkylated with Iodoacetamide, and digested using trypsin overnight at 37°C. Subsequently, the digested sample was analyzed by nano Liquid Chromatography tandem Mass Spectrometry (LC-MS/MS) on a ThermoScientific Orbitrap Velos. The digest was loaded and a gradient elution was over a 10 cm 75 μm ID C18 column at 400nL/min for 30 minutes. Product ion data were searched against the NCBI protein database using Mascot and X-Tandem! search engines. Mascot files were assessed in Scaffold for filtering to assess false discovery rates, common contaminants, and non-specific interactions (also identified in IgG sample), to show only correct protein identifications.

Gene Set Enrichment Analysis

We performed gene ontology (GO), Kegg pathway and protein domain enrichment analysis of all immunoprecipitated proteins using the functional annotation tool, DAVID V6.8. To correct for multiple testing we considered functional enrichment only for categories with a Benjamini-adjusted p-value <0.01."

Bibliography

Adachi, K., M. Toyota, Y. Sasaki, T. Yamashita, S. Ishida, M. Ohe-Toyota, R. Maruyama, Y. Hinoda, T. Saito, K. Imai, R. Kudo and T. Tokino (2004). "Identification of SCN3B as a novel p53-inducible proapoptotic gene." Oncogene **23**(47): 7791-7798.

Aeby, A., C. Sculier, A. A. Bouza, B. Askar, D. Lederer, A.-S. Schoonjans, M. Vander Ghinst, B. Ceulemans, J. Offord, L. F. Lopez-Santiago and L. L. Isom (2019). "SCN1B-linked early infantile developmental and epileptic encephalopathy." Annals of Clinical and Translational Neurology **6**(12): 2354-2367.

Agsten, M., S. Hessler, S. Lehnert, T. Volk, A. Rittger, S. Hartmann, C. Raab, D. Y. Kim, T. W. Groemer, M. Schwake, C. Alzheimer and T. Huth (2015). "BACE1 modulates gating of KCNQ1 (Kv7.1) and cardiac delayed rectifier KCNQ1/KCNE1 (IKs)." J Mol Cell Cardiol **89**(Pt B): 335-348.

Al-Chalabi, A., L. H. van den Berg and J. Veldink (2017). "Gene discovery in amyotrophic lateral sclerosis: implications for clinical management." Nat Rev Neurol **13**(2): 96-104.

Alders, M. and I. Christiaans (1993). Long QT Syndrome. GeneReviews(R). R. A. Pagon, M. P. Adam, H. H. Ardinger et al. Seattle (WA), University of Washington, Seattle

University of Washington, Seattle. GeneReviews is a registered trademark of the University of Washington, Seattle. All rights reserved.

Aman, T. K., T. M. Grieco-Calub, C. Chen, R. Rusconi, E. A. Slat, L. L. Isom and I. M. Raman (2009). "Regulation of persistent Na current by interactions between beta subunits of voltage-gated Na channels." J Neurosci **29**(7): 2027-2042.

Andersson, E. R., R. Sandberg and U. Lendahl (2011). "Notch signaling: simplicity in design, versatility in function." Development **138**(17): 3593-3612.

Andrikopoulos, P., S. P. Fraser, L. Patterson, Z. Ahmad, H. Burcu, D. Ottaviani, J. K. Diss, C. Box, S. A. Eccles and M. B. Djamgoz (2011). "Angiogenic functions of voltage-gated Na+ Channels in human endothelial cells: modulation of vascular endothelial growth factor (VEGF) signaling." J Biol Chem **286**(19): 16846-16860.

Aoyagi-Ikeda, K., T. Maeno, H. Matsui, M. Ueno, K. Hara, Y. Aoki, F. Aoki, T. Shimizu, H. Doi, K. Kawai-Kowase, T. Iso, T. Suga, M. Arai and M. Kurabayashi (2011). "Notch Induces Myofibroblast Differentiation of Alveolar Epithelial Cells via Transforming Growth Factor–β–Smad3 Pathway." American Journal of Respiratory Cell and Molecular Biology **45**(1): 136-144.

Aster, J. C., S. C. Blacklow and W. S. Pear (2011). "Notch signalling in T-cell lymphoblastic leukaemia/lymphoma and other haematological malignancies." J Pathol **223**(2): 262-273.

Audenaert, D., L. Claes, B. Ceulemans, A. Lofgren, C. Van Broeckhoven and P. De Jonghe (2003). "A deletion in SCN1B is associated with febrile seizures and early-onset absence epilepsy." Neurology **61**(6): 854-856.

Auerbach, D. S., J. Jones, B. C. Clawson, J. Offord, G. M. Lenk, I. Ogiwara, K. Yamakawa, M. H. Meisler, J. M. Parent and L. L. Isom (2013). "Altered cardiac electrophysiology and SUDEP in a model of Dravet syndrome." PLoS One **8**(10): e77843.

Bant, J. S. and I. M. Raman (2010). "Control of transient, resurgent, and persistent current by open-channel block by Na channel beta4 in cultured cerebellar granule neurons." Proc Natl Acad Sci U S A **107**(27): 12357-12362.

Bao, Y., B. C. Willis, C. R. Frasier, L. F. Lopez-Santiago, X. Lin, R. Ramos-Mondragon, D. S. Auerbach, C. Chen, Z. Wang, J. Anumonwo, H. H. Valdivia, M. Delmar, J. Jalife and L. L. Isom (2016). "Scn2b Deletion in Mice Results in Ventricular and Atrial Arrhythmias." Circ Arrhythm Electrophysiol **9**(12).

Barao, S., A. Gartner, E. Leyva-Diaz, G. Demyanenko, S. Munck, T. Vanhoutvin, L. Zhou, M. Schachner, G. Lopez-Bendito, P. F. Maness and B. De Strooper (2015). "Antagonistic Effects of BACE1 and APH1B-gamma-Secretase Control Axonal Guidance by Regulating Growth Cone Collapse." Cell Rep **12**(9): 1367-1376.

Baum, L., B. S. Haerian, H. K. Ng, V. C. Wong, P. W. Ng, C. H. Lui, N. C. Sin, C. Zhang, B. Tomlinson, G. W. Wong, H. J. Tan, A. A. Raymond, Z. Mohamed and P. Kwan (2014). "Case-control association study of polymorphisms in the voltage-gated sodium channel genes SCN1A, SCN2A, SCN3A, SCN1B, and SCN2B and epilepsy." Hum Genet **133**(5): 651-659.

Bharadwaj, M. and O. A. Bizzozero (1995). "Myelin P0 glycoprotein and a synthetic peptide containing the palmitoylation site are both autoacylated." J Neurochem **65**(4): 1805-1815.

Bhattacharyya, R., C. Barren and D. M. Kovacs (2013). "Palmitoylation of amyloid precursor protein regulates amyloidogenic processing in lipid rafts." J Neurosci **33**(27): 11169-11183.

Blackburn-Munro, G. and S. M. Fleetwood-Walker (1999). "The sodium channel auxiliary subunits beta1 and beta2 are differentially expressed in the spinal cord of neuropathic rats." Neuroscience **90**(1): 153-164.

Blanc, M., F. David, L. Abrami, D. Migliozzi, F. Armand, J. Burgi and F. G. van der Goot (2015). "SwissPalm: Protein Palmitoylation database." F1000Res **4**: 261.

Borghetti, G., C. A. Eisenberg, S. Signore, A. Sorrentino, K. Kaur, A. Andrade-Vicenty, J. G. Edwards, M. Nerkar, K. Qanud, D. Sun, P. Goichberg, A. Leri, P. Anversa, L. M. Eisenberg, J. T. Jacobson, T. H. Hintze and M. Rota (2018). "Notch signaling modulates the electrical behavior of cardiomyocytes." Am J Physiol Heart Circ Physiol **314**(1): H68-h81.

Bouza, A. A. and L. L. Isom (2017). "Voltage-Gated Sodium Channel beta Subunits and Their Related Diseases." Handb Exp Pharmacol.

Bouza, A. A. and L. L. Isom (2018). "Voltage-Gated Sodium Channel beta Subunits and Their Related Diseases." Handb Exp Pharmacol **246**: 423-450.

Bouza, A. A., Nnamdi Edokobi, Alexa M. Pinsky, James Offord, PhD, Lin Piao, MD, PhD, Anatoli N. Lopatin, PhD, Luis F. Lopez-Santiago, PhD, and Lori L. Isom, PhD (2020). "Voltage-gated sodium channel β1 subunits mediate excitation-transcription coupling through regulated intramembrane proteolysis." In Review.

Brackenbury, W. J. (2012). "Voltage-gated sodium channels and metastatic disease." Channels (Austin) **6**(5): 352-361.

Brackenbury, W. J., J. D. Calhoun, C. Chen, H. Miyazaki, N. Nukina, F. Oyama, B. Ranscht and L. L. Isom (2010). "Functional reciprocity between Na+ channel Nav1.6 and beta1 subunits in the coordinated regulation of excitability and neurite outgrowth." Proc Natl Acad Sci U S A **107**(5): 2283-2288.

Brackenbury, W. J., T. H. Davis, C. Chen, E. A. Slat, M. J. Detrow, T. L. Dickendesher, B. Ranscht and L. L. Isom (2008). "Voltage-gated Na+ channel beta1 subunit-mediated neurite outgrowth requires Fyn kinase and contributes to postnatal CNS development in vivo." J Neurosci **28**(12): 3246-3256.

Brackenbury, W. J. and L. L. Isom (2011). "Na Channel beta Subunits: Overachievers of the Ion Channel Family." Front Pharmacol **2**: 53.

Brackenbury, W. J., Y. Yuan, H. A. O'Malley, J. M. Parent and L. L. Isom (2013). "Abnormal neuronal patterning occurs during early postnatal brain development of Scn1b-null mice and precedes hyperexcitability." Proc Natl Acad Sci U S A **110**(3): 1089-1094.

Bray, S. J. and M. Gomez-Lamarca (2018). "Notch after cleavage." Curr Opin Cell Biol **51**: 103-109.

Breunig, J. J., J. Silbereis, F. M. Vaccarino, N. Sestan and P. Rakic (2007). "Notch regulates cell fate and dendrite morphology of newborn neurons in the postnatal dentate gyrus." Proc Natl Acad Sci U S A **104**(51): 20558-20563.

Brigidi, G. S., B. Santyr, J. Shimell, B. Jovellar and S. X. Bamji (2015). "Activity-regulated trafficking of the palmitoyl-acyl transferase DHHC5." Nat Commun **6**: 8200.

Brigidi, G. S., Y. Sun, D. Beccano-Kelly, K. Pitman, M. Mobasser, S. L. Borgland, A. J. Milnerwood and S. X. Bamji (2014). "Palmitoylation of delta-catenin by DHHC5 mediates activity-induced synapse plasticity." Nat Neurosci **17**(4): 522-532.

Buas, M. F., S. Kabak and T. Kadesch (2009). "Inhibition of myogenesis by Notch: Evidence for multiple pathways." Journal of Cellular Physiology **218**(1): 84-93.

Buffington, S. A. and M. N. Rasband (2013). "Na+ channel-dependent recruitment of Navbeta4 to axon initial segments and nodes of Ranvier." J Neurosci **33**(14): 6191-6202.

Cai, J., X. Qi, N. Kociok, S. Skosyrski, A. Emilio, Q. Ruan, S. Han, L. Liu, Z. Chen, C. Bowes Rickman, T. Golde, M. B. Grant, P. Saftig, L. Serneels, B. de Strooper, A. M. Joussen and M. E. Boulton (2012). "beta-Secretase (BACE1) inhibition causes retinal pathology by vascular dysregulation and accumulation of age pigment." EMBO Mol Med **4**(9): 980-991.

Calhoun, J. D. and L. L. Isom (2014). "The role of non-pore-forming beta subunits in physiology and pathophysiology of voltage-gated sodium channels." Handb Exp Pharmacol **221**: 51-89.

Cao, L., G. T. Rickenbacher, S. Rodriguez, T. W. Moulia and M. W. Albers (2012). "The precision of axon targeting of mouse olfactory sensory neurons requires the BACE1 protease." Sci Rep **2**: 231.

Cao, X. and T. C. Sudhof (2001). "A transcriptionally [correction of transcriptively] active complex of APP with Fe65 and histone acetyltransferase Tip60." Science **293**(5527): 115-120.

Cao, X. and T. C. Sudhof (2004). "Dissection of amyloid-beta precursor protein-dependent transcriptional transactivation." J Biol Chem **279**(23): 24601-24611.

Carey, R. M., B. A. Balcz, I. Lopez-Coviella and B. E. Slack (2005). "Inhibition of dynamin-dependent endocytosis increases shedding of the amyloid precursor protein ectodomain and reduces generation of amyloid beta protein." BMC Cell Biol **6**: 30.

Catterall, W. A. "From Ionic Currents to Molecular Mechanisms." Neuron **26**(1): 13-25.

Chadwick, N., L. Zeef, V. Portillo, C. Fennessy, F. Warrander, S. Hoyle and A. M. Buckle (2009). "Identification of novel Notch target genes in T cell leukaemia." Mol Cancer **8**: 35.

Chavez-Gutierrez, L., L. Bammens, I. Benilova, A. Vandersteen, M. Benurwar, M. Borgers, S. Lismont, L. Zhou, S. Van Cleynenbreugel, H. Esselmann, J. Wiltfang, L. Serneels, E. Karran, H. Gijsen, J. Schymkowitz, F. Rousseau, K. Broersen and B. De Strooper (2012). "The mechanism of gamma-Secretase dysfunction in familial Alzheimer disease." Embo j **31**(10): 2261-2274.

Chen, C., V. Bharucha, Y. Chen, R. E. Westenbroek, A. Brown, J. D. Malhotra, D. Jones, C. Avery, P. J. Gillespie, 3rd, K. A. Kazen-Gillespie, K. Kazarinova-Noyes, P. Shrager, T. L. Saunders, R. L. Macdonald, B. R. Ransom, T. Scheuer, W. A. Catterall and L. L. Isom (2002). "Reduced sodium channel density, altered voltage dependence of inactivation, and increased

susceptibility to seizures in mice lacking sodium channel beta 2-subunits." <u>Proc Natl Acad Sci U S A</u> **99**(26): 17072-17077.

Chen, C., J. D. Calhoun, Y. Zhang, L. Lopez-Santiago, N. Zhou, T. H. Davis, J. L. Salzer and L. L. Isom (2012). "Identification of the cysteine residue responsible for disulfide linkage of Na+ channel alpha and beta2 subunits." <u>J Biol Chem</u> **287**(46): 39061-39069.

Chen, C., R. E. Westenbroek, X. Xu, C. A. Edwards, D. R. Sorenson, Y. Chen, D. P. McEwen, H. A. O'Malley, V. Bharucha, L. S. Meadows, G. A. Knudsen, A. Vilaythong, J. L. Noebels, T. L. Saunders, T. Scheuer, P. Shrager, W. A. Catterall and L. L. Isom (2004). "Mice lacking sodium channel beta1 subunits display defects in neuronal excitability, sodium channel expression, and nodal architecture." <u>J Neurosci</u> **24**(16): 4030-4042.

Chen, Q., X. Liu, L. Xu, Y. Wang, S. Wang, Q. Li, Y. Huang and T. Liu (2016). "Long non-coding RNA BACE1-AS is a novel target for anisomycin-mediated suppression of ovarian cancer stem cell proliferation and invasion." <u>Oncol Rep</u> **35**(4): 1916-1924.

Cheret, C., M. Willem, F. R. Fricker, H. Wende, A. Wulf-Goldenberg, S. Tahirovic, K. A. Nave, P. Saftig, C. Haass, A. N. Garratt, D. L. Bennett and C. Birchmeier (2013). "Bace1 and Neuregulin-1 cooperate to control formation and maintenance of muscle spindles." <u>Embo j</u> **32**(14): 2015-2028.

Chioni, A. M., W. J. Brackenbury, J. D. Calhoun, L. L. Isom and M. B. Djamgoz (2009). "A novel adhesion molecule in human breast cancer cells: voltage-gated Na+ channel beta1 subunit." <u>Int J Biochem Cell Biol</u> **41**(5): 1216-1227.

Chook, Y. M. and K. E. Suel (2011). "Nuclear import by karyopherin-betas: recognition and inhibition." <u>Biochim Biophys Acta</u> **1813**(9): 1593-1606.

Chyung, J. H. and D. J. Selkoe (2003). "Inhibition of receptor-mediated endocytosis demonstrates generation of amyloid beta-protein at the cell surface." <u>J Biol Chem</u> **278**(51): 51035-51043.

Cole, S. L. and R. Vassar (2007). "The Alzheimer's disease beta-secretase enzyme, BACE1." <u>Mol Neurodegener</u> **2**: 22.

Contreras-Cornejo, H., G. Saucedo-Correa, J. Oviedo-Boyso, J. J. Valdez-Alarcón, V. M. Baizabal-Aguirre, M. Cajero-Juárez and A. Bravo-Patiño (2016). "The CSL proteins, versatile transcription factors and context dependent corepressors of the notch signaling pathway." <u>Cell Div</u> **11**: 12.

Coward, K., A. Jowett, C. Plumpton, A. Powell, R. Birch, S. Tate, C. Bountra and P. Anand (2001). "Sodium channel beta1 and beta2 subunits parallel SNS/PN3 alpha-subunit changes in injured human sensory neurons." <u>Neuroreport</u> **12**(3): 483-488.

Das, D., F. Lanner, H. Main, E. R. Andersson, O. Bergmann, C. Sahlgren, N. Heldring, O. Hermanson, E. M. Hansson and U. Lendahl (2010). "Notch induces cyclin-D1-dependent proliferation during a specific temporal window of neural differentiation in ES cells." <u>Dev Biol</u> **348**(2): 153-166.

Davis, T. H., C. Chen and L. L. Isom (2004). "Sodium channel beta1 subunits promote neurite outgrowth in cerebellar granule neurons." <u>J Biol Chem</u> **279**(49): 51424-51432.

Davis, T. H., C. Chen and L. L. Isom (2004). "Sodium Channel β1 Subunits Promote Neurite Outgrowth In Cerebellar Granule Neurons." <u>J. Biol. Chem.</u> **279**: 51424-51432.

Deschenes, I., A. A. Armoundas, S. P. Jones and G. F. Tomaselli (2008). "Post-transcriptional gene silencing of KChIP2 and Navbeta1 in neonatal rat cardiac myocytes reveals a functional association between Na and Ito currents." <u>J Mol Cell Cardiol</u> **45**(3): 336-346.

Deschenes, I. and G. F. Tomaselli (2002). "Modulation of Kv4.3 current by accessory subunits." <u>FEBS Lett</u> **528**(1-3): 183-188.

Dhar Malhotra, J., C. Chen, I. Rivolta, H. Abriel, R. Malhotra, L. N. Mattei, F. C. Brosius, R. S. Kass and L. L. Isom (2001). "Characterization of sodium channel alpha- and beta-subunits in rat and mouse cardiac myocytes." Circulation **103**(9): 1303-1310.

Di Ventura, B. and B. Kuhlman (2016). "Go in! Go out! Inducible control of nuclear localization." Curr Opin Chem Biol **34**: 62-71.

Diss, J. K., S. P. Fraser, M. M. Walker, A. Patel, D. S. Latchman and M. B. Djamgoz (2008). "Beta-subunits of voltage-gated sodium channels in human prostate cancer: quantitative in vitro and in vivo analyses of mRNA expression." Prostate Cancer Prostatic Dis **11**(4): 325-333.

Dohda, T., A. Maljukova, L. Liu, M. Heyman, D. Grander, D. Brodin, O. Sangfelt and U. Lendahl (2007). "Notch signaling induces SKP2 expression and promotes reduction of p27Kip1 in T-cell acute lymphoblastic leukemia cell lines." Exp Cell Res **313**(14): 3141-3152.

Dunckley, T., T. G. Beach, K. E. Ramsey, A. Grover, D. Mastroeni, D. G. Walker, B. J. LaFleur, K. D. Coon, K. M. Brown, R. Caselli, W. Kukull, R. Higdon, D. McKeel, J. C. Morris, C. Hulette, D. Schmechel, E. M. Reiman, J. Rogers and D. A. Stephan (2006). "Gene expression correlates of neurofibrillary tangles in Alzheimer's disease." Neurobiol Aging **27**(10): 1359-1371.

Edbauer, D., E. Winkler, J. T. Regula, B. Pesold, H. Steiner and C. Haass (2003). "Reconstitution of gamma-secretase activity." Nat Cell Biol **5**(5): 486-488.

El-Husseini Ael, D., E. Schnell, S. Dakoji, N. Sweeney, Q. Zhou, O. Prange, C. Gauthier-Campbell, A. Aguilera-Moreno, R. A. Nicoll and D. S. Bredt (2002). "Synaptic strength regulated by palmitate cycling on PSD-95." Cell **108**(6): 849-863.

Evin, G., A. Barakat and C. L. Masters (2010). "BACE: Therapeutic target and potential biomarker for Alzheimer's disease." Int J Biochem Cell Biol **42**(12): 1923-1926.

Fendri-Kriaa, N., F. Kammoun, I. H. Salem, C. Kifagi, E. Mkaouar-Rebai, I. Hsairi, A. Rebai, C. Triki and F. Fakhfakh (2011). "New mutation c.374C>T and a putative disease-associated haplotype within SCN1B gene in Tunisian families with febrile seizures." Eur J Neurol **18**(5): 695-702.

Ficker, D. M., E. L. So, W. K. Shen, J. F. Annegers, P. C. O'Brien, G. D. Cascino and P. G. Belau (1998). "Population-based study of the incidence of sudden unexplained death in epilepsy." Neurology **51**(5): 1270-1274.

Fielden, M. R., J. Werner, J. A. Jamison, A. Coppi, D. Hickman, R. T. Dunn, 2nd, E. Trueblood, L. Zhou, C. A. Afshari and R. Lightfoot-Dunn (2015). "Retinal Toxicity Induced by a Novel beta-secretase Inhibitor in the Sprague-Dawley Rat." Toxicol Pathol **43**(4): 581-592.

Fleig, L., N. Bergbold, P. Sahasrabudhe, B. Geiger, L. Kaltak and M. K. Lemberg (2012). "Ubiquitin-dependent intramembrane rhomboid protease promotes ERAD of membrane proteins." Mol Cell **47**(4): 558-569.

Forrester, M. T., D. T. Hess, J. W. Thompson, R. Hultman, M. A. Moseley, J. S. Stamler and P. J. Casey (2011). "Site-specific analysis of protein S-acylation by resin-assisted capture." J Lipid Res **52**(2): 393-398.

Gaborit, N., S. Le Bouter, V. Szuts, A. Varro, D. Escande, S. Nattel and S. Demolombe (2007). "Regional and tissue specific transcript signatures of ion channel genes in the non-diseased human heart." J Physiol **582**(Pt 2): 675-693.

Gataullina, S. and O. Dulac (2017). "From genotype to phenotype in Dravet disease." Seizure **44**: 58-64.

Gilchrist, J., S. Das, F. Van Petegem and F. Bosmans (2013). "Crystallographic insights into sodium-channel modulation by the beta4 subunit." Proc Natl Acad Sci U S A **110**(51): E5016-5024.

Giri, B., V. D. Dixit, M. C. Ghosh, G. D. Collins, I. U. Khan, K. Madara, A. T. Weeraratna and D. D. Taub (2007). "CXCL12-induced partitioning of flotillin-1 with lipid rafts plays a role in CXCR4 function." Eur J Immunol **37**(8): 2104-2116.

Glasscock, E., J. W. Yoo, T. T. Chen, T. L. Klassen and J. L. Noebels (2010). "Kv1.1 potassium channel deficiency reveals brain-driven cardiac dysfunction as a candidate mechanism for sudden unexplained death in epilepsy." J Neurosci **30**(15): 5167-5175.

Gomez-Ospina, N., G. Panagiotakos, T. Portmann, S. P. Pasca, D. Rabah, A. Budzillo, J. P. Kinet and R. E. Dolmetsch (2013). "A promoter in the coding region of the calcium channel gene CACNA1C generates the transcription factor CCAT." PLoS One **8**(4): e60526.

Gomez-Ospina, N., F. Tsuruta, O. Barreto-Chang, L. Hu and R. Dolmetsch (2006). "The C terminus of the L-type voltage-gated calcium channel Ca(V)1.2 encodes a transcription factor." Cell **127**(3): 591-606.

Gorlich, D., P. Henklein, R. A. Laskey and E. Hartmann (1996). "A 41 amino acid motif in importin-alpha confers binding to importin-beta and hence transit into the nucleus." Embo j **15**(8): 1810-1817.

Gorlich, D. and R. W. Kriwacki (2016). "Editorial Overview: Functional and Mechanistic Landscape of the Nuclear Pore Complex." J Mol Biol **428**(10 Pt A): 1947-1948.

Goth, C. K., A. Halim, S. A. Khetarpal, D. J. Rader, H. Clausen and K. T. Schjoldager (2015). "A systematic study of modulation of ADAM-mediated ectodomain shedding by site-specific O-glycosylation." Proc Natl Acad Sci U S A **112**(47): 14623-14628.

Gray, B., C. Hasdemir, J. Ingles, T. Aiba, N. Makita, V. Probst, A. A. M. Wilde, R. Newbury-Ecob, M. N. Sheppard, C. Semsarian, R. W. Sy and E. R. Behr (2018). "Lack of genotype-phenotype correlation in Brugada Syndrome and Sudden Arrhythmic Death Syndrome families with reported pathogenic SCN1B variants." Heart Rhythm **15**(7): 1051-1057.

Grieco, T. M., J. D. Malhotra, C. Chen, L. L. Isom and I. M. Raman (2005). "Open-channel block by the cytoplasmic tail of sodium channel beta4 as a mechanism for resurgent sodium current." Neuron **45**(2): 233-244.

Haapasalo, A. and D. M. Kovacs (2011). "The many substrates of presenilin/gamma-secretase." J Alzheimers Dis **25**(1): 3-28.

Haass, C., A. Y. Hung, M. G. Schlossmacher, D. B. Teplow and D. J. Selkoe (1993). "beta-Amyloid peptide and a 3-kDa fragment are derived by distinct cellular mechanisms." J Biol Chem **268**(5): 3021-3024.

Hakim, P., N. Brice, R. Thresher, J. Lawrence, Y. Zhang, A. P. Jackson, A. A. Grace and C. L. Huang (2010). "Scn3b knockout mice exhibit abnormal sino-atrial and cardiac conduction properties." Acta Physiol (Oxf) **198**(1): 47-59.

Hakim, P., I. S. Gurung, T. H. Pedersen, R. Thresher, N. Brice, J. Lawrence, A. A. Grace and C. L. Huang (2008). "Scn3b knockout mice exhibit abnormal ventricular electrophysiological properties." Prog Biophys Mol Biol **98**(2-3): 251-266.

Hemming, M. L., J. E. Elias, S. P. Gygi and D. J. Selkoe (2009). "Identification of beta-secretase (BACE1) substrates using quantitative proteomics." PLoS One **4**(12): e8477.

Hernandez-Plata, E., C. S. Ortiz, B. Marquina-Castillo, I. Medina-Martinez, A. Alfaro, J. Berumen, M. Rivera and J. C. Gomora (2012). "Overexpression of NaV 1.6 channels is associated with the invasion capacity of human cervical cancer." Int J Cancer **130**(9): 2013-2023.

Hesdorffer, D. C., T. Tomson, E. Benn, J. W. Sander, L. Nilsson, Y. Langan, T. S. Walczak, E. Beghi, M. J. Brodie and W. A. Hauser (2012). "Do antiepileptic drugs or generalized tonic-clonic seizure frequency increase SUDEP risk? A combined analysis." Epilepsia **53**(2): 249-252.

Hicks, C., S. H. Johnston, G. diSibio, A. Collazo, T. F. Vogt and G. Weinmaster (2000). "Fringe differentially modulates Jagged1 and Delta1 signalling through Notch1 and Notch2." Nat Cell Biol **2**(8): 515-520.

Hitt, B., S. M. Riordan, L. Kukreja, W. A. Eimer, T. W. Rajapaksha and R. Vassar (2012). "beta-Site amyloid precursor protein (APP)-cleaving enzyme 1 (BACE1)-deficient mice exhibit a close homolog of L1 (CHL1) loss-of-function phenotype involving axon guidance defects." J Biol Chem **287**(46): 38408-38425.

Hitt, B. D., T. C. Jaramillo, D. M. Chetkovich and R. Vassar (2010). "BACE1-/- mice exhibit seizure activity that does not correlate with sodium channel level or axonal localization." Mol Neurodegener **5**: 31.

Holst, A. G., S. Saber, M. Houshmand, E. V. Zaklyazminskaya, Y. Wang, H. K. Jensen, L. Refsgaard, S. Haunso, J. H. Svendsen, M. S. Olesen and J. Tfelt-Hansen (2012). "Sodium current and potassium transient outward current genes in Brugada syndrome: screening and bioinformatics." Can J Cardiol **28**(2): 196-200.

Hu, D., H. Barajas-Martinez, A. Medeiros-Domingo, L. Crotti, C. Veltmann, R. Schimpf, J. Urrutia, A. Alday, O. Casis, R. Pfeiffer, E. Burashnikov, G. Caceres, D. J. Tester, C. Wolpert, M. Borggrefe, P. Schwartz, M. J. Ackerman and C. Antzelevitch (2012). "A novel rare variant in SCN1Bb linked to Brugada syndrome and SIDS by combined modulation of Na(v)1.5 and K(v)4.3 channel currents." Heart Rhythm **9**(5): 760-769.

Hu, X., Q. Fan, H. Hou and R. Yan (2016). "Neurological dysfunctions associated with altered BACE1-dependent Neuregulin-1 signaling." J Neurochem **136**(2): 234-249.

Hu, X., W. He, X. Luo, K. E. Tsubota and R. Yan (2013). "BACE1 regulates hippocampal astrogenesis via the Jagged1-Notch pathway." Cell Rep **4**(1): 40-49.

Hu, X., C. W. Hicks, W. He, P. Wong, W. B. Macklin, B. D. Trapp and R. Yan (2006). "Bace1 modulates myelination in the central and peripheral nervous system." Nat Neurosci **9**(12): 1520-1525.

Hu, X., X. Zhou, W. He, J. Yang, W. Xiong, P. Wong, C. G. Wilson and R. Yan (2010). "BACE1 deficiency causes altered neuronal activity and neurodegeneration." J Neurosci **30**(26): 8819-8829.

Hull, J. M. and L. L. Isom (2018). "Voltage-gated sodium channel beta subunits: The power outside the pore in brain development and disease." Neuropharmacology **132**: 43-57.

Isom, L. L. (2002). "The role of sodium channels in cell adhesion." Front Biosci **7**: 12-23.

Isom, L. L. and W. A. Catterall (1996). "Na+ channel subunits and Ig domains." Nature **383**(6598): 307-308.

Isom, L. L., K. S. De Jongh and W. A. Catterall (1994). "Auxiliary subunits of voltage-gated ion channels." Neuron **12**(6): 1183-1194.

Isom, L. L., K. S. De Jongh, D. E. Patton, B. F. Reber, J. Offord, H. Charbonneau, K. Walsh, A. L. Goldin and W. A. Catterall (1992). "Primary structure and functional expression of the beta 1 subunit of the rat brain sodium channel." Science **256**(5058): 839-842.

Isom, L. L., D. S. Ragsdale, K. S. De Jongh, R. E. Westenbroek, B. F. Reber, T. Scheuer and W. A. Catterall (1995). "Structure and function of the beta 2 subunit of brain sodium channels, a transmembrane glycoprotein with a CAM motif." Cell **83**(3): 433-442.

Isom, L. L., T. Scheuer, A. B. Brownstein, D. S. Ragsdale, B. J. Murphy and W. A. Catterall (1995). "Functional Co-expression of the 1 and Type IIA Subunits of Sodium Channels in a Mammalian Cell Line." Journal of Biological Chemistry **270**(7): 3306-3312.

Isom, L. L., T. Scheuer, A. B. Brownstein, D. S. Ragsdale, B. J. Murphy and W. A. Catterall (1995). "Functional co-expression of the b1 and type IIA a subunits of sodium channels in a mammalian cell line." J. Biol. Chem. **270**: 3306-3312.

Jansen, K. and L. Lagae (2010). "Cardiac changes in epilepsy." Seizure **19**(8): 455-460.

Jansson, K. H., J. E. Lynch, N. Lepori-Bui, K. J. Czymmek, R. L. Duncan and R. A. Sikes (2012). "Overexpression of the VSSC-associated CAM, beta-2, enhances LNCaP cell metastasis associated behavior." Prostate **72**(10): 1080-1092.

Johnson, D., M. L. Montpetit, P. J. Stocker and E. S. Bennett (2004). "The sialic acid component of the beta1 subunit modulates voltage-gated sodium channel function." J Biol Chem **279**(43): 44303-44310.

Kageyama, R., T. Ohtsuka, H. Shimojo and I. Imayoshi (2009). "Dynamic regulation of Notch signaling in neural progenitor cells." Curr Opin Cell Biol **21**(6): 733-740.

Kalume, F., R. E. Westenbroek, C. S. Cheah, F. H. Yu, J. C. Oakley, T. Scheuer and W. A. Catterall (2013). "Sudden unexpected death in a mouse model of Dravet syndrome." J Clin Invest **123**(4): 1798-1808.

Kaplan, D. I., L. L. Isom and S. Petrou (2016). "Role of Sodium Channels in Epilepsy." Cold Spring Harb Perspect Med **6**(6).

Kazarinova-Noyes, K., J. D. Malhotra, D. P. McEwen, L. N. Mattei, E. O. Berglund, B. Ranscht, S. R. Levinson, M. Schachner, P. Shrager, L. L. Isom and Z. C. Xiao (2001). "Contactin associates with Na+ channels and increases their functional expression." J Neurosci **21**(19): 7517-7525.

Kazen-Gillespie, K. A., D. S. Ragsdale, M. R. D'Andrea, L. N. Mattei, K. E. Rogers and L. L. Isom (2000). "Cloning, localization, and functional expression of sodium channel beta1A subunits." J Biol Chem **275**(2): 1079-1088.

Kelleher, R. J., 3rd and J. Shen (2017). "Presenilin-1 mutations and Alzheimer's disease." Proc Natl Acad Sci U S A **114**(4): 629-631.

Kim, D. Y., B. W. Carey, H. Wang, L. A. Ingano, A. M. Binshtok, M. H. Wertz, W. H. Pettingell, P. He, V. M. Lee, C. J. Woolf and D. M. Kovacs (2007). "BACE1 regulates voltage-gated sodium channels and neuronal activity." Nat Cell Biol **9**(7): 755-764.

Kim, D. Y., M. T. Gersbacher, P. Inquimbert and D. M. Kovacs (2011). "Reduced sodium channel Na(v)1.1 levels in BACE1-null mice." J Biol Chem **286**(10): 8106-8116.

Kim, D. Y., L. A. Ingano, B. W. Carey, W. H. Pettingell and D. M. Kovacs (2005). "Presenilin/gamma-secretase-mediated cleavage of the voltage-gated sodium channel beta2-subunit regulates cell adhesion and migration." J Biol Chem **280**(24): 23251-23261.

Kim, D. Y., L. A. Mackenzie Ingano, B. W. Carey, W. P. Pettingell and D. M. Kovacs (2005). "Presenilin/gamma -secretase-mediated cleavage of the voltage-gated sodium channel beta 2 subunit regulates cell adhesion and migration." J Biol Chem.

Kim, H. S., E. M. Kim, J. P. Lee, C. H. Park, S. Kim, J. H. Seo, K. A. Chang, E. Yu, S. J. Jeong, Y. H. Chong and Y. H. Suh (2003). "C-terminal fragments of amyloid precursor protein exert neurotoxicity by inducing glycogen synthase kinase-3beta expression." Faseb j **17**(13): 1951-1953.

Ko, S. H., P. W. Lenkowski, H. C. Lee, J. P. Mounsey and M. K. Patel (2005). "Modulation of Na(v)1.5 by beta1-- and beta3-subunit co-expression in mammalian cells." Pflugers Arch **449**(4): 403-412.

Kobayashi, D., M. Zeller, T. Cole, M. Buttini, L. McConlogue, S. Sinha, S. Freedman, R. G. Morris and K. S. Chen (2008). "BACE1 gene deletion: impact on behavioral function in a model of Alzheimer's disease." Neurobiol Aging **29**(6): 861-873.

Komeili, A. and E. K. O'Shea (2000). "Nuclear transport and transcription." <u>Curr Opin Cell Biol</u> **12**(3): 355-360.

Koo, E. H. and S. L. Squazzo (1994). "Evidence that production and release of amyloid beta-protein involves the endocytic pathway." <u>J Biol Chem</u> **269**(26): 17386-17389.

Kopan, R. (2012). "Notch signaling." <u>Cold Spring Harb Perspect Biol</u> **4**(10).

Kopan, R. and M. X. G. Ilagan (2004). "γ-Secretase: proteasome of the membrane?" <u>Nature Reviews Molecular Cell Biology</u> **5**(6): 499-504.

Kopan, R., J. S. Nye and H. Weintraub (1994). "The intracellular domain of mouse Notch: a constitutively activated repressor of myogenesis directed at the basic helix-loop-helix region of MyoD." <u>Development</u> **120**(9): 2385-2396.

Krous, H. F., J. B. Beckwith, R. W. Byard, T. O. Rognum, T. Bajanowski, T. Corey, E. Cutz, R. Hanzlick, T. G. Keens and E. A. Mitchell (2004). "Sudden infant death syndrome and unclassified sudden infant deaths: a definitional and diagnostic approach." <u>Pediatrics</u> **114**(1): 234-238.

Kruger, L. C. and L. L. Isom (2016). "Voltage-Gated Na+ Channels: Not Just for Conduction." <u>Cold Spring Harb Perspect Biol</u> **8**(6).

Kruger, L. C., H. A. O'Malley, J. M. Hull, A. Kleeman, G. A. Patino and L. L. Isom (2016). "beta1-C121W Is Down But Not Out: Epilepsy-Associated Scn1b-C121W Results in a Deleterious Gain-of-Function." <u>J Neurosci</u> **36**(23): 6213-6224.

Laedermann Cé, J., N. Syam, M. Pertin, I. Decosterd and H. Abriel (2013). "β1- and β3- voltage-gated sodium channel subunits modulate cell surface expression and glycosylation of Na(v)1.7 in HEK293 cells." <u>Front Cell Neurosci</u> **7**.

Lal, M. and M. Caplan (2011). "Regulated Intramembrane Proteolysis: Signaling Pathways and Biological Functions." <u>Physiology</u> **26**(1): 34-44.

Lal, M. and M. Caplan (2011). "Regulated intramembrane proteolysis: signaling pathways and biological functions." <u>Physiology (Bethesda)</u> **26**(1): 34-44.

Lee, Y. J. and T. H. Ch'ng (2020). "RIP at the Synapse and the Role of Intracellular Domains in Neurons." <u>Neuromolecular Med</u> **22**(1): 1-24.

Lemberg, M. K. and M. Freeman (2007). "Cutting Proteins within Lipid Bilayers: Rhomboid Structure and Mechanism." <u>Molecular Cell</u> **28**(6): 930-940.

Levental, I., D. Lingwood, M. Grzybek, U. Coskun and K. Simons (2010). "Palmitoylation regulates raft affinity for the majority of integral raft proteins." <u>Proc Natl Acad Sci U S A</u> **107**(51): 22050-22054.

Li, H., Y. Chen, B. Zhou, Y. Peng, Y. Sheng and L. Rao (2011). "Polymorphisms of presenilin-1 gene associate with dilated cardiomyopathy susceptibility." <u>Mol Cell Biochem</u> **358**(1-2): 31-36.

Li, R. G., Q. Wang, Y. J. Xu, M. Zhang, X. K. Qu, X. Liu, W. Y. Fang and Y. Q. Yang (2013). "Mutations of the SCN4B-encoded sodium channel beta4 subunit in familial atrial fibrillation." <u>Int J Mol Med</u> **32**(1): 144-150.

Lichtenthaler, S. F., C. Haass and H. Steiner (2011). "Regulated intramembrane proteolysis – lessons from amyloid precursor protein processing." <u>Journal of Neurochemistry</u> **117**(5): 779-796.

Lichtenthaler, S. F., M. K. Lemberg and R. Fluhrer (2018). "Proteolytic ectodomain shedding of membrane proteins in mammals-hardware, concepts, and recent developments." <u>Embo j</u> **37**(15).

Lin, X., H. O'Malley, C. Chen, D. Auerbach, M. Foster, A. Shekhar, M. Zhang, W. Coetzee, J. Jalife, G. I. Fishman, L. Isom and M. Delmar (2014). "Scn1b deletion leads to increased tetrodotoxin-sensitive sodium current, altered intracellular calcium homeostasis and arrhythmias in murine hearts." <u>J Physiol</u>.

Lin, X., H. O'Malley, C. Chen, D. Auerbach, M. Foster, A. Shekhar, M. Zhang, W. Coetzee, J. Jalife, G. I. Fishman, L. Isom and M. Delmar (2015). "Scn1b deletion leads to increased tetrodotoxin-sensitive sodium current, altered intracellular calcium homeostasis and arrhythmias in murine hearts." J Physiol **593**(6): 1389-1407.

Lo, W. L., D. L. Donermeyer and P. M. Allen (2012). "A voltage-gated sodium channel is essential for the positive selection of CD4(+) T cells." Nat Immunol **13**(9): 880-887.

Lopez-Santiago, L. F., W. J. Brackenbury, C. Chen and L. L. Isom (2011). "Na+ channel Scn1b gene regulates dorsal root ganglion nociceptor excitability in vivo." J Biol Chem **286**(26): 22913-22923.

Lopez-Santiago, L. F., W. J. Brackenbury, C. Chen and L. L. Isom (2011). "Na+ channel SCN1B regulates dorsal root ganglion nociceptor excitability in vivo." J Biol Chem.

Lopez-Santiago, L. F., L. S. Meadows, S. J. Ernst, C. Chen, J. D. Malhotra, D. P. McEwen, A. Speelman, J. L. Noebels, S. K. Maier, A. N. Lopatin and L. L. Isom (2007). "Sodium channel Scn1b null mice exhibit prolonged QT and RR intervals." J Mol Cell Cardiol **43**(5): 636-647.

Lopez-Santiago, L. F., M. Pertin, X. Morisod, C. Chen, S. Hong, J. Wiley, I. Decosterd and L. L. Isom (2006). "Sodium channel beta2 subunits regulate tetrodotoxin-sensitive sodium channels in small dorsal root ganglion neurons and modulate the response to pain." J Neurosci **26**(30): 7984-7994.

Lu, L., P. Sirish, Z. Zhang, R. L. Woltz, N. Li, V. Timofeyev, A. A. Knowlton, X. D. Zhang, E. N. Yamoah and N. Chiamvimonvat (2015). "Regulation of gene transcription by voltage-gated L-type calcium channel, Cav1.3." J Biol Chem **290**(8): 4663-4676.

Maier, S. K., R. E. Westenbroek, K. A. McCormick, R. Curtis, T. Scheuer and W. A. Catterall (2004). "Distinct subcellular localization of different sodium channel alpha and beta subunits in single ventricular myocytes from mouse heart." Circulation **109**(11): 1421-1427.

Main, H., K. L. Lee, H. Yang, S. Haapa-Paananen, H. Edgren, S. Jin, C. Sahlgren, O. Kallioniemi, L. Poellinger, B. Lim and U. Lendahl (2010). "Interactions between Notch- and hypoxia-induced transcriptomes in embryonic stem cells." Exp Cell Res **316**(9): 1610-1624.

Malhotra, J. D., K. Kazen-Gillespie, M. Hortsch and L. L. Isom (2000). "Sodium channel beta subunits mediate homophilic cell adhesion and recruit ankyrin to points of cell-cell contact." J Biol Chem **275**(15): 11383-11388.

Malhotra, J. D., M. C. Koopmann, K. A. Kazen-Gillespie, N. Fettman, M. Hortsch and L. L. Isom (2002). "Structural requirements for interaction of sodium channel b1 subunits with ankyrin." J Biol Chem **277**(29): 26681-26688.

Malhotra, J. D., M. C. Koopmann, K. A. Kazen-Gillespie, N. Fettman, M. Hortsch and L. L. Isom (2002). "Structural requirements for interaction of sodium channel beta 1 subunits with ankyrin." J Biol Chem **277**(29): 26681-26688.

Malhotra, J. D., V. Thyagarajan, C. Chen and L. L. Isom (2004). "Tyrosine-phosphorylated and nonphosphorylated sodium channel beta1 subunits are differentially localized in cardiac myocytes." J Biol Chem **279**(39): 40748-40754.

Marionneau, C., Y. Carrasquillo, A. J. Norris, R. R. Townsend, L. L. Isom, A. J. Link and J. M. Nerbonne (2012). "The Sodium Channel Accessory Subunit Navβ1 Regulates Neuronal Excitability through Modulation of Repolarizing Voltage-Gated K(+) Channels." J Neurosci **32**(17): 5716-5727.

Massey, C. A., L. P. Sowers, B. J. Dlouhy and G. B. Richerson (2014). "SUDEP Mechanisms: The pathway to prevention." Nat Rev Neurol **10**(5): 271-282.

Mattsson, N., M. Axelsson, S. Haghighi, C. Malmestrom, G. Wu, R. Anckarsater, S. Sankaranarayanan, U. Andreasson, S. Fredrikson, A. Gundersen, L. Johnsen, T. Fladby, A. Tarkowski, E. Trysberg, A. Wallin, H. Anckarsater, J. Lycke, O. Andersen, A. J. Simon, K. Blennow and H. Zetterberg (2009). "Reduced cerebrospinal fluid BACE1 activity in multiple sclerosis." Mult Scler 15(4): 448-454.

McCarthy, A. J., C. Coleman-Vaughan and J. V. McCarthy (2017). "Regulated intramembrane proteolysis: emergent role in cell signalling pathways." Biochem Soc Trans 45(6): 1185-1202.

McCormick, K. A., L. L. Isom, D. Ragsdale, D. Smith, T. Scheuer and W. A. Catterall (1998). "Molecular determinants of Na+ channel function in the extracellular domain of the beta1 subunit." J Biol Chem 273(7): 3954-3962.

McEwen, D. P., C. Chen, L. S. Meadows, L. Lopez-Santiago and L. L. Isom (2009). "The voltage-gated Na+ channel beta3 subunit does not mediate trans homophilic cell adhesion or associate with the cell adhesion molecule contactin." Neurosci Lett 462(3): 272-275.

McEwen, D. P. and L. L. Isom (2004). "Heterophilic interactions of sodium channel beta1 subunits with axonal and glial cell adhesion molecules." J Biol Chem 279(50): 52744-52752.

McEwen, D. P., L. S. Meadows, C. Chen, V. Thyagarajan and L. L. Isom (2004). "Sodium channel beta1 subunit-mediated modulation of Nav1.2 currents and cell surface density is dependent on interactions with contactin and ankyrin." J Biol Chem 279(16): 16044-16049.

Meadows, L., J. D. Malhotra, A. Stetzer, L. L. Isom and D. S. Ragsdale (2001). "The intracellular segment of the sodium channel beta 1 subunit is required for its efficient association with the channel alpha subunit." J Neurochem 76(6): 1871-1878.

Meadows, L. S., J. Malhotra, A. Loukas, V. Thyagarajan, K. A. Kazen-Gillespie, M. C. Koopman, S. Kriegler, L. L. Isom and D. S. Ragsdale (2002). "Functional and biochemical analysis of a sodium channel beta1 subunit mutation responsible for generalized epilepsy with febrile seizures plus type 1." J Neurosci 22(24): 10699-10709.

Medeiros-Domingo, A., T. Kaku, D. J. Tester, P. Iturralde-Torres, A. Itty, B. Ye, C. Valdivia, K. Ueda, S. Canizales-Quinteros, M. T. Tusie-Luna, J. C. Makielski and M. J. Ackerman (2007). "SCN4B-encoded sodium channel beta4 subunit in congenital long-QT syndrome." Circulation 116(2): 134-142.

Mei, L. and K. A. Nave (2014). "Neuregulin-ERBB signaling in the nervous system and neuropsychiatric diseases." Neuron 83(1): 27-49.

Meier-Stiegen, F., R. Schwanbeck, K. Bernoth, S. Martini, T. Hieronymus, D. Ruau, M. Zenke and U. Just (2010). "Activated Notch1 target genes during embryonic cell differentiation depend on the cellular context and include lineage determinants and inhibitors." PLoS One 5(7): e11481.

Mikhailik, A., J. Mazella, S. Liang and L. Tseng (2009). "Notch ligand-dependent gene expression in human endometrial stromal cells." Biochem Biophys Res Commun 388(3): 479-482.

Miyazaki, H., F. Oyama, R. Inoue, T. Aosaki, T. Abe, H. Kiyonari, Y. Kino, M. Kurosawa, J. Shimizu, I. Ogiwara, K. Yamakawa, Y. Koshimizu, F. Fujiyama, T. Kaneko, H. Shimizu, K. Nagatomo, K. Yamada, T. Shimogori, N. Hattori, M. Miura and N. Nukina (2014). "Singular localization of sodium channel beta4 subunit in unmyelinated fibres and its role in the striatum." Nat Commun 5: 5525.

Miyazaki, H., F. Oyama, H. K. Wong, K. Kaneko, T. Sakurai, A. Tamaoka and N. Nukina (2007). "BACE1 modulates filopodia-like protrusions induced by sodium channel beta4 subunit." Biochem Biophys Res Commun 361(1): 43-48.

Morgan, K., E. B. Stevens, B. Shah, P. J. Cox, A. K. Dixon, K. Lee, R. D. Pinnock, J. Hughes, P. J. Richardson, K. Mizuguchi and A. P. Jackson (2000). "beta 3: an additional auxiliary subunit of

the voltage-sensitive sodium channel that modulates channel gating with distinct kinetics." Proc Natl Acad Sci U S A **97**(5): 2308-2313.

Morrison, S. J., S. E. Perez, Z. Qiao, J. M. Verdi, C. Hicks, G. Weinmaster and D. J. Anderson (2000). "Transient Notch activation initiates an irreversible switch from neurogenesis to gliogenesis by neural crest stem cells." Cell **101**(5): 499-510.

Nakano, Y. and W. Shimizu (2016). "Genetics of long-QT syndrome." J Hum Genet **61**(1): 51-55.

Namadurai, S., D. Balasuriya, R. Rajappa, M. Wiemhofer, K. Stott, J. Klingauf, J. M. Edwardson, D. Y. Chirgadze and A. P. Jackson (2014). "Crystal structure and molecular imaging of the Nav channel beta3 subunit indicates a trimeric assembly." J Biol Chem **289**(15): 10797-10811.

Nashef, L., E. L. So, P. Ryvlin and T. Tomson (2012). "Unifying the definitions of sudden unexpected death in epilepsy." Epilepsia **53**(2): 227-233.

Nejatbakhsh, N. and Z. P. Feng (2011). "Calcium binding protein-mediated regulation of voltage-gated calcium channels linked to human diseases." Acta Pharmacol Sin **32**(6): 741-748.

Nelson, M., R. Millican-Slater, L. C. Forrest and W. J. Brackenbury (2014). "The sodium channel beta1 subunit mediates outgrowth of neurite-like processes on breast cancer cells and promotes tumour growth and metastasis." Int J Cancer **135**(10): 2338-2351.

Nguyen, H. M., H. Miyazaki, N. Hoshi, B. J. Smith, N. Nukina, A. L. Goldin and K. G. Chandy (2012). "Modulation of voltage-gated K+ channels by the sodium channel beta1 subunit." Proc Natl Acad Sci U S A **109**(45): 18577-18582.

Noritake, J., Y. Fukata, T. Iwanaga, N. Hosomi, R. Tsutsumi, N. Matsuda, H. Tani, H. Iwanari, Y. Mochizuki, T. Kodama, Y. Matsuura, D. S. Bredt, T. Hamakubo and M. Fukata (2009). "Mobile DHHC palmitoylating enzyme mediates activity-sensitive synaptic targeting of PSD-95." J Cell Biol **186**(1): 147-160.

Nutini, M., A. Spalloni, F. Florenzano, R. E. Westenbroek, C. Marini, W. A. Catterall, G. Bernardi and P. Longone (2011). "Increased expression of the beta3 subunit of voltage-gated Na+ channels in the spinal cord of the SOD1G93A mouse." Mol Cell Neurosci **47**(2): 108-118.

O'Malley, H. A. and L. L. Isom (2015). "Sodium channel beta subunits: emerging targets in channelopathies." Annu Rev Physiol **77**: 481-504.

O'Malley, H. A., A. B. Shreiner, G. H. Chen, G. B. Huffnagle and L. L. Isom (2009). "Loss of Na+ channel beta2 subunits is neuroprotective in a mouse model of multiple sclerosis." Mol Cell Neurosci **40**(2): 143-155.

Oakley, J. C., F. Kalume and W. A. Catterall (2011). "Insights into pathophysiology and therapy from a mouse model of Dravet syndrome." Epilepsia **52 Suppl 2**: 59-61.

Ogiwara, I., T. Nakayama, T. Yamagata, H. Ohtani, E. Mazaki, S. Tsuchiya, Y. Inoue and K. Yamakawa (2012). "A homozygous mutation of voltage-gated sodium channel beta(I) gene SCN1B in a patient with Dravet syndrome." Epilepsia **53**(12): e200-203.

Olesen, M. S., A. G. Holst, J. H. Svendsen, S. Haunso and J. Tfelt-Hansen (2012). "SCN1Bb R214Q found in 3 patients: 1 with Brugada syndrome and 2 with lone atrial fibrillation." Heart Rhythm **9**(5): 770-773.

Olesen, M. S., T. Jespersen, J. B. Nielsen, B. Liang, D. V. Moller, P. Hedley, M. Christiansen, A. Varro, S. P. Olesen, S. Haunso, N. Schmitt and J. H. Svendsen (2011). "Mutations in sodium channel beta-subunit SCN3B are associated with early-onset lone atrial fibrillation." Cardiovasc Res **89**(4): 786-793.

Oyama, F., H. Miyazaki, N. Sakamoto, C. Becquet, Y. Machida, K. Kaneko, C. Uchikawa, T. Suzuki, M. Kurosawa, T. Ikeda, A. Tamaoka, T. Sakurai and N. Nukina (2006). "Sodium channel

beta4 subunit: down-regulation and possible involvement in neuritic degeneration in Huntington's disease transgenic mice." J Neurochem **98**(2): 518-529.

Ozaki, T., Y. Li, H. Kikuchi, T. Tomita, T. Iwatsubo and A. Nakagawara (2006). "The intracellular domain of the amyloid precursor protein (AICD) enhances the p53-mediated apoptosis." Biochem Biophys Res Commun **351**(1): 57-63.

Palomero, T., W. K. Lim, D. T. Odom, M. L. Sulis, P. J. Real, A. Margolin, K. C. Barnes, J. O'Neil, D. Neuberg, A. P. Weng, J. C. Aster, F. Sigaux, J. Soulier, A. T. Look, R. A. Young, A. Califano and A. A. Ferrando (2006). "NOTCH1 directly regulates c-MYC and activates a feed-forward-loop transcriptional network promoting leukemic cell growth." Proceedings of the National Academy of Sciences **103**(48): 18261-18266.

Pandis, D. and N. Scarmeas (2012). "Seizures in Alzheimer Disease: Clinical and Epidemiological Data." Epilepsy Currents **12**(5): 184-187.

Pardossi-Piquard, R. and F. Checler (2012). "The physiology of the beta-amyloid precursor protein intracellular domain AICD." J Neurochem **120 Suppl 1**: 109-124.

Paris, D., A. Quadros, N. Patel, A. DelleDonne, J. Humphrey and M. Mullan (2005). "Inhibition of angiogenesis and tumor growth by beta and gamma-secretase inhibitors." Eur J Pharmacol **514**(1): 1-15.

Patino, G. A., W. J. Brackenbury, Y. Bao, L. F. Lopez-Santiago, H. A. O'Malley, C. Chen, J. D. Calhoun, R. G. Lafreniere, P. Cossette, G. A. Rouleau and L. L. Isom (2011). "Voltage-gated Na+ channel beta1B: a secreted cell adhesion molecule involved in human epilepsy." J Neurosci **31**(41): 14577-14591.

Patino, G. A., L. R. Claes, L. F. Lopez-Santiago, E. A. Slat, R. S. Dondeti, C. Chen, H. A. O'Malley, C. B. Gray, H. Miyazaki, N. Nukina, F. Oyama, P. De Jonghe and L. L. Isom (2009). "A functional null mutation of SCN1B in a patient with Dravet syndrome." J Neurosci **29**(34): 10764-10778.

Pedrozo, Z., N. Torrealba, C. Fernandez, D. Gatica, B. Toro, C. Quiroga, A. E. Rodriguez, G. Sanchez, T. G. Gillette, J. A. Hill, P. Donoso and S. Lavandero (2013). "Cardiomyocyte ryanodine receptor degradation by chaperone-mediated autophagy." Cardiovasc Res **98**(2): 277-285.

Percher, A., S. Ramakrishnan, E. Thinon, X. Yuan, J. S. Yount and H. C. Hang (2016). "Mass-tag labeling reveals site-specific and endogenous levels of protein S-fatty acylation." Proc Natl Acad Sci U S A **113**(16): 4302-4307.

Pertin, M., R. R. Ji, T. Berta, A. J. Powell, L. Karchewski, S. N. Tate, L. L. Isom, C. J. Woolf, N. Gilliard, D. R. Spahn and I. Decosterd (2005). "Upregulation of the voltage-gated sodium channel beta2 subunit in neuropathic pain models: characterization of expression in injured and non-injured primary sensory neurons." J Neurosci **25**(47): 10970-10980.

Pink, A. E., M. A. Simpson, N. Desai, R. C. Trembath and J. N. W. Barker (2013). "γ-Secretase Mutations in Hidradenitis Suppurativa: New Insights into Disease Pathogenesis." Journal of Investigative Dermatology **133**(3): 601-607.

Qin, N., M. R. D'Andrea, M. L. Lubin, N. Shafaee, E. E. Codd and A. M. Correa (2003). "Molecular cloning and functional expression of the human sodium channel beta1B subunit, a novel splicing variant of the beta1 subunit." Eur J Biochem **270**(23): 4762-4770.

Radtke, F., N. Fasnacht and H. R. Macdonald (2010). "Notch signaling in the immune system." Immunity **32**(1): 14-27.

Rajapaksha, T. W., W. A. Eimer, T. C. Bozza and R. Vassar (2011). "The Alzheimer's beta-secretase enzyme BACE1 is required for accurate axon guidance of olfactory sensory neurons and normal glomerulus formation in the olfactory bulb." Mol Neurodegener **6**: 88.

Ransdell, J. L., E. Dranoff, B. Lau, W. L. Lo, D. L. Donermeyer, P. M. Allen and J. M. Nerbonne (2017). "Loss of Navbeta4-Mediated Regulation of Sodium Currents in Adult Purkinje Neurons Disrupts Firing and Impairs Motor Coordination and Balance." Cell Rep **19**(3): 532-544.

Ratcliffe, C. F., Y. Qu, K. A. McCormick, V. C. Tibbs, J. E. Dixon, T. Scheuer and W. A. Catterall (2000). "A sodium channel signaling complex: modulation by associated receptor protein tyrosine phosphatase beta." Nat Neurosci **3**(5): 437-444.

Ratcliffe, C. F., R. E. Westenbroek, R. Curtis and W. A. Catterall (2001). "Sodium channel beta1 and beta3 subunits associate with neurofascin through their extracellular immunoglobulin-like domain." J Cell Biol **154**(2): 427-434.

Rawson, R. B., N. G. Zelenski, D. Nijhawan, J. Ye, J. Sakai, M. T. Hasan, T. Y. Chang, M. S. Brown and J. L. Goldstein (1997). "Complementation cloning of S2P, a gene encoding a putative metalloprotease required for intramembrane cleavage of SREBPs." Mol Cell **1**(1): 47-57.

Reid, C. A., B. Leaw, K. L. Richards, R. Richardson, V. Wimmer, C. Yu, E. L. Hill-Yardin, H. Lerche, I. E. Scheffer, S. F. Berkovic and S. Petrou (2014). "Reduced dendritic arborization and hyperexcitability of pyramidal neurons in a Scn1b-based model of Dravet syndrome." Brain **137**(Pt 6): 1701-1715.

Remme, C. A. and C. R. Bezzina (2010). "Sodium channel (dys)function and cardiac arrhythmias." Cardiovasc Ther **28**(5): 287-294.

Reverter, M., C. Rentero, S. V. de Muga, A. Alvarez-Guaita, V. Mulay, R. Cairns, P. Wood, K. Monastyrskaya, A. Pol, F. Tebar, J. Blasi, T. Grewal and C. Enrich (2011). "Cholesterol transport from late endosomes to the Golgi regulates t-SNARE trafficking, assembly, and function." Mol Biol Cell **22**(21): 4108-4123.

Ricci, M. T., S. Menegon, S. Vatrano, G. Mandrile, N. Cerrato, P. Carvalho, M. De Marchi, F. Gaita, C. Giustetto and D. F. Giachino (2014). "SCN1B gene variants in Brugada Syndrome: a study of 145 SCN5A-negative patients." Sci Rep **4**: 6470.

Riuro, H., P. Beltran-Alvarez, A. Tarradas, E. Selga, O. Campuzano, M. Verges, S. Pagans, A. Iglesias, J. Brugada, P. Brugada, F. M. Vazquez, G. J. Perez, F. S. Scornik and R. Brugada (2013). "A missense mutation in the sodium channel beta2 subunit reveals SCN2B as a new candidate gene for Brugada syndrome." Hum Mutat **34**(7): 961-966.

Riuro, H., O. Campuzano, E. Arbelo, A. Iglesias, M. Batlle, F. Perez-Villa, J. Brugada, G. J. Perez, F. S. Scornik and R. Brugada (2014). "A missense mutation in the sodium channel beta1b subunit reveals SCN1B as a susceptibility gene underlying long QT syndrome." Heart Rhythm **11**(7): 1202-1209.

Roger, S., J. Rollin, A. Barascu, P. Besson, P. I. Raynal, S. Iochmann, M. Lei, P. Bougnoux, Y. Gruel and J. Y. Le Guennec (2007). "Voltage-gated sodium channels potentiate the invasive capacities of human non-small-cell lung cancer cell lines." Int J Biochem Cell Biol **39**(4): 774-786.

Sachse, C. C., Y. H. Kim, M. Agsten, T. Huth, C. Alzheimer, D. M. Kovacs and D. Y. Kim (2013). "BACE1 and presenilin/gamma-secretase regulate proteolytic processing of KCNE1 and 2, auxiliary subunits of voltage-gated potassium channels." Faseb j **27**(6): 2458-2467.

Sachse, C. C., Y. H. Kim, M. Agsten, T. Huth, C. Alzheimer, D. M. Kovacs and D. Y. Kim (2013). "BACE1 and presenilin/γ-secretase regulate proteolytic processing of KCNE1 and 2, auxiliary subunits of voltage-gated potassium channels." Faseb j **27**(6): 2458-2467.

Sakai, J., R. B. Rawson, P. J. Espenshade, D. Cheng, A. C. Seegmiller, J. L. Goldstein and M. S. Brown (1998). "Molecular identification of the sterol-regulated luminal protease that cleaves SREBPs and controls lipid composition of animal cells." Mol Cell **2**(4): 505-514.

Sanchez-Sandoval, A. L. and J. C. Gomora (2019). "Contribution of voltage-gated sodium channel β-subunits to cervical cancer cells metastatic behavior." Cancer Cell Int **19**: 35.

Sannerud, R., C. Esselens, P. Ejsmont, R. Mattera, L. Rochin, A. K. Tharkeshwar, G. De Baets, V. De Wever, R. Habets, V. Baert, W. Vermeire, C. Michiels, A. J. Groot, R. Wouters, K. Dillen, K. Vints, P. Baatsen, S. Munck, R. Derua, E. Waelkens, G. S. Basi, M. Mercken, M. Vooijs, M. Bollen, J. Schymkowitz, F. Rousseau, J. S. Bonifacino, G. Van Niel, B. De Strooper and W. Annaert (2016). "Restricted Location of PSEN2/gamma-Secretase Determines Substrate Specificity and Generates an Intracellular Abeta Pool." Cell **166**(1): 193-208.

Sardi, S. P., J. Murtie, S. Koirala, B. A. Patten and G. Corfas (2006). "Presenilin-dependent ErbB4 nuclear signaling regulates the timing of astrogenesis in the developing brain." Cell **127**(1): 185-197.

Scheffer, I. E., L. A. Harkin, B. E. Grinton, L. M. Dibbens, S. J. Turner, M. A. Zielinski, R. Xu, G. Jackson, J. Adams, M. Connellan, S. Petrou, R. M. Wellard, R. S. Briellmann, R. H. Wallace, J. C. Mulley and S. F. Berkovic (2007). "Temporal lobe epilepsy and GEFS+ phenotypes associated with SCN1B mutations." Brain **130**(Pt 1): 100-109.

Schroder, E., M. Byse and J. Satin (2009). "L-type calcium channel C terminus autoregulates transcription." Circ Res **104**(12): 1373-1381.

Selkoe, D. J. and M. S. Wolfe (2007). "Presenilin: running with scissors in the membrane." Cell **131**(2): 215-221.

Shah, B. S., E. B. Stevens, M. I. Gonzalez, S. Bramwell, R. D. Pinnock, K. Lee and A. K. Dixon (2000). "beta3, a novel auxiliary subunit for the voltage-gated sodium channel, is expressed preferentially in sensory neurons and is upregulated in the chronic constriction injury model of neuropathic pain." Eur J Neurosci **12**(11): 3985-3990.

Shah, B. S., E. B. Stevens, R. D. Pinnock, A. K. Dixon and K. Lee (2001). "Developmental expression of the novel voltage-gated sodium channel auxiliary subunit beta3, in rat CNS." J Physiol **534**(Pt 3): 763-776.

Shank, L. C. and B. M. Paschal (2005). "Nuclear transport of steroid hormone receptors." Crit Rev Eukaryot Gene Expr **15**(1): 49-73.

Shimizu, H., H. Miyazaki, N. Ohsawa, S. Shoji, Y. Ishizuka-Katsura, A. Tosaki, F. Oyama, T. Terada, K. Sakamoto, M. Shirouzu, S. Sekine, N. Nukina and S. Yokoyama (2016). "Structure-based site-directed photo-crosslinking analyses of multimeric cell-adhesive interactions of voltage-gated sodium channel beta subunits." Sci Rep **6**: 26618.

Shimizu, H., A. Tosaki, N. Ohsawa, Y. Ishizuka-Katsura, S. Shoji, H. Miyazaki, F. Oyama, T. Terada, M. Shirouzu, S. I. Sekine, N. Nukina and S. Yokoyama (2017). "Parallel homodimer structures of the extracellular domains of the voltage-gated sodium channel beta4 subunit explain its role in cell-cell adhesion." J Biol Chem.

Spampanato, J., J. A. Kearney, G. de Haan, D. P. McEwen, A. Escayg, I. Aradi, B. T. MacDonald, S. I. Levin, I. Soltesz, P. Benna, E. Montalenti, L. L. Isom, A. L. Goldin and M. H. Meisler (2004). "A novel epilepsy mutation in the sodium channel SCN1A identifies a cytoplasmic domain for beta subunit interaction." J Neurosci **24**(44): 10022-10034.

Spasic, D. and W. Annaert (2008). "Building gamma-secretase: the bits and pieces." J Cell Sci **121**(Pt 4): 413-420.

Srinivasan, J., M. Schachner and W. A. Catterall (1998). "Interaction of voltage-gated sodium channels with the extracellular matrix molecules tenascin-C and tenascin-R." Proceedings of the National Academy of Sciences **95**(26): 15753-15757.

Surges, R. and J. W. Sander (2012). "Sudden unexpected death in epilepsy: mechanisms, prevalence, and prevention." Curr Opin Neurol **25**(2): 201-207.

Takahashi, N., S. Kikuchi, Y. Dai, K. Kobayashi, T. Fukuoka and K. Noguchi (2003). "Expression of auxiliary beta subunits of sodium channels in primary afferent neurons and the effect of nerve injury." Neuroscience **121**(2): 441-450.

Tan, B. H., K. N. Pundi, D. W. Van Norstrand, C. R. Valdivia, D. J. Tester, A. Medeiros-Domingo, J. C. Makielski and M. J. Ackerman (2010). "Sudden infant death syndrome-associated mutations in the sodium channel beta subunits." Heart Rhythm **7**(6): 771-778.

Tester, D. J. and M. J. Ackerman (2014). "GENETICS OF LONG QT SYNDROME." Methodist Debakey Cardiovasc J **10**(1): 29-33.

Theile, J. W., B. W. Jarecki, A. D. Piekarz and T. R. Cummins (2011). "Nav1.7 mutations associated with paroxysmal extreme pain disorder, but not erythromelalgia, enhance Navbeta4 peptide-mediated resurgent sodium currents." J Physiol **589**(Pt 3): 597-608.

Valdivia, C. R., A. Medeiros-Domingo, B. Ye, W. K. Shen, T. J. Algiers, M. J. Ackerman and J. C. Makielski (2010). "Loss-of-function mutation of the SCN3B-encoded sodium channel {beta}3 subunit associated with a case of idiopathic ventricular fibrillation." Cardiovasc Res **86**(3): 392-400.

Van Norstrand, D. W. and M. J. Ackerman (2009). "Sudden infant death syndrome: do ion channels play a role?" Heart Rhythm **6**(2): 272-278.

van Tetering, G. and M. Vooijs (2011). "Proteolytic cleavage of Notch: "HIT and RUN"." Curr Mol Med **11**(4): 255-269.

Vassar, R., B. D. Bennett, S. Babu-Khan, S. Kahn, E. A. Mendiaz, P. Denis, D. B. Teplow, S. Ross, P. Amarante, R. Loeloff, Y. Luo, S. Fisher, J. Fuller, S. Edenson, J. Lile, M. A. Jarosinski, A. L. Biere, E. Curran, T. Burgess, J. C. Louis, F. Collins, J. Treanor, G. Rogers and M. Citron (1999). "Beta-secretase cleavage of Alzheimer's amyloid precursor protein by the transmembrane aspartic protease BACE." Science **286**(5440): 735-741.

Vassar, R., D. M. Kovacs, R. Yan and P. C. Wong (2009). "The beta-secretase enzyme BACE in health and Alzheimer's disease: regulation, cell biology, function, and therapeutic potential." J Neurosci **29**(41): 12787-12794.

Veeraraghavan, R., G. S. Hoeker, A. Alvarez-Laviada, D. Hoagland, X. Wan, D. R. King, J. Sanchez-Alonso, C. Chen, J. Jourdan, L. L. Isom, I. Deschenes, J. W. Smyth, J. Gorelik, S. Poelzing and R. G. Gourdie (2018). "The adhesion function of the sodium channel beta subunit (beta1) contributes to cardiac action potential propagation." Elife **7**.

von Rotz, R. C., B. M. Kohli, J. Bosset, M. Meier, T. Suzuki, R. M. Nitsch and U. Konietzko (2004). "The APP intracellular domain forms nuclear multiprotein complexes and regulates the transcription of its own precursor." J Cell Sci **117**(Pt 19): 4435-4448.

Wallace, R. H., I. E. Scheffer, G. Parasivam, S. Barnett, G. B. Wallace, G. R. Sutherland, S. F. Berkovic and J. C. Mulley (2002). "Generalized epilepsy with febrile seizures plus: mutation of the sodium channel subunit SCN1B." Neurology **58**(9): 1426-1429.

Wallace, R. H., D. W. Wang, R. Singh, I. E. Scheffer, A. L. George, H. A. Phillips, K. Saar, A. Reis, E. W. Johnson, G. R. Sutherland, S. F. Berkovic and J. C. Mulley (1998). "Febrile seizures and generalized epilepsy associated with a mutation in the Na+-channel sz1 subunit gene SCN1B." Nat Genet **19**(4): 366-370.

Wang, H., A. Megill, P. C. Wong, A. Kirkwood and H. K. Lee (2014). "Postsynaptic target specific synaptic dysfunctions in the CA3 area of BACE1 knockout mice." PLoS One **9**(3): e92279.

Wang, H., L. Song, F. Laird, P. C. Wong and H. K. Lee (2008). "BACE1 knock-outs display deficits in activity-dependent potentiation of synaptic transmission at mossy fiber to CA3 synapses in the hippocampus." J Neurosci **28**(35): 8677-8681.

Wang, P., Q. Yang, X. Wu, Y. Yang, L. Shi, C. Wang, G. Wu, Y. Xia, B. Yang, R. Zhang, C. Xu, X. Cheng, S. Li, Y. Zhao, F. Fu, Y. Liao, F. Fang, Q. Chen, X. Tu and Q. K. Wang (2010). "Functional dominant-negative mutation of sodium channel subunit gene SCN3B associated with atrial fibrillation in a Chinese GeneID population." Biochem Biophys Res Commun **398**(1): 98-104.

Watanabe, H., D. Darbar, D. W. Kaiser, K. Jiramongkolchai, S. Chopra, B. S. Donahue, P. J. Kannankeril and D. M. Roden (2009). "Mutations in sodium channel beta1- and beta2-subunits associated with atrial fibrillation." Circ Arrhythm Electrophysiol **2**(3): 268-275.

Watanabe, H., T. T. Koopmann, S. Le Scouarnec, T. Yang, C. R. Ingram, J. J. Schott, S. Demolombe, V. Probst, F. Anselme, D. Escande, A. C. Wiesfeld, A. Pfeufer, S. Kaab, H. E. Wichmann, C. Hasdemir, Y. Aizawa, A. A. Wilde, D. M. Roden and C. R. Bezzina (2008). "Sodium channel beta1 subunit mutations associated with Brugada syndrome and cardiac conduction disease in humans." J Clin Invest **118**(6): 2260-2268.

Weerkamp, F., T. C. Luis, B. A. E. Naber, E. E. L. Koster, L. Jeannotte, J. J. M. van Dongen and F. J. T. Staal (2006). "Identification of Notch target genes in uncommitted T-cell progenitors: no direct induction of a T-cell specific gene program." Leukemia **20**(11): 1967-1977.

Weggen, S. and D. Beher (2012). "Molecular consequences of amyloid precursor protein and presenilin mutations causing autosomal-dominant Alzheimer's disease." Alzheimers Res Ther **4**(2): 9.

Willem, M., A. N. Garratt, B. Novak, M. Citron, S. Kaufmann, A. Rittger, B. DeStrooper, P. Saftig, C. Birchmeier and C. Haass (2006). "Control of peripheral nerve myelination by the beta-secretase BACE1." Science **314**(5799): 664-666.

Wimmer, V. C., C. A. Reid, S. Mitchell, K. L. Richards, B. B. Scaf, B. T. Leaw, E. L. Hill, M. Royeck, M. T. Horstmann, B. A. Cromer, P. J. Davies, R. Xu, H. Lerche, S. F. Berkovic, H. Beck and S. Petrou (2010). "Axon initial segment dysfunction in a mouse model of genetic epilepsy with febrile seizures plus." J Clin Invest **120**(8): 2661-2671.

Wolfe, M. S. (2019). "Dysfunctional gamma-Secretase in Familial Alzheimer's Disease." Neurochem Res **44**(1): 5-11.

Wolfe, M. S., J. De Los Angeles, D. D. Miller, W. Xia and D. J. Selkoe (1999). "Are Presenilins Intramembrane-Cleaving Proteases? Implications for the Molecular Mechanism of Alzheimer's Disease." Biochemistry **38**(35): 11223-11230.

Wong, H. K., T. Sakurai, F. Oyama, K. Kaneko, K. Wada, H. Miyazaki, M. Kurosawa, B. De Strooper, P. Saftig and N. Nukina (2005). "beta Subunits of voltage-gated sodium channels are novel substrates of beta-site amyloid precursor protein-cleaving enzyme (BACE1) and gamma-secretase." J Biol Chem **280**(24): 23009-23017.

Xiao, Z. C., D. S. Ragsdale, J. D. Malhotra, L. N. Mattei, P. E. Braun, M. Schachner and L. L. Isom (1999). "Tenascin-R is a functional modulator of sodium channel beta subunits." J Biol Chem **274**(37): 26511-26517.

Xu, H., W. Guo and J. M. Nerbonne (1999). "Four kinetically distinct depolarization-activated K+ currents in adult mouse ventricular myocytes." J Gen Physiol **113**(5): 661-678.

Xu, R., E. A. Thomas, E. V. Gazina, K. L. Richards, M. Quick, R. H. Wallace, L. A. Harkin, S. E. Heron, S. F. Berkovic, I. E. Scheffer, J. C. Mulley and S. Petrou (2007). "Generalized epilepsy

with febrile seizures plus-associated sodium channel beta1 subunit mutations severely reduce beta subunit-mediated modulation of sodium channel function." Neuroscience **148**(1): 164-174.

Yan, R. (2017). "Physiological Functions of the beta-Site Amyloid Precursor Protein Cleaving Enzyme 1 and 2." Front Mol Neurosci **10**: 97.

Yan, R., Q. Fan, J. Zhou and R. Vassar (2016). "Inhibiting BACE1 to reverse synaptic dysfunctions in Alzheimer's disease." Neurosci Biobehav Rev **65**: 326-340.

Yan, Z., K. Cui, D. M. Murray, C. Ling, Y. Xue, A. Gerstein, R. Parsons, K. Zhao and W. Wang (2005). "PBAF chromatin-remodeling complex requires a novel specificity subunit, BAF200, to regulate expression of selective interferon-responsive genes." Genes Dev **19**(14): 1662-1667.

Yu, F. H., R. E. Westenbroek, I. Silos-Santiago, K. A. McCormick, D. Lawson, P. Ge, H. Ferriera, J. Lilly, P. S. DiStefano, W. A. Catterall, T. Scheuer and R. Curtis (2003). "Sodium channel beta4, a new disulfide-linked auxiliary subunit with similarity to beta2." J Neurosci **23**(20): 7577-7585.

Yuan, L., J. T. Koivumaki, B. Liang, L. G. Lorentzen, C. Tang, M. N. Andersen, J. H. Svendsen, J. Tfelt-Hansen, M. Maleckar, N. Schmitt, M. S. Olesen and T. Jespersen (2014). "Investigations of the Navbeta1b sodium channel subunit in human ventricle; functional characterization of the H162P Brugada syndrome mutant." Am J Physiol Heart Circ Physiol **306**(8): H1204-1212.

Yuan, Y., H. A. O'Malley, M. A. Smaldino, A. A. Bouza, J. M. Hull and L. L. Isom (2019). "Delayed maturation of GABAergic signaling in the Scn1a and Scn1b mouse models of Dravet Syndrome." Sci Rep **9**(1): 6210.

Zhang, Y. W., R. Wang, Q. Liu, H. Zhang, F. F. Liao and H. Xu (2007). "Presenilin/gamma-secretase-dependent processing of beta-amyloid precursor protein regulates EGF receptor expression." Proc Natl Acad Sci U S A **104**(25): 10613-10618.

Zhao, Y. T., Y. B. Guo, L. Gu, X. X. Fan, H. Q. Yang, Z. Chen, P. Zhou, Q. Yuan, G. J. Ji and S. Q. Wang (2017). "Sensitized signalling between L-type Ca2+ channels and ryanodine receptors in the absence or inhibition of FKBP12.6 in cardiomyocytes." Cardiovasc Res **113**(3): 332-342.

Zhao, Y. T., C. R. Valdivia, G. B. Gurrola, P. P. Powers, B. C. Willis, R. L. Moss, J. Jalife and H. H. Valdivia (2015). "Arrhythmogenesis in a catecholaminergic polymorphic ventricular tachycardia mutation that depresses ryanodine receptor function." Proc Natl Acad Sci U S A **112**(13): E1669-1677.

Zhou, J., A. Jeron, B. London, X. Han and G. Koren (1998). "Characterization of a slowly inactivating outward current in adult mouse ventricular myocytes." Circ Res **83**(8): 806-814.

Zhou, T. T., Z. W. Zhang, J. Liu, J. P. Zhang and B. H. Jiao (2012). "Glycosylation of the sodium channel beta4 subunit is developmentally regulated and involves in neuritic degeneration." Int J Biol Sci **8**(5): 630-639.

Zuhl, A. M., C. E. Nolan, M. A. Brodney, S. Niessen, K. Atchison, C. Houle, D. A. Karanian, C. Ambroise, J. W. Brulet, E. M. Beck, S. D. Doran, B. T. O'Neill, C. W. Am Ende, C. Chang, K. F. Geoghegan, G. M. West, J. C. Judkins, X. Hou, D. R. Riddell and D. S. Johnson (2016). "Chemoproteomic profiling reveals that cathepsin D off-target activity drives ocular toxicity of beta-secretase inhibitors." Nat Commun **7**: 13042.